A Thesis for the Degree of Doctor of Philosophy in Pharmacology

Structure Determination of Bioactive Metabolites from Marine-Derived Fungi and Simultaneous Analysis of Herbal Medicines by HPLC-DAD-ELSD-MS

August 2015

by
Lijuan Liao

Natural Products Science Major, College of Pharmacy
Doctoral Course in the Graduate School
Seoul National University

Abstract

Structure Determination of Bioactive Metabolites from Marine-Derived Fungi and Simultaneous Analysis of Herbal Medicines by HPLC-DAD-ELSD-MS

Lijuan Liao
Natural Products Science Major
College of Pharmacy
Doctoral Course in the Graduate School
Seoul National University

Part A. Structure Determination of Bioactive Metabolites from Marine-Derived Fungi

Marine natural products have been proven to be a prolific source of novel therapeutic agents that have demonstrated significant activities in various pathological conditions including cancer, viral infection, inflammation, analgesia, and immune modulation. The marine-derived fungi is one of the three dominated phylogenetic groups, have shown great diversity of their secondary metabolites and a wide range novel secondary

metabolites have been isolated since 1980s. Marine-derived fungi alone have produced more than 400 novel compounds, of which several have exhibited potent and diverse bioactivities. The purpose of this study is to investigate new marine natural products from marine-derived fungi and study their biological activities. During the course of searching for bioactive metabolites from marine-derived fungi, two strains *Penicillium* sp. and *Aspergillus* sp. were selected for chemical investigation based on LC-ESIMS analysis and bioassay screening of the crude extracts. Secondary metabolites from the selected fungi were isolated and structure determination based on 1D, 2D NMR, and IR, UV, OR and MS. As a result, 9 novel compounds and 9 known compounds were structurally determined using integrated spectroscopic analysis and chemical approaches. These compounds belonged to various structural classes: meroterpenoids, alkaloids, anthroquinones, and lipopeptides. The biological activities of the isolated compounds were studied on various bioactivity tests: cytotoxicity, antimicrobial activities, inhibition against the enzymes isocitrate lyase (ICL), sortase A (SrtA) and Na^+/K^+-ATPase, and quinone reductase. Structure-activity relationships were also deduced.

Part B. Simultaneous Analysis of Herbal Medicines by HPLC-DAD-ELSD-MS

Traditional herbal medicines have been practiced to maintain health and treat diseases especially in the Asia communities for more than 2,000 years. Increment of worldwide attention and concomitant pharmaceutical research has made it essential to carry out the quality control measurement for the herbal medicines. However, serious hindrance has been attributed to the lack of recognition and regulation of professions, qualified practitioners, quality-controlled herbal medicines, and evidence-based clinical studies. Thus it is urgently needed to establish a comprehensive qualified evaluation method that could accurately reflect the quality of herbal medicines. The purpose of this study is developing simultaneous analysis methods of bioactive compounds in herbal medicines. Two herbal medicines, which are Kalopanacis Cortex and Semen Ziziphus jujuba were subjected to the current study. In herbal medicines, it is hard to consider that single or a few compounds would determine the overall pharmacological activities. Rather, it is more likely that multiple compounds act simultaneously and attribute to the therapeutic function of the herbal medicine. For this reason, most bioactive metabolite in the selected herbal medicines were analyzed and determined. In particular, three phenolics and nine hedergenin saponins were selected for the analysis of Kalopanacis Cortex. Moreover, one alkaloid, five flavonoid saponins and three jujuboside saponins from Semen

Ziziphus jujuba were also analyzed. The methods based on HPLC-DAD-ELSD-MS was established for the quantitative and qualitative analysis of a selected folk medicine. Various validation parameters, such as linearity, limit of detection, limit of quantification, recovery, accuracy, and precision, were successfully obtained. In addition, the efficiencies of diverse extraction methods were compared for the development of a standard analytic method. The verified methods were successfully applied to the quantitative determination of representative metabolites in commercial samples from Korea, Myanmar and China.

Keywords: marine natural products, marine-derived fungi, structure determination, herbal medicines, simultaneous analysis

Student number: 2011-30822

List of Contents

List of Tables

List of Figures

Part A.

Structure Determination of Bioactive Metabolites from Marine-Derived Fungi

I. Introduction

Marine microorganisms are tiny, single-celled organisms that live in the ocean and account for more than 98% of ocean biomass. In contrast to the terrestrial microorganisms, the environment of marine microorganisms is extreme and changeable with the high salinity, high pressure, low oxygen, and insufficient light, which made them produce bioactive and structurally unique secondary metabolites.[1-6] Since late 1990s, the numbers of new compounds isolated from the marine microbes increased steeply.[7] This trend has accelerated in recent years due to both the demand of mass bioactive compounds and the technical progress in related field, such as microbial genetics and bioinformatics.[8] Marine microbes, particularly actinomycete bacteria and fungi, produce a wide variety of biologically active and structurally unique metabolites.[2-6] Hundreds of novel compounds are isolated from these organisms annually.[7] A wide range of pharmacological activities of these compounds as antitumor/anticancer, antimicrobial, antiviral, and cytotoxic activities against several cell lines have been reported.[6, 10-12] Until 2010, several compounds from marine microbes are in clinical or preclinical studies.[13-16]

Marine-derived fungi, as one of the major marine microbes, which is

comprised of marine fungi and facultative species that are found in terrestrial ecosystem as well but grow well in the marine environment. Based on the sources of the marine-derived fungi, the distribution of taxonomic diversity and all compounds isolated has been graphically summarized in Figures 1 and 2.[3, 17] The greatest taxonomic diversity and the largest number compounds come from strains derived from sponges (33%). The highest number of novel metabolites also come from those isolated from sponges. Marine algae and drifting woods come next that is reminiscent of abundance of algaecolous and wood-digesting fungal strains.[3, 17]

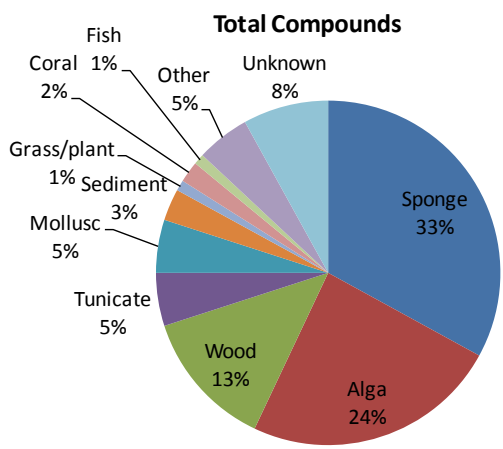

Figure 1. The distribution of compounds from marine-derived fungi by their sources (or origins).

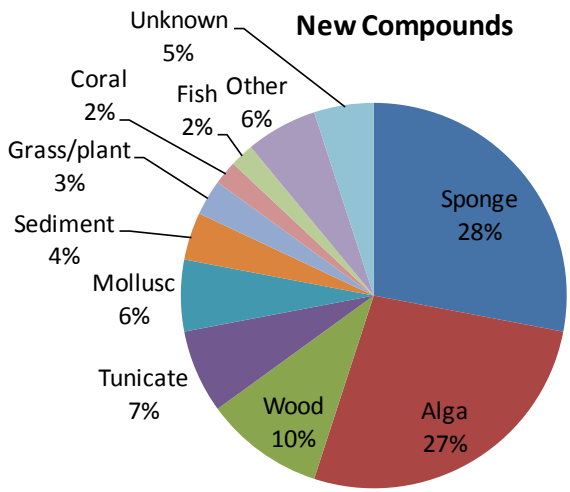

Figure 2. The distribution of new compounds from marine-derived fungi by their sources (or origins).

The marine-derived fungi that have shown great diversity of their secondary metabolites and a wide range novel secondary metabolites have been isolated since 1980s. The diverse novel bioactive metabolites have been reported which show anticancer, antibacterial, antifungal, antiviral, antiplasmodial, anti-inflammatory could be beneficial for pharmaceutical therapeutics.[18]

The representative examples of novel bioactive secondary metabolites from marine-derived fungi was illustrated in

Figure 3.

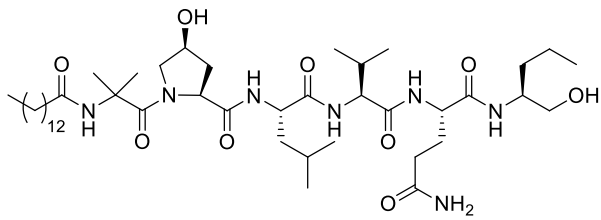

Halovir A
Antiviral activity against HSV-1 and HSV-2 (ED_{50} : 280 nM)
Source : Genus *Scytalidium*

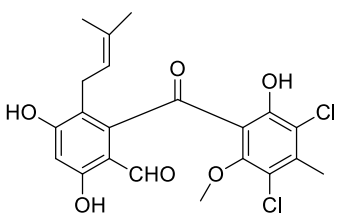

Pestalone
Antibiotic activity against methicilin-resistant *Staphylococcus aureus* (MIC = 37 ng/mL) and vancomycin-resistant *Enterococcus faecium* (MIC = 78 ng/mL)
Source : genus *Pestalotia*

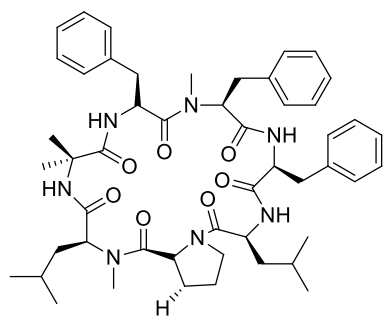

Scytalidamide A
Cytotoxic activity against HCT-116
(IC50 = 2.7 μM)
Source : genus *Scytalidium*

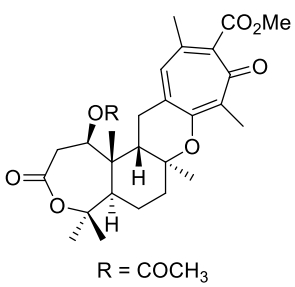

R = $COCH_3$

Tropolactone B
Cytotoxic activity against HCT-116
(IC50 = 10.9 μg/mL)
Source : genus *Aspergillus*

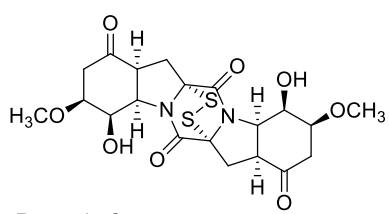

Rostratin C
Cytotoxic activity against HCT-116
(IC50 = 0.76 μg/mL)
Source : *Exserohilum rostratum*

Figure 3. Examples of novel bioactive secondary metabolites from marine-derived fungi.[19-23]

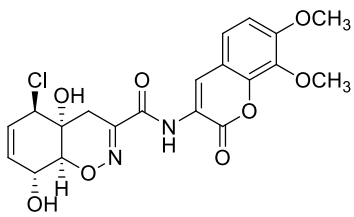

Trichodermamide
Cytotoxic activity against HCT-116
(IC_{50} = 0.32 μg/mL)
Source : *Trichoderma virens*

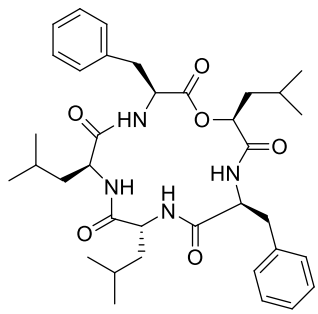

Zygosporamide
Cytotoxic activity against SF-268 (GI_{50} = 6.5 nM)
and RXF 393 ($GI_{50} \leq$ 5.0 nm)
Source : *Zygosporium masonii*

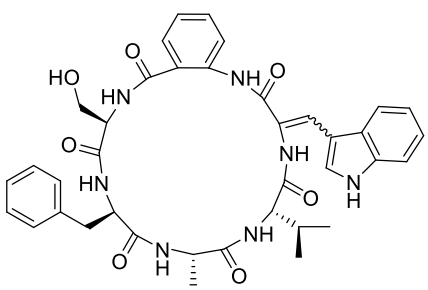

Z-, sclerotide A; E-, sclerotide B
Antifungal activity against *Candida albicans*
(MIC = 7.0 and 3.5 μM respectively)
Source : *Aspergillus sclerotorium*

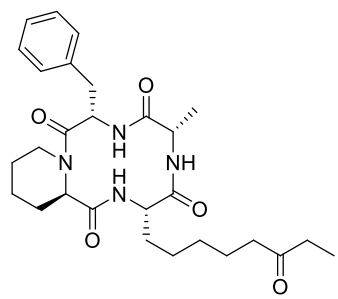

Microsporin A
Cytotoxic activity against HCT-116
(IC50 = 0.6 μg/mL)
Source : *Microsporum* cf. *gypseum*

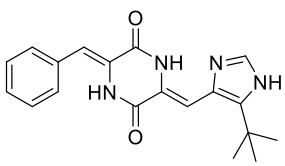

Plinabulin (NPI-2358)

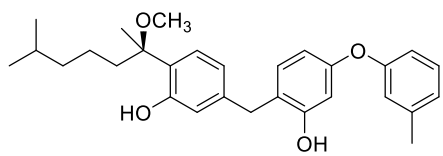

Expansol B
Cytotoxic activity against A549 (IC_{50}= 1.9 μM)
Source : *Penicillium expansum*

Figure 3. Examples of novel bioactive secondary metabolites from marine-derived fungi (continued).[24-29]

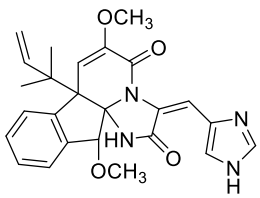

Oxaline
Inhibited tubulin polymerization
Source : *Penicillium sp*. FKI-0779

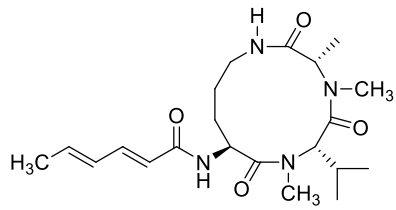

Sclerotiotides B
Antifungal activity against *Candida albicans*
(MIC = 3.8 μM)
Source : *Aspergillus sclerotiorum* PT06-1

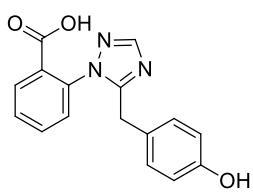

Penipanoid A
Cytotoxicity against SMMC-772
(IC50 = 54.2 μM)
Source : *Penicillium paneum* SD-44

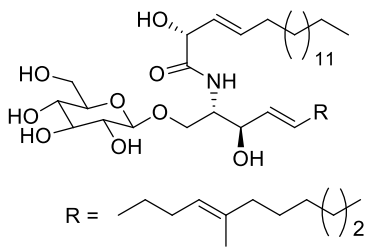

Chrysogeside B
Antimicrobial activity against *Enterobacter aerogenes*
(MIC = 1.72 μM)
Source : *Penicillium chrysogenum*

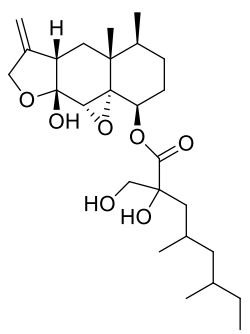

Cryptosphaerolide
Cytotoxicity against HCT-116 cells
(IC_{50} = 4.5 μM)
Source : *Cryptosphaeria* sp

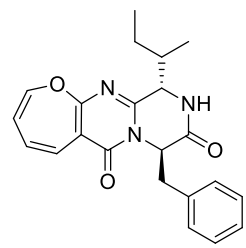

Protuboxepins A
Cytotoxicity against HL-60 cells
(IC50 = 75 μM)
Source : *Aspergillus sp*. SF-5044

Figure 3. Examples of novel bioactive secondary metabolites from marine-derived fungi (continued).[30-35]

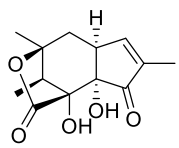

Acremostrictin
antioxidant-related DPPH
(IC50 = 2.5 μM)
Source : *Acemonium strictum*

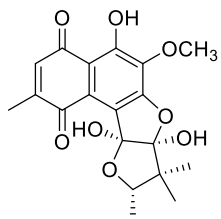

Herqueidiketal
significant inhibitory against sortase A
(IC50 = 23.6 μM)
Source : *Penicillium* sp.

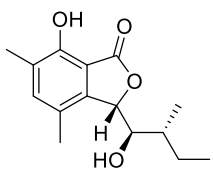

Chrysoarticulin C
Moderate activity against sortase A
(IC50 = 95.1 μM)
Source : *Chrysosporium articulatum*

Figure 3. Examples of novel bioactive secondary metabolites from marine-derived fungi.[36-38]

The purpose of this thesis is to investigate new marine natural products from the marine-derived fungi which were isolated from the marine

sediment and marine organisms that mostly were sponges collected from off the coast of Korea.

In this research, several media were used for the isolation of fungi. Those media are follows:

YMM	Mannitol 2 g, malt extract 4 g, yeast extract 2 g, agar 16 g, artificial seawater 1 L.
YPMBFe	Yeast extract 2 g, peptone 2 g, mannitol 4 g, KBr 5 mL/L of 20 g/L in purified H_2O, $FePO_4$ 5 mL/L of 8 g/L in purified H_2O, agar 16 g, artificial seawater 1 L.
YPM	Yeast extract 2 g, peptone 2 g, mannitol 4 g, crab meal 2 g, agar 16 g, artificial seawater 1 L.
YPM2	Yeast extract 2 g, peptone 2 g, mannitol 4 g, crab meal 2 g, calcium carbonate 1 g, agar 16 g, artificial seawater 1 L
YPG	Yeast extract 5 g, peptone 5 g, glucose 10 g, agar 16 g, artificial seawater 1 L.
MB 2216	Marine broth 2216 37.4 g, glycerol 20 g, agar 16 g, purified H_2O 1 L.

The bacterial inhibitors, penicillin G sodium salt and streptomycin sulphate, were added into the culture media with a concentration 150 mg/L, respectively.

During my research for bioactive compounds from marine fungi, in total more than 200 fungal strains were isolated from marine sediment and marine organisms that mostly isolated from sponges.

The pure strains were further investigated by performing small scale cultivation and extraction for screenings. Strains selection was conducted by LC-ESIMS based on the chemical constituents and cytotoxicity towards K562 and A549. The selected strains were chosen for a large cultivation and isolation of the new compounds. The first strain is F446 which was isolated from marine sediment, the LC-ESIMS profile of the extract revealed the presence of novel compounds which prompted us to investigate its metabolites in detail (Figure 4). And the organic extract showed a mild cytotoxicity (LC_{50} = 192 μg/mL) against the K562 human leukemia cell line. The F446 was identified to be *Penicillium* sp.. The second strain was F452 which was isolated from marine-submerged decaying wood from Korea, the LC-ESIMS profile of the extract revealed the presence of diverse secondary metabolites (Figure 5). F452 was identified as *Aspergillus* sp..

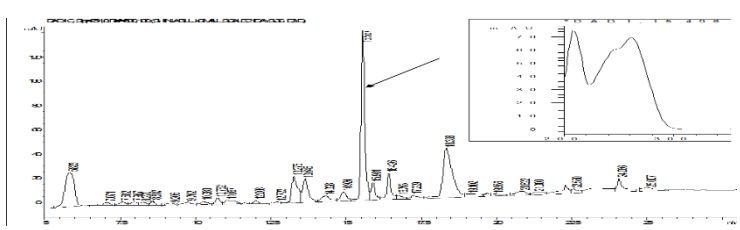

Figure 4. LC-MS profile of the broth extract of strain F446.

HPLC with C18 (Phenomenex, 5 μm, 4.6 x 100 mm), elution by H_2O-MeCN, gradient (90:10 to 0:100 in 20 min, then 0:100 in 5 min), 0.7 mL/min, UV detection at 254 nm.

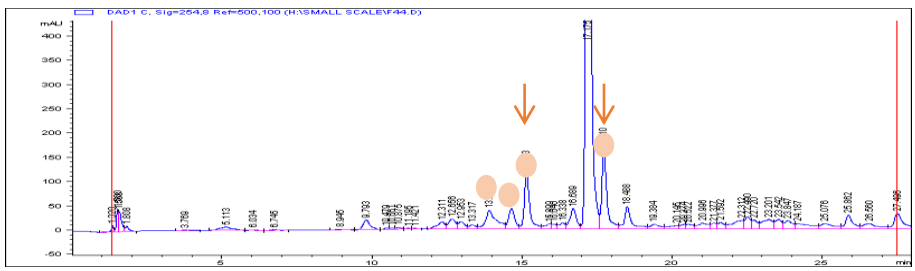

Figure 5. LC-MS profile of the broth extract of strain F452.

HPLC with C18 (Phenomenex, 5 μm, 4.6 x 100 mm), elution by H_2O-MeCN, gradient (90:10 to 0:100 in 20 min, then 0:100 in 5 min), 0.7 mL/min, UV detection at 254 nm.

The large scale cultivation, extraction and separation using diverse chromatographic methods were conducted to yield 9 new compounds and 9 known compounds from F466 and F452 in total. Structure elucidation was performed mainly using 1D and 2D NMR techniques and chemical characterization of the isolated metabolites.

The biological activity assays were performed for antimicrobioal,

and cytotoxic activities, inhibition against the enzymes isocitrate lyase (ICL) and reduction of quinone reductase, sortase A (SrtA) and Na^+/K^+-ATPase. The cytotoxicity of the test compounds were conducted on A549, K562, HCT116, MDA-MB231, SNU638, and SK-HEP1 cancer cell lines.[39-41] Quinone reductase was conducted on murine Hepa 1c1c7 cells.[42] Sortase A (SrtA) and isocitrate lyase (ICL),[43,44] which are not found in mammalian species, were selected as target enzyme since they play crucial roles in the virulence or survival of various human-pathogenic bacteria and fungi. In addition, the inhibitory activity against Na^+/K^+-ATPase, which plays a crucial role in cellular function, was also tested.[45]

II. Penicillipyrones A and B, Meroterpenoids from the Marine-derived Fungus *Penicillium* sp.

Two novel meroterpenoids, Penicillipyrones A (**1**) and B (**2**), together with methyl 8-hydroxy-6-methyl-9-oxo-9H-xanthene-1-carboxylate (**3**) and coniochaetone B (**4**) were isolated from the marine-derived fungus *Penicillium* sp.. Based upon the results of combined spectroscopic analyses, these compounds were structurally elucidated to be triprenyl γ-lactones from a new skeletal class derived from a unique pattern of linkage between the prenyl and pyrone moieties. The new compounds exhibited weak cytotoxicities against K562 and A549 cell lines. Compound **2** also elicited a significant induction of quinone reductase.

2-1. Introduction

Fungi from marine environments are widely recognized as very prolific sources of biologically active and structurally unique secondary metabolites.[2-6] Although studies on these organisms began much later than their counterparts in terrestrial environments, more than a hundred novel compounds have been found annually since the late 1990s.[7] Consequently, fungi, along with actinomycete bacteria, from marine environments are

regarded as a new frontier for research into natural products.

In our search for novel bioactive compounds from marine fungi, we reported acremostrictin, a highly oxygenated metabolite of a new structural class from *Acremonium strictum*.[36] In addition, there have recent reports of novel polyaromatic compounds and hydroxybenzolactones from marine-derived *Penicillium* sp.[37] and *Chrysosporium articulatum*, respectively.[38] In our continued search, a strain of *Penicillium* sp. was collected from a marine sediment from Korea, whose organic extract showed a mild cytotoxicity (LC_{50} = 192 μg/mL) against the K562 human leukemia cell line. More importantly the LC-ESIMS profile of the *Penicillium* sp. extract revealed the presence of novel compounds which prompted us to investigate its metabolites in detail. Large-scale culture of the strain followed by the extraction of the broth and chromatographic separation led to the isolation of two new meroterpenoids. Here, we report the structural determinations of the penicillipyrones A (**1**) and B (**2**) (Figure 1), triprenyl γ-pyrones of a novel skeletal class. These compounds exhibited weak inhibition against K562 and A549 cell lines as well as significant induction (compound **2**) of quinone reductase (QR) in Hepa 1c1c7 murine hepatoma cells.

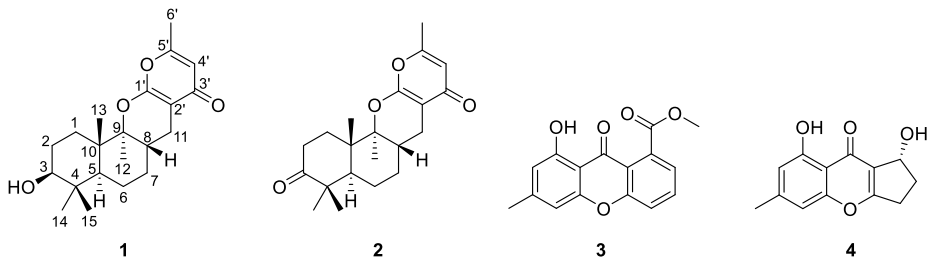

Figure 6. The chemical structures of compounds **1** - **4**.

2-2. Results and discussion

The molecular formula of penicillipyrone A (**1**) was deduced to be $C_{21}H_{30}O_4$ by HRFABMS analysis. The ^{13}C NMR data of this compound showed signals from a carbonyl carbon at a δ_C value of 180.2 and four olefinic carbons at δ_C values of 163.3, 160.6, 111.8, and 98.0 (Table 1). The highly differentiated chemical shifts of the olefinic carbons, in conjunction with the seven degrees of unsaturation inherent in the molecular formula, suggested the presence of a conjugated cyclic lactone or ketone moiety, such as an α- or γ-pyrone. The strong absorption band at 1665 cm^{-1} in the IR data as well as the absorption maxima at 210, 243 and 257 nm in the UV data were indicative of the latter, a γ-pyrone moiety. [46]

In addition to the downfield carbon signals, the ^{13}C NMR data also showed signals of two oxygenated carbons at δ_C values of 89.5 and 78.6 and

fourteen upfield carbon atoms: 2 x C, 2 x CH, 5 x CH_2, and 5 x CH_3. The high occurrence of methyl groups in the NMR data revealed the polyprenyl-containing meroterpenoid nature of this compound.

Given this information, the planar structure of compound **1** was determined by a combination of the ^{1}H COSY, HSQC and HMBC experiments. In particular, the HMBC correlations between the upfield methyl protons and their neighboring carbons were crucial to defining the triprenyl portion of compound **1** (Figure 7). The two singlet methyl protons at δ_H values of 1.00 and 0.84 showed long-range correlations to the neighboring carbons at δ_C values of 78.6, 39.1 and 47.6 as well as the mutual correlations with their carbons at δ_C values of 15.3 and 28.4, revealed that these are the terminal isopropyl head of the triprenyl-derived ring system. Starting from the methine protons at δ_H values of 3.22 and 1.23, which are attached at the carbons at δ_C values of 78.6 (C-3) and 39.1 (C-5), respectively, and are also neighbors to the isopropyl moiety, the ^{1}H COSY NMR data revealed the presence of two linear proton spin systems (Figure 7). The C-1 and C-5 carbons at δ_C values of 29.7 and 47.6, which contained the protons belonging to each of the spin systems, showed long-range correlations with a singlet methyl proton at a δ_H value of 1.08 (H-13) in the HMBC data. Thus, a six-membered carbocycle was constructed from these data and an additional

correlation between H-13 and a quaternary carbon at a δ_C value of 41.8 (C-10).

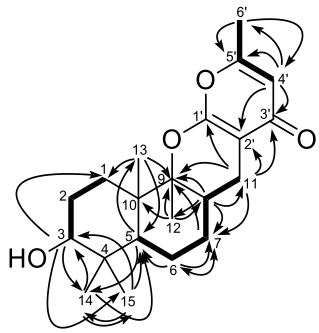

Figure 7. The COSY (bold line) and selected gHMBC (arrows) correlations of compound **1**.

Meanwhile, an oxygen-containing carbon at a δ_C value of 89.5 was placed at the neighboring C-9 position by its HMBC correlation with the H-13 methyl proton. Another six-membered ring was also established by the HMBC correlations of a singlet methyl proton at a δ_H value of 1.22 (H-12) with the prepositioned C-9 and C-10 atoms as well as a methine carbon at a δ_C value of 33.5 (C-8) whose proton at a δ_H value of 2.01 was determined to belonged to a linear spin system starting from the H-5 methine proton.

The terminus of the triprenyl portion was deduced to be the C-11 methylene whose carbon and proton signals were assigned to be those at a δ_C value of 22.0 and δ_H values of 2.53 and 1.93 by the ^{1}H COSY data of the

linear proton spin system starting from H-5 as well as from the carbon-proton correlations of H-8/C-11, H-11/C-7 and H-11/C-9 in the HMBC data (Figure 7). The characteristic shifts of the carbon atom and protons of this methylene group indicated the direct attachment of an aromatic moiety, γ-pyrone, at this position that was confirmed by the long-range correlations of the methylene protons with the carbons at δ_C values of 180.2 (C-3′), 163.3 (C-1′) and 98.0 (C-2′). The remaining three carbons at δ_C values of 160.6 (C-5′), 111.8 (C-4′) and 19.2 (C-6′) were also placed on this methylpyrone by a series of HMBC correlations between H-4′/C-2′, H-4′/C-3′, H-4′/C-5′, H-4′/C-6′, H-6′/C-4′, and H-6′/C-5′. Meanwhile, 2-D NMR based carbon assignments, in conjunction with the molecular formula, confirmed the presence of a γ-pyrone moiety by the downfield shifts of the C-1′ and C-5′ carbons at δ_C values of 163.3 and 160.6, respectively.[46] Although the lack of protons at these positions prohibited direct evidences, the downfield shift of C-9 at a δ_C value of 89.5 showed an ether bridge between this and carbon atom C-1′.[46, 47] Thus, the planar structure of penicillipyrone A (**1**) was unambiguously determined.

Penicillipyrone A possesses asymmetric carbon centers at C-3, C-5, C-8, C-9, and C-10. The relative configurations at these centers were determined by a combination of 1-D NMR data and NOESY analysis (Figure 8). First, the H-3 and H-5 protons were placed at the axial orientation by the

large vicinal proton-proton couplings (10.0 and 12.9 Hz). Starting from these protons, those axially oriented to same side of the rings were found by NOESY cross-peaks to be: H-1α (δ_H 1.67)/H-5, H-1α/H-12, H-3/H-14, H-5/H-14, H-6α (δ_H 1.64)/H-14, H-7α (δ_H 1.14)/H-11α (δ_H 1.93), and H-7α/H-12. Those axially oriented to the opposite side of H-3 and H-5 were also determined by the NOESY data to be: H-2β (δ_H 1.66)/H-13, H-2β/H-15, H-6β (δ_H 1.47)/H-13, H-6β/H-15, H-6/H-8, H-8/H-13, and H-13/H-15. Overall these data determined that the orientations for both the A/B and B/C ring junctures were *trans*, which was supported by the characteristic upfield shifts of the bridgehead methyl groups and the downfield shifts of the ring juncture methines in the ^{13}C NMR data.

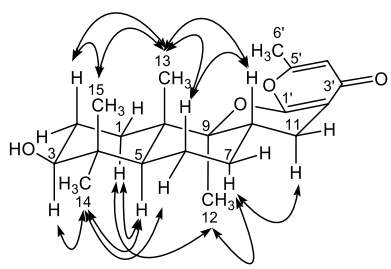

Figure 8. The selected NOE correlations of compound **1**.

Having the relative configurations through the NMR data, the absolute configurations were assigned by Mosher analysis in which the *S* configuration at the hydroxy-bearing C-3 was deduced from Δδ values

between the MTPA esters (Figure 9). Therefore, the overall absolute configurations were assigned as 3*S*, 5*S*, 8*S*, 9*S*, and 10*S*. Thus the structure of penicillipyrone A (**1**) was determined to be that of a triprenyl-γ-pyrone meroterpenoid from a new skeletal class.

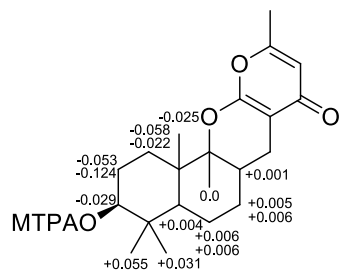

Figure 9. The Δδ ($\delta_{(S\text{-ester})}$-$\delta_{(R\text{-ester})}$) values of MTPA esterification for compound **1**.

The structure of penicillipyrone A (**1**) was found to be a meroterpenoid of cyclic triterpenyl-γ-pyrone. A literature survey showed that structurally related prenylated α- and/or γ-pyrones are found from diverse organisms,[48-52] such as sponges, fungi and plants, and have also been synthetically prepared.[53] However, the cyclization pattern of the prenyl portion of **1** significantly differed from the other known meroterpenoids. As depicted in Scheme 1, using pyripyrone E whose biosynthesis has been proven experimentally as an example,[54] the removal of the pyrophosphate group generally induced the attack of pyrone moiety at the terminal isoprene

unit. Then sequential epoxidation, ring opening and cyclization occurred in the carbon framework of pyrone-containing meroterpenoids. However, the unique framework of **1** required an alternative biosynthetic pathway because the vinyl methyl group (C-11) of the third isoprene unit was directly linked to the pyrone moiety in **1** instead of the terminal methylene carbon (C-12) of the prenyl portion as seen in the ordinary linkage. A plausible mechanism is, after the preliminary removal of pyrophosphate and the formation of a linear sesquiterpene alcohol, epoxidation and cyclization may occur prior to the attachment of the pyrone moiety that may be driven by the cation generated by a cyclization of the prenyl moiety. To the best of our knowledge, this is an unprecedented mode of linkage among the pyrone-containing meroterpenoids.

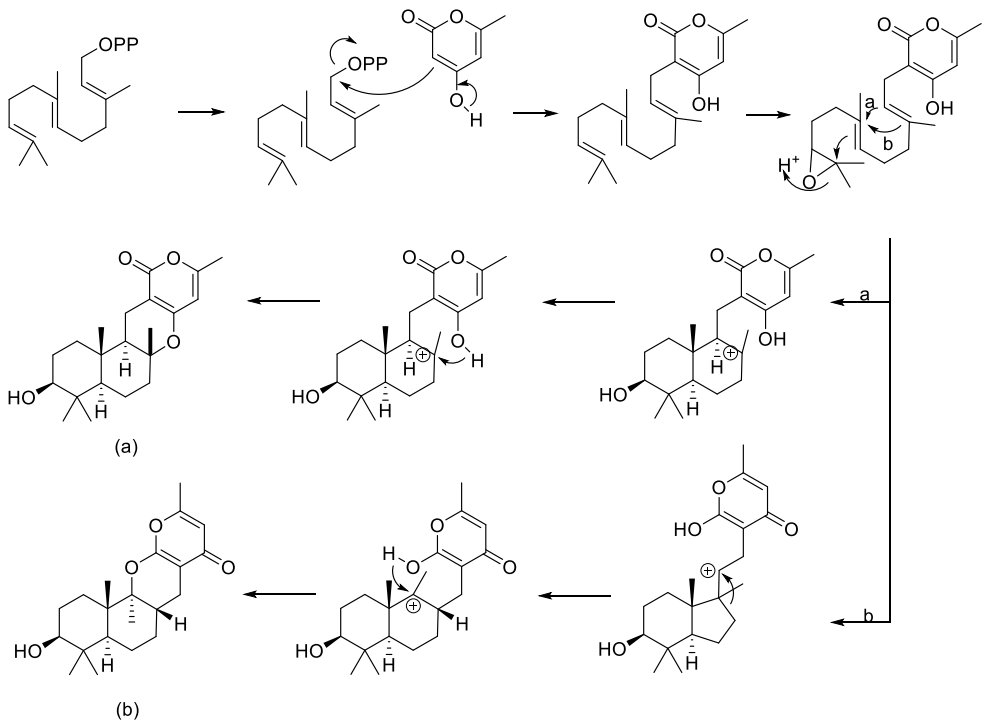

Schem 1. Comparison of bioynthetic pathyways of meroterpenoids.

The molecular formula of penicillipyrone B (**2**) was deduced to be $C_{21}H_{28}O_4$ by HRFABMS analysis. The NMR data of this compound was very similar to that of **1**, with the most noticeable difference being the replacement of the C-3 oxymethine, which had signals at a δ_C value of 78.6 and a δ_H value of 3.22 with a carbonyl carbon having a signal at a δ_C value of 215.5. This interpretation was readily confirmed by a combination of 2-D NMR experiments, in which all of the proton-proton and carbon-proton correlations obtained supported the placement of a ketone group at C-3. NOESY data

showed the same cross-peaks among the ring juncture protons as **1**, allowing the assignment of the 5*R*, 8*S*, 9*S*, and 10*S* configurations, which were also supported by the comparison of the optical rotations ($[\alpha]_D^{25}$ = +51.4 and +25.7 for **1** and **2**, respectively). Thus penicillipyrone B (**2**) was structurally elucidated to be a 3-keto derivative of **1**.

In our bioactivity measurements, compounds **1** and **2** exhibited weak cytotoxicities toward the K562 (LC_{50} = 27.84 and 50.16 μM for **1** and **2**, respectively, doxorubicin was uesd as a positive control with a LC_{50} = 0.99 μM) and A549 (LC_{50} = 15.43, 17.25 and 1.18 μM for **1**, **2** and doxorubicin, respectively) cell lines. However, compounds **1** and **2** were inactive (MIC > 100 μg/mL) against various Gram-positive and Gram-negative bacteria and pathogenic fungi.

Compound **2** also exhibited a significant induction of QR in a dosage-dependent manner in murine Hepa 1c1c7 cells over the concentration range of 5–40 μM. At a concentration of 40 μM, the induction was 1.9-times that of blank control (0.1% DMSO), which was comparable with that of *β*-NF (2 μM), a positive control (Figure 10). Contrastingly, compound **1**, which possessed the 3-hydroxy group, failed to show a noticeable induction in the given concentration, implying that the ketone moiety at C-3 of **2** plays a

crucial role in its QR inducing activity. QR, a representative detoxification enzyme, is known to play an important anticancer role through the reduction of electrophilic quinones.[55] Therefore, the significant induction of penicillipyrone B (**2**) with significant induction of QR may be suggestive of a potential role in cancer prevention.

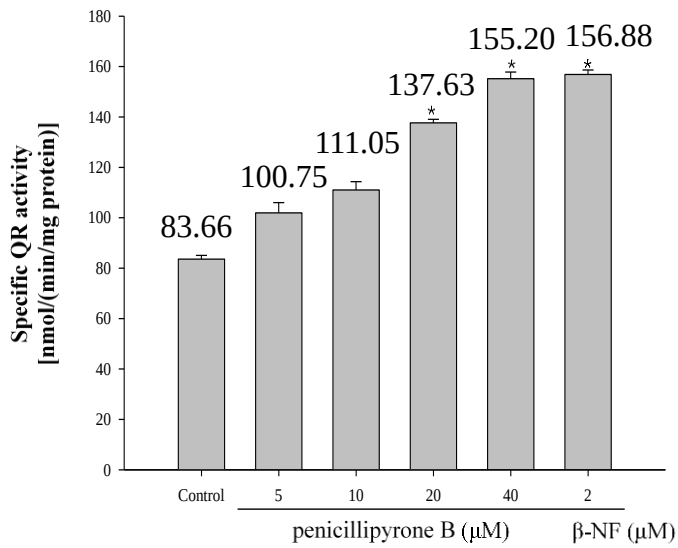

Figure 10. Effects of penicillipyrone B (**2**) on induction of quinone reductase in murine Hepa 1c1c7 cells. Cells were grown for 24 h and then exposed to penicillipyrone B (**2**) for 24 h. Quinone reductase activity were measured in cell lysates by reduction of a tetrazolium dye and expressed a nmol/min/mg protein. Values represent the mean ± SD of four determinanats. Asterisks (*)

denote significant differences between the penicillipyrone B (**2**) treated group and the control group ($P < 0.05$).

2-3. Experimental section

General Experimental Procedures. Optical rotations were measured on a JASCO P-1020 polarimeter using a 1 cm cell. IR spectra were recorded on a Jasco 4200 FT-IR spectrometer, using a ZnSe cell. UV spectra were acquired with a Hitachi U-3010 spectrophotometer. NMR spectra were recorded on Bruker Avance 500 spectrometer. Proton and carbon NMR spectra were measured in $CDCl_3$ solution at 500 and 125 MHz, respectively. High-resolution fast-atom bombardment mass spectrometry (HRFABMS) data were acquired using Jeol JMS 700 mass spectrometer with *meta*-nitrobenzyl alcohol (NBA) as a matrix in the Korea Basic Science Institute (Daegu, Korea). HPLC were performed on a Spectrasystem p2000 equipped with a refractive index detector (Spectrasystem RI-150). All solvents used were spectroscopic grade or distilled from glass prior to use.

Isolation and Identification of Fungal Strain. The fungal strain *Penicillium* sp. (strain number F446) was isolated from marine sediments at the depth of –25 m collected from Geomun-do (Island), Korea, in October 2011. F446 was identified using standard molecular biological protocols by

DNA amplification and sequencing of the ITS region. Genomic DNA extraction was performed using Intron's i-genomic BYF DNA Extraction Mini Kit according to the manufacturer's protocol. The nucleotide sequence of F446 has been deposited in the GenBank database under the accession number JF901804. The 18S rDNA sequence of this strain showed 99% identity with *Penicillium citrinum* a2s6-6 (GenBank accession number KF146984).

Fermentation and Isolation. The isolated strain was cultured on marine broth agar plate (37.4 g Difco marine broth 2216, 20.0 g glycerol, 16.0 g agar in 1 L artificial seawater) for 7 days. Agar plugs (1 cm × 1 cm, 10 pieces for 1 L) were inoculated into 2.8 L Glass Fernbach Flask, 24 flasks in all, containing MB media (37.4 g Difco marine broth 2216 and 20.0 g glycerol in 1 L artificial seawater). The fermentation was conducted at 28 ^{o}C on a rotary shaker at 150 rpm for 3 weeks. The mycelia and culture broth were separated by filtration, and the broth was extracted with EtOAc. The solvent was evaporated to obtain an organic extract (1.4 g). The extract was separated by C_{18} reversed-phase vacuum flash chromatography using a sequential mixture of MeOH and H_2O as eluents (seven fractions in gradient, H_2O–MeOH, from 60:40 to 0:100), acetone, and finally EtOAc. On the basis of the results of ^{1}H-NMR analysis, the fractions eluted with H_2O–MeOH (30:70)

(96 mg) was chosen for separation. The fraction eluted with H_2O–MeOH (30:70) was separated by semipreparative reversed-phase HPLC (H_2O–MeCN, 70:30, 1.0 mL/min) to afford compound **1** (8.9 mg), compound **2** (4.5 mg).

Penicillipyrone A (**1**): pale yellow amorphous solid, $[\alpha]_D^{25}$ +51.4 (*c* 0.5, acetone); UV (MeOH) λ_{max} (log ε) 210 (3.83), 243 (3.83), 257 (3.85) nm; IR (ZnSe) ν_{max} 3394 (br), 2942, 2874, 1665, 1572, 1449 cm^{-1}; HRFABMS, *m/z* 347.2224 $[M+H]^+$ (Calcd for $C_{21}H_{31}O_4$, 347.2222).

Penicillipyrone B (**2**): pale yellow amorphous solid, $[\alpha]_D^{25}$ +25.7 (*c* 0.5, acetone); UV (MeOH) λ_{max} (log ε) 210 (3.80), 243 (3.81), 256 (3.82) nm; IR (ZnSe) ν_{max} 2944, 2876, 1666, 1579, 1431 cm^{-1}; HRFABMS, *m/z* 345.2064 $[M+H]^+$ (Calcd for $C_{21}H_{29}O_4$, 345.2066).

MTPA Esterifications of 1. To a solution of **1** (2.0 mg) in 1.0 mL of pyridine (distilled over CaH_2), were added 10 μL of triethylamine and 20 μL of (-)-(*R*)-MTPA chloride. The mixture was stirred under N_2 for 1 h at room temperature. After the consumption of the starting material was confirmed by thin-layer chromatography, the solvent was removed under vacuum and the residue was purified by analytical HPLC (YMC-ODS column, 4.6 × 250 mm;

H_2O–MeOH, 15:85, 1.0 mL/min) to afford the (*S*)-MTPA ester of **1**, **1S**. The corresponding (*R*)-MTPA ester of **1**, **1R** was also obtained from the same esterification reaction with (+)-(*S*)-MTPA chloride. ^{1}H NMR ($CDCl_3$, 600 MHz) of **1S**: δ_H 7.533–7.417 (5 H, m, aromatic), 6.143 (1 H, s, H-4'), 4.708 (1 H, dd, *J* = 11.2, 4.4 Hz, H-3), 3.521 (3 H, s, OMe), 2.567 (1 H, dd, *J* = 15.9, 4.7 Hz, H-11), 2.234 (3 H, s, H-6'), 2.031 (1 H, dddd, *J* = 11.7, 9.0, 4.7, 4.7 Hz, H-8), 1.971 (1 H, dd, *J* = 15.9, 11.7 Hz, H-11), 1.910 (1 H, m, H-7), 1.885 (1 H, m, H-2), 1.783 (1 H, m, H-1), 1.730 (1 H, m, H-1), 1.711 (1 H, m, H-2), 1.662 (1 H, m, H-6), 1.490 (1 H, dq, *J* = 12.9, 4.7 Hz, H-6), 1.347 (1 H, dd, *J* = 12.9, 3.2 Hz, H-5), 1.260 (3 H, s, H-12), 1.181 (1 H, m, H-7), 1.103 (3 H, s, H-13), 0.921 (3 H, s, H-15), 0.871 (3 H, s, H-14); ESI-MS *m/z* 563.2, $[M+H]^+$ (calcd for $C_{31}H_{38}F_3O_6$, 563.3). ^{1}H NMR ($CDCl_3$, 600 MHz) of **1R**: δ_H 7.554–7.410 (5 H, m, aromatic), 6.113 (1 H, s, H-4'), 4.737 (1 H, dd, *J* = 11.0, 4.4 Hz, H-3), 3.576 (3 H, s, OMe), 2.562 (1 H, dd, *J* = 15.9, 4.6 Hz, H-11), 2.230 (3 H, s, H-6'), 2.030 (1 H, dddd, *J* = 11.7, 9.0, 4.6, 4.6 Hz, H-8), 1.965 (1 H, dd, *J* = 15.9, 11.7 Hz, H-11), 1.938 (1 H, m, H-2), 1.905 (1 H, m, H-7), 1.835 (1 H, m, H-2), 1.805 (1 H, m, H-1), 1.788 (1 H, m, H-1), 1.656 (1 H, m, H-6), 1.484 (1 H, dq, *J* = 12.9, 4.7 Hz, H-6), 1.343 (1 H, dd, *J* = 12.9, 3.2 Hz, H-5), 1.259 (3 H, s, H-12), 1.175 (1 H, m, H-7), 1.128 (3 H, s, H-13), 0.866 (3 H, s, H-15), 0.840 (3 H, s, H-14); ESI-MS *m/z* 563.2, $[M+H]^+$ (calcd

for $C_{31}H_{38}F_3O_6$, 563.3).

Biological Assays. Quinone reductase (QR) activity in Hepa 1c1c7 murine hepatoma cells was performed in accordance with literature protocols.[42] Anti-microbial and cytotoxicities assays were also carried out in accordance with primary literatures.[56, 57]

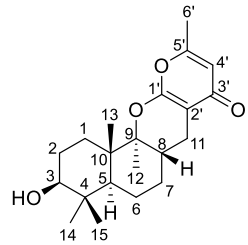

Table 1. ^{13}C and ^{1}H NMR assignment for compound **1** in $CDCl_3$

Position	δ_C	δ_H
1	29.7, CH_2	1.67, m; 1.75, m
2	27.1, CH_2	1.73, m; 1.66, m
3	78.6, CH	3.22, dd (10.0, 3.0)
4	39.1, C	
5	47.6, CH	1.23, dd (12.9, 3.2)
6	20.9, CH_2	1.64, m; 1.47, m
7	28.9, CH_2	1.14, dq (12.9, 4.7); 1.88, m
8	33.5, CH	2.01, dddd (11.7, 9.0, 4.7, 4.7)
9	89.5, C	
10	41.8, C	
11	22.0, CH_2	1.93, dd (15.9, 11.7); 2.53, dd (15.9, 4.7)
12	13.1, CH_3	1.22, s
13	14.5, CH_3	1.08, s
14	28.4, CH_3	1.00, s
15	15.3, CH_3	0.84, s
1’	163.3, C	
2’	98.0, C	
3’	180.2, C	
4’	111.8, CH	5.96, brs
5’	160.6, C	
6’	19.2, CH_3	2.19, brs

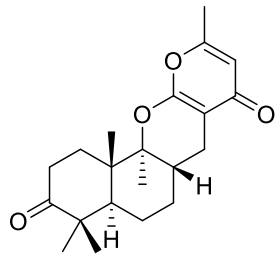

Table 2. ^{13}C and ^{1}H NMR assignment for compound **2** in $CDCl_3$

Position	δ_C	δ_H
1	30.8, CH_2	2.02, m; 2.03, m
2	34.5, CH_2	2.42, dt (15.6, 4.5); 2.70, ddd (15.6, 12.1, 7.3)
3	215.5, C	
4	47.8, C	
5	48.8, CH	1.70, dd (10.8, 5.1)
6	22.1, CH_2	1.62, m; 1.61, m
7	28.7, CH_2	1.21, dq (12.9, 4.4); 1.94, m
8	28.7, CH	2.10, dddd (12.0, 9.3, 5.2, 4.4)
9	88.8, C	
10	41.5, C	
11	22.0, CH_2	1.95, dd (16.4, 12.0); 2.58, dd (16.4, 5.2)
12	13.2, CH_3	1.27, s
13	14.1, CH_3	1.29, s
14	26.2, CH_3	1.11, s
15	21.8, CH_3	1.09, s
1’	163.0, C	
2’	98.1, C	
3’	180.1, C	
4’	111.9, CH	5.98, brs
5’	160.7, C	
6’	19.3, CH_3	2.21, brs

III. Alkaloidal Metabolites from a Marine-Derived *Aspergillus* sp. Fungus

Fumiquinazoline S (**5**), a new quinazoline-containing alkaloid, and the known fumiquinazolines F (**10**) and L (**11**) of the same structural class were isolated from the solid-substrate culture of an *Aspergillus* sp. fungus collected from marine-submerged wood. In addition, isochaetominines A-C (**6**-**8**) and 14-*epi*-isochaetominine C (**9**), new alkaloids possessing an unusual amino acid-based tetracyclic core framework related to the fumiquinazolines, and together with nidurufin (**12**), versiconol (**13**), sterigmatocystin (**14**), 7-deoxysterigmatocystin (**15**), and isobenzofuranone (**16**) were isolated from the same fungal strain. The structures of these compounds were determined by combined spectroscopic methods, and the absolute configurations were assigned by NOESY, ROESY and advanced Marfey's analyses along with biogenetic considerations. The new compounds exhibited weak inhibition against Na^+/K^+-ATPase.

3-1. Introduction

Microorganisms in marine environments have been widely recognized as emerging sources of biologically active and structurally unique secondary metabolites.[2-6] Dominated by three major phylogenetic groups,

actinomycete and non-actinomycete bacteria and fungi, the novel natural products from marine microorganisms have shown a noticeable increase since 1997.[3] Marine fungi alone have produced more than 400 novel compounds, of which several have exhibited potent and diverse bioactivities.[7,8]

In our search for bioactive metabolites from the fungi of marine environments, we have recently reported novel compounds, such as acremostrictin, chrysoarticulins, herqueiazoles, herqueidiketal, and penicillipyrones, possessing unusual carbon frameworks and/or functionalities, thus contributing to the chemical library from marine-derived fungi.[36-38,58] Several of these compounds have exhibited moderate to significant inhibition of sortase A (chrysoarticulin C and herqueidiketal),[37,38] significant induction of quinone reductase (penicillipyrone B),[58] and moderate antioxidant activity (acremostrictin).[36] During our search, a strain of *Aspergillus* was collected from marine-submerged decaying wood from Korea, with an organic extract that showed moderate cytotoxicity (IC_{50} 170 μg/mL) against the K562 human leukemia cell line. Furthermore, the LC-ESIMS profile of the extract revealed the presence of diverse secondary metabolites, which prompted our detailed investigation of the extract metabolites.

A solid-substrate culture of the strain followed by an extraction and chromatographic separation led to the isolation of several new alkaloids. In this study, we report the structure determinations of fumiquinazoline S (**5**), isochaetominines A-C (**6**-**8**) and 14-*epi*-isochaetominine C (**9**), and the known congeners, fumiquinazolines F (**10**) and L (**11**) based on combined spectroscopic and chemical analyses (Figure 11). Fumiquinazoline S is a new member of the fumiquinazoline class of alkaloids, which has been reported in a number of marine-derived *Aspergillus*, *Acremonium* and *Scopulariopsis* fungal strains. Fumiquinazolines A-P have been reported in the literature. However, fumiquinazolines K and L were doubly designated.[59-61] Accordingly, our new compound was designated fumiquinazoline S instead of either Q or R.[59-66] The isochaetominines are structurally related to the recently reported chaetominine from the terrestrial endophytic fungus *Chaetomium* sp.[67] Our isolation of the fumiquinazolines and the isochaetominines from a common fungal strain provides insight into the biogenetic relationships of these quinazoline-containing natural products. Although these compounds were not significantly active against the K562 and A549 cell lines, several of them showed weak inhibition against Na^+/K^+-ATPase.

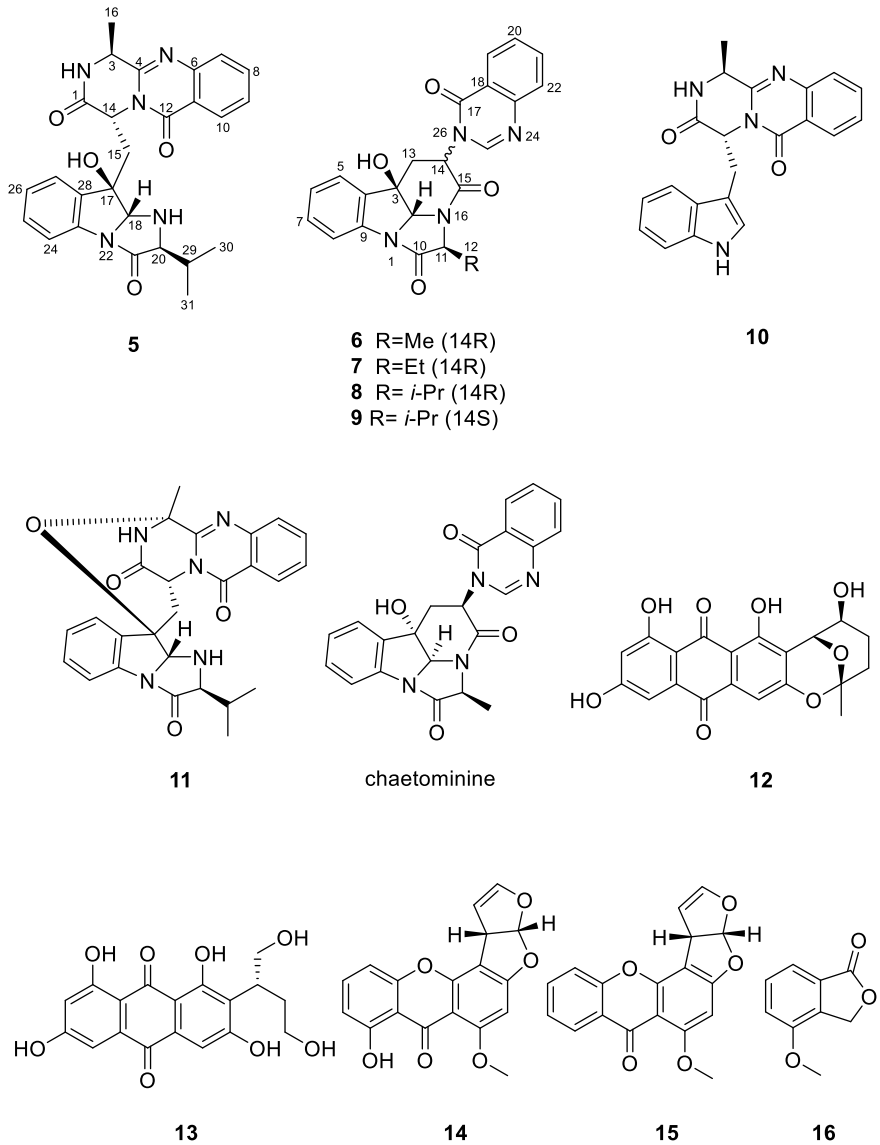

Figure 11. The chemical structrues of compounds **5-16**.

3-2. Results and discussion

The molecular formula of fumiquinazoline S (**5**) was deduced as

$C_{26}H_{27}N_5O_4$ by the HRFABMS analysis. The spectroscopic data of this compound revealed the characteristic features of fumiquinazolines. That is, the presence of 12 carbon signals in the aromatic region (δ_C 150-110) in the ^{13}C NMR data, along with the corresponding proton signals (δ_H 8.2-7.0) in the ^{1}H NMR data and aromatic E bands in the UV spectrum, was indicative of two benzene rings in **5** (Table 3). Four carbon signals at δ_C 172.1, 168.9, 160.2, and 153.3 in the ^{13}C NMR data were thought to represent either carbonyl or imine carbons, which was implied by the molecular formula and the strong absorption bands at 1730 and 1681 cm^{-1} in the IR spectrum.

The gross structure of compound **5** was determined by a combination of 2D NMR analyses as well as comparison with the congeners **10** and **11**. First, the COSY data showed a linear spin system of four aromatic protons resonating at δ_H 8.12, 7.82, 7.66, and 7.53, thus revealing the presence of a 1,2-disubstituted benzene whose carbons were also assigned by the HSQC and HMBC data. The attachment of a carbonyl carbon at δ_C 160.2 to the ring quaternary carbon at δ_C 120.0 was secured by its HMBC correlation with a ring proton at δ_H 8.12, designating a benzamide for this portion (C-6~C-12) (Figure 12). The COSY and HSQC data also defined two spin systems consisting of a methine (δ_C 51.8, δ_H 5.58; C-14) and a methylene (δ_C 35.4, δ_H 2.58 and 1.82; C-15), and a methyl (δ_C 16.6, δ_H 1.58; C-16) and a methine

group (δ_C 48.6, δ_H 4.95; C-3), respectively. The HMBC correlations of these protons and an exchangeable one at δ_H 8.61 (2-NH) with the neighboring carbons accomplished a 4-oxo-quinazoline-δ-lactam system found in several fumiquinazolines.[61,63]

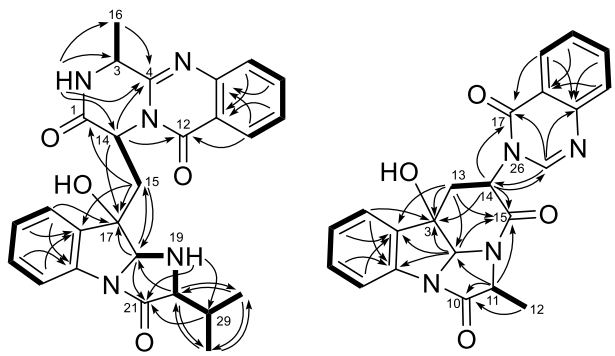

Figure 12. The COSY (bold line) and selected HMBC (arrows) correlations of compounds **5** and **6**.

The combined 2D NMR data also revealed the presence of another 1,2-disubstituted benzene (C-23~C-28) in **5** (Table 3). The extension of this ring to a 3-alkylindole-3-ol moiety as well as its connection to the upper portion of the molecule via a methylene (C-15) was accomplished by the HMBC correlations of an oxygenated carbon at δ_C 80.1 (C-17) and a methine carbon at δ_C 88.2 (C-18) with neighboring protons and carbons (Figure 12). The remaining portion of the molecule was also found to have a valine (Val)-

derived residue by the COSY data which showed a long spin system consisting of protons at δ_H 5.26 (H-18), 3.51 (19-NH), 3.54 (H-20), 1.98 (H-29), 0.96 (H-30), and 0.93 (H-31). The HMBC correlations of several of these protons with a carbonyl carbon at δ_C 172.1 (C-21) allowed the construction of an imidazolidinone moiety (Figure 12). Thus, the planar structure of fumiquinazoline S (**5**) was determined as a new derivative of the fumiquinazoline class possessing a Val-derived residue.

A structural comparison of the congeners revealed a biogenetic relationship between **5** and **11,** whose absolute configurations were assigned by X-ray crystallographic analysis.[61] Although several biosynthetic postulations would be plausible for the structural conversion between these compounds, the configurations at C-14, C-17, C-18, and C-20 are likely to be the same in these two compounds, whereas the configuration at the reaction center C-3 in **5** may be either intact or reversed, depending on the reaction pathway. This hypothesis was supported by the ROESY data for **5** in which a conspicuous cross-peak was found at H-18/H-29 (Figure 13). Although the desired cross-peak at 17-OH/H-18 was not found, it was compensated by another cross-peak at H-15 (δ_H 2.58)/H-20 because a DFT model calculation (Supporting Information) revealed a spatial proximity between these protons only by the β-orientation of the 17-OH proton at the tetracyclic frame.

Similarly, H-14 was placed at the β-orientation based on the cross-peaks at H-3/H-15 (δ_H 2.58), H-3/H-15 (δ_H 1.82), and H-14/H-27.

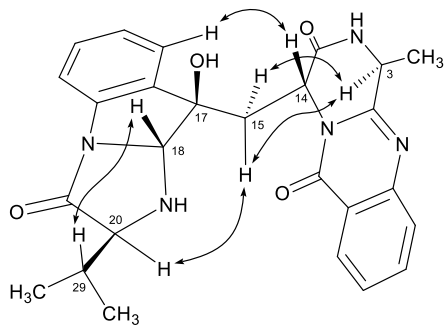

Figure 13. Selected ROESY correlations of compound **5**.

The significant ROESY correlations of H-3 with both of the H-15 methylene protons coupled with the lack of a ROESY correlation of H-16 with the latter protons assigned an α-orientation for the H-3 to the quinazoline plane, which was supported by the ^{13}C NMR data. A literature study showed that the C-3 asymmetric center significantly influences the chemical shifts of the C-16 methyl carbon (*cis* δ_C ~24.9, *trans* δ_C ~16.8), possibly due to the spatial crowding of the substituents at C-14 (*cis* δ_C ~52.7 and *trans* δ_C ~49.2).[62-64] The chemical shifts of C-16 and C-14 at δ_C 16.9 and 49.1 in $CDCl_3$, respectively, in the ^{13}C NMR data fit well with the α-orientation (*trans* orientation of C-15 with C-16) of H-3 (Supporting Information). Thus, the relative configurations of the stereogenic carbon centers of **5** were

unambiguously assigned throughout the molecule. Compound **5** has a Val-derived unit at C-21. The absolute configuration of this unit was determined to be L by advanced Marfey's analysis (Experimental Section).[68] Therefore, the overall absolute configuration of **5** was assigned as 3*S*, 14*R*, 17*R*, 18*R*, and 20*S*.

The molecular formula of isochaetominine A (**6**) was deduced as $C_{22}H_{18}N_4O_4$ by the HRFABMS analysis. The gross NMR features of this compound were highly reminiscent of **5**, indicating the presence of a quinazoline and a 3-alkylindolin-3-ol as substructures. The replacement of the Val-derived residue with an alanine (Ala)-derived one was also found by the NMR data (δ_C 174.4, 59.7, and 13.8, δ_H 4.58 and 1.57). However, a detailed examination of the ^{13}C and ^{1}H NMR data revealed that the signals of the several carbons and protons, particularly those near the δ-lactam C-14, noticeably differ from those of **5** in the chemical shifts and the multiplicities, which prompted an extensive interpretation of the full spectroscopic data (Table 4).

First, a combination of the COSY, HSQC and HMBC data secured the presence of a 1,2-disubstituted benzene in **6** and assigned all of the carbons and protons in this moiety. A three-bond HMBC correlation with an

aromatic proton at δ_H 8.14 (H-19) placed a carbonyl carbon at δ_C 159.9 as a substituent (C-17) (Figure 12). Interestingly, this carbon showed an additional correlation with an isolated singlet proton at δ_H 8.25, which correlated with the aromatic carbon at δ_C 127.2 (C-22). The downfield chemical shift of this proton-bearing carbon at δ_C 146.7 defined it as an amidine methine carbon (C-25), corresponding to the C-4 carbon in **5**. Therefore, unlike the additional 6-membered lactam system present in **5** and other fumiquinazoline metabolites, the 4-oxo-quinazoline moiety of **6** was directly attached to the remaining portion of the compound through a single bond at N-26, which is discussed later.

A combination of 2D NMR data revealed the presence of another 1,2-disubstituted benzene moiety. Despite the noticeable shifts of the protons and the carbons in the NMR data, the extension to a 3-alkylindolin-3-ol, identical to **5**, was accomplished by the HMBC analysis (H-2/C-3, H-2/C-4, H-2/C-9, and H-5/C-3, Figure 12). The connection of the Ala-derived residue to the indolinol moiety through the construction of an imidazolidinone ring was also accomplished long-range correlations at H-11/C-2 and H-11/C-10 and H-11/C-15. Thus, **6** was found to possess the same indolinol-imidazolidinone tricyclic substructure as found in **5**.

Compound **6** possessed a three-carbon moiety (C-13, C-14 and C-15) connecting the indolinol and quinazoline moieties. The ^{13}C NMR data for **6** also showed signals of three carbons at δ_C 164.2 (C), 55.6 (CH) and 34.7 (CH_2) having corresponding multiplicities to those of **5**. Although the chemical shifts of these carbons and their attached protons at δ_H 4.88, 2.92 and 2.65 in the ^1H NMR data were significantly shifted compared with those of **5**, the COSY and HMBC data showed the same linear assembly of these groups in **6**. In addition, the HMBC data showed the key correlations at H-2/C-15, H-13/C-2, H-13/C-3, H-13/C-4, and H-14/C-3, constructing a δ-lactam moiety consisting of indolinol-imidazolidinone and three carbons at C-13, C-14 and C-15 (Figure 12). As previously mentioned, the connection between this lactam and 4-oxo-quinazoline via a C-N single bond was also accomplished by the long-range correlations at H-14/C-17, H-14/C-25 and H-25/C-14 in the HMBC data. Thus, the planar structure of isochaetominine A (**6**) was defined as a 4-oxo-quinazoline-containing alkaloid, identical to chaetominine.[67]

A comparison of the main framework of this compound with that of fumiquinazolines **5**, **10** and **11** indicated that **6** and the fumiquinazolines are biogenetically related, but that the exact relationship is unclear at this time. A literature study revealed that the hexacyclic framework of **6** is unusual; the only previous example is the recently found chaetominine from the terrestrial

endophytic *Chaetomium* sp. fungus whose planar structure is identical to **6**. However, the NMR chemical shifts of several carbons and protons of these compounds significantly differ from each other, suggesting a diastereomeric relationship between them.

Compound **6** possessed four asymmetric carbon centers at C-2, C-3, C-11, and C-14 with configurations assigned by NOESY (Figure 14) and the chemical analyses. The H-2 methine proton showed strong cross-peaks with the 3-OH and H-12 in the NOESY data, placing all of these protons on the same face of the tetracyclic plane. In contrast, the H-14 methine proton did not exhibit cross-peaks with any of these protons but showed strong cross-peaks with both of the neighboring H-13 methylenes, matching the *gauche* conformation based on the proton coupling constants ($J_{11,12}$ = 7.0 and 5.1 Hz) on the pseudo boat form of the lactam ring deduced by DFT model study (Supporting Information). Therefore, H-14 must be oriented on the opposite face of the tetracyclic plane, which coincided well with the cross-peak at H-2/H-25. For compound **6**, the absolute configuration of the Ala-derived residue at C-10 was determined as L by advanced Marfey's analysis (Supporting Information). These results assigned the 2*R*, 3*R*, 11*S*, and 14*R* absolute configuration, which was distinguished from the 2*S*, 3*S*, 11*S*, and 14*R* configuration of chaetominine based on X-ray crystallographic

analysis.[67] Therefore, compound **6** is the a *bis*-epimer of chaetominine at C-2 and C-3.

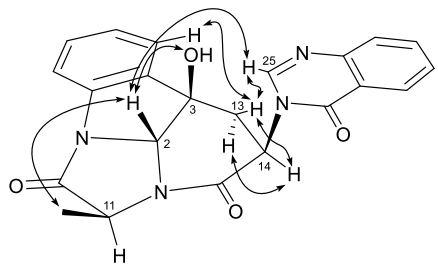

6

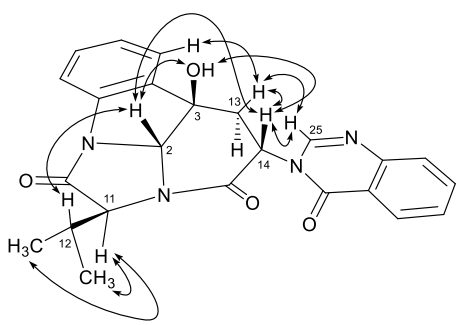

9

Figure 14. Selected NOESY and ROESY correlations of compounds **6** and **9**.

Isochaetominine B (**7**) was isolated as a pale yellow solid, which was determined as $C_{23}H_{20}N_4O_4$ by HRFABMS analysis. The NMR data for this compound were similar to those of **6,** and all of the key structural features were intact in **7**. In the ^{13}C NMR data, the only significant difference was the

addition of a methylene carbon at δ_C 21.7 (Table 5). A corresponding difference was found in the ^{1}H NMR data in which the signals of the new methylene protons were observed at δ_H 2.06 and 2.00. In addition, the multiplicity of a doublet methyl proton was changed to a triplet (J = 7.3 Hz) (Table 5). These spectroscopic differences were readily accommodated by the replacement of the C-12 methyl with an ethyl group, which was confirmed by combined 2D NMR methods. Therefore, the Ala-derived residue must be replaced with a 2-amino-butanoic acid-derived residue. The ROESY data showed the same cross-peaks as **7**, which along with the L configuration for the newly appeared 2-amino-butanoic acid residue by advanced Marfey's analysis, assigned the same absolute configuration as **6**. Thus, the structure of isochaetominine B (**7**) was defined as a new alkaloid possessing an unusual L-2-amino-butanoic acid-derived lactam moiety.

The molecular formula of isochaetominine C (**8**) was deduced as $C_{24}H_{22}N_4O_4$ by HRFABMS analysis. The NMR data for this compound were similar to those of **7,** with the replacement of signals of the C-12 group to an isopropyl group (δ_C 28.2, 20.2 and 18.7, δ_H 2.44, 1.15 and 1.12) (Table 6). This replacement of an Ala-derived residue in **6** with a valine (Val)-derived one was confirmed by the combined 2D NMR data. The NOESY cross-peaks at H-2/3-OH, H-2/H-12 and H-13/H-14 along with the L configuration of the

newly appeared Val-derived residue by advanced Marfey's analysis assigned the same 2*R*, 3*R*, 11*S*, and 14*R* configuration as **6** and **7**. Thus, the structure of isochaetominine C (**8**) was determined as a new alkaloid, possessing an L-Val-derived lactam moiety.

Finally, the molecular formula of 14-*epi*-isochaetominine C (**9**) was deduced as $C_{24}H_{22}N_4O_4$, which is identical to **8**, by HRFABMS analysis. Despite the noticeable shifts of several carbons, the ^{13}C NMR data for this compound showed the same signal distribution and multiplicities as **8** (Table 7). The same trend was also found in the ^{1}H NMR data in which most of the signals showed similar chemical shifts and coupling constants as **9** (Table 7). Accordingly, **8** and **9** must be diastereomeric to each other, which was supported by the combined COSY, HSQC and HMBC analyses in which the identical proton-proton and carbon-proton correlations were found between these compounds. The ROESY data showed cross-peaks at H-2/3-OH and H-2/H-12, confirming the same *syn* orientations for these protons as for the other isochaetominines (Figure 14). However, additional cross-peaks were found at H-2/H-14 and 3-OH/H-14, adding the H-14 methine proton in a *syn* orientation to the other key protons. Furthermore, the 4-oxo-quinazoline moiety was spatially close to the main framework by the cross-peaks at H-13/H-25 and H-14/H-25. Because the L-configuration was found for the Val-

derived moiety (C-10, C-11, C-12, C-27, C-28) by advanced Marfey's analysis, the overall ROESY data confidently assigned the 2*R*, 3*R*, 11*S*, and 14*S* configuration for **9**, reversed at C-14 from **6**-**8**. This interpretation coincides well with the ^{13}C and ^{1}H NMR data in which the conspicuous differences were concentrated at the signals of the carbons and the protons near C-14 (Table 7). This conclusion was further supported by the opposite sign of the specific rotation of **9** compared with the other isochaetominines. Thus, the structure of **9** was determined as the 14-*epi*-derivative of isochaetominine C (**8**).

Certain fumiquinazoline metabolites have been reported to exhibit weak activities against cancer cell lines,[62,63] proliferation of cancer cell lines,[66] and/or fungal strains,[64] whereas chaetominine exhibited cytotoxicity against K562 leukemia and SW1116 colon cancer cell lines comparable to 5-fluorouracil.[67] In our measurement of cytotoxicity, however, **5**-**11** were inactive (**5**-**9**: IC_{50} > 13-50 μM, **10** and **11**: IC_{50} > 100 μM) against the K562 and A549 cell lines.[39] In the antimicrobial activity tests against selected strains of Gram-positive and Gram-negative bacteria and pathogenic fungi, only compound **10** displayed weak inhibition (MIC 50 μM) against *Bacillus subtilis*.[57] These alkaloids also exhibited a weak inhibition (IC_{50} were 34, 78, 20, 38, 57, 17, and 20 μM for **5**-**11**, respectively) against Na^+/K^+-ATPase.[41]

None of these compounds were active against the enzymes sortase A or isocitrate lyase.

In conclusion, five new alkaloidal metabolites, fumiquinazoline S (**5**), isochaetominines A-C (**6**-**8**) and 14-*epi*-isochaetominine C (**9**), along with the known fumiquinazolines F (**10**) and L (**11**), were isolated from a marine-derived *Aspergillus* sp. fungus. Compound **5** is a new member of the fumiquinazoline alkaloids, whereas **6**-**9** had a structural similarity only with chaetominine, which has been recently isolated from a terrestrial endophytic fungus. Furthermore, the differences in the relative and absolute configurations among these compounds provide additional structural novelty to the isochaetomines. These compounds exhibited weak inhibition against Na^+/K^+-ATPase.

3-3. Experimental section

General Experimental Procedures. The optical rotations were measured on a JASCO P-1020 polarimeter using a 1 cm cell. The UV spectra were acquired with a Hitachi U-3010 spectrophotometer. The CD spectra were obtained on a Chirascan-plus CD spectrometer. The IR spectra were recorded on a JASCO 4200 FT-IR spectrometer, using a ZnSe cell. The NMR spectra were recorded on Bruker Avance 400, 500 and 600 spectrometers. The

proton and carbon NMR spectra were measured in a DMSO-d_6 solution at 400 and 100 MHz (**5**), 600 and 150 MHz (**6**), and 500 and 125 MHz (**7**-**9**), respectively. HRFABMS data were acquired using a Jeol JMS 700 mass spectrometer with *meta*-nitrobenzyl alcohol (NBA) as the matrix at the Korea Basic Science Institute (Daegu, Korea). The HPLC analyses were performed on a Spectrasystem p2000 equipped with a refractive index detector (Spectrasystem RI-150). All of the solvents used were spectroscopic grade or distilled from glass prior to use.

Isolation and Identification of the Fungal Strain. The fungal strain *Aspergillus* sp. (strain number F452) was isolated from submerged decaying wood off of the shore of Jeju Island, Korea, in November 2011. The strain was identified using standard molecular biological protocols by DNA amplification and sequencing of the ITS region. The genomic DNA extraction was performed using Intron's i-genomic BYF DNA Extraction Mini Kit according to the manufacturer's protocol. The nucleotide sequence of F452 has been deposited in the GenBank database under the accession number KF384188. The 18S rDNA sequence of this strain showed a 99% identity with *Aspergillus versicolor* Ppf48 (GenBank accession number GU586852).

Fermentation and Isolation. The isolated strain was cultivated on a

YPG agar plate (5 g yeast extract, 5 g peptone, 10 g glucose, and 16.0 g agar, 24.8 g artificial sea salt; Instant Ocean in 1 L distilled H_2O) for 7 days. The agar plugs (1 cm × 1 cm, 5 pieces each) were inoculated into 100 mL of the YPG media in a 250 mL Erlenmeyer flask for 7 days, then separately transferred to 2.8 L glass Fernbach flasks with rice media (1 g peptone, 1 g yeast extract, 200 g rice, 5 g artificial sea salt; Instant Ocean in 200 mL distilled H_2O in each flask, boiled in an autoclave for 20 min at 120 ℃; 8 flasks total). The fermentation in the rice media was conducted under static conditions for 6 weeks and then was extracted by EtOAc (1 L × 3). The solvent was evaporated to obtain a brown organic extract (5.8 g). The extract was separated by C_{18} reversed-phase vacuum flash chromatography using a sequential mixture of MeOH and H_2O as the eluents (seven fractions in the gradient, H_2O–MeOH, from 60:40 to 0:100), acetone, and, finally, EtOAc. Based on the results of the ^{1}H-NMR analysis, the fractions that eluted with H_2O–MeOH (40:60) (1010 mg) and (30:70) (1019 mg) were chosen for the separation. The fraction that eluted with H_2O–MeOH (40:60) was separated by semi-preparative reversed-phase HPLC (H_2O–MeOH, 50:50, 2.0 mL/min) to afford compounds **5** and **9**. The fraction that eluted with H_2O–MeOH (30:70) was separated by semi-preparative reversed-phase HPLC (H_2O–MeOH, 40:60, 2.0 mL/min) to yield, in order of elution, compounds **6**,

7, **8**, **10** and **11**. The purified metabolites were isolated in the following amounts: 6.4, 10.0, 9.4, 4.0, 8.9, 3.2, and 5.5 mg for **5-11**, respectively.

Fumiquinazoline S (**5**): pale yellow amorphous solid, $[\alpha]_D^{25}$ -105 (*c* 0.5, MeOH), -151 (*c* 0.25, $CHCl_3$); UV (MeOH) λ_{max} (log ε) 205 (4.37), 226 (4.14), 257 (3.80), 266 (3.62), 279 (3.36), 304 (3.05), 317 (2.93) nm; CD (MeOH) λ (Δε) 210 (+13.64), 233 (-12.88), 287 (-1.33) nm; IR (ZnSe) ν_{max} 3395, 1730, 1681, 1605 cm^{-1}; ^1H and ^{13}C NMR data, Table 3; HRFABMS *m/z* 474.2143 $[M+H]^+$ (calcd for $C_{26}H_{28}N_5O_4$, 474.2141).

Isochaetominine A (**6**): pale yellow amorphous solid, $[\alpha]_D^{25}$ -63 (*c* 0.5, MeOH); UV (MeOH) λ_{max} (log ε) 204 (4.60), 225 (4.44), 275(4.07), 305 (3.35) nm; CD (MeOH) λ (Δε) 204 (-15.10), 219 (+5.78), 247 (-3.24), 285 (+0.52), 304 (-1.57) nm; IR (ZnSe) ν_{max} 3364 (br), 1725, 1673, 1607 cm^{-1}; ^1H and ^{13}C NMR data, Table 4, respectively; HRFABMS *m/z* 403.1404 $[M+H]^+$ (calcd for $C_{22}H_{19}N_4O_4$, 403.1406).

Isochaetominine B (**7**): pale yellow amorphous solid, $[\alpha]_D^{25}$ -73 (*c* 0.6, MeOH); UV (MeOH) λ_{max} (log ε) 208 (4.60), 226 (4.45), 275 (4.09), 305 (3.34) nm; CD (MeOH) λ (Δε) 203 (-18.11), 218 (+8.17), 243 (-13.14), 286 (+0.75), 303 (-1.30) nm; IR (ZnSe) ν_{max} 3358 (br), 1726, 1678, 1608 cm^{-1}; ^1H

and ^{13}C NMR data, Table 5, respectively; HRFABMS *m/z* 417.1566 $[M+H]^+$ (calcd for $C_{23}H_{21}N_4O_4$, 417.1563).

Isochaetominine C (**8**): pale yellow amorphous solid, $[\alpha]_D^{25}$ -90 (*c* 0.6, MeOH); UV (MeOH) λ_{max} (log ε) 204 (4.58), 224 (4.42), 274 (4.03), 303 (3.33) nm; CD (MeOH) λ (Δε) 201 (-19.25), 217 (+9.06), 244 (-6.53), 274 (+0.29), 303 (-2.28) nm; IR (ZnSe) ν_{max} 3362 (br), 1723, 1676, 1610 cm^{-1}; ^1H and ^{13}C NMR data, Table 6, respectively; HRFABMS *m/z* 431.1721 $[M+H]^+$ (calcd for $C_{24}H_{23}N_4O_4$, 431.1719).

14-*epi*-Isochaetominine C (**9**): pale yellow amorphous solid, $[\alpha]_D^{25}$ +33 (*c* 0.7, MeOH); UV (MeOH) λ_{max} (log ε) 204 (4.58), 224 (4.42), 274 (4.03), 302 (3.30) nm; CD (MeOH) λ (Δε) 204 (-15.10), 219 (+5.78), 247 (-3.24), 285 (+0.52), 305 (+0.85) nm; IR (ZnSe) ν_{max} 3370 (br), 1726, 1677, 1609 cm^{-1}; ^1H and ^{13}C NMR data, Table 7, respectively; HRFABMS *m/z* 431.1720 $[M+H]^+$ (calcd for $C_{24}H_{23}N_4O_4$, 431.1719).

Advanced Marfey's Analysis of Compounds 5-9.[68] Compound **5** (0.4 mg) was dissolved in 0.5 mL of 6 N HCl and heated to 110 ℃ for 1 h. The solution was evaporated with distilled H_2O three times to remove the trace HCl under vacuum. The divided hydrolysate (0.2 mg each) was treated

with 100 μL of 1 N $NaHCO_3$ followed by 50 μL of 1% L- or D- FDAA in acetone. The mixture was stirred at 80 ℃ for 15 min. After quenching by the addition of 50 μL 2 N HCl, the mixture was analyzed by ESI-LC/MS to assign the chirality of the amino acids. The retention times of the L- and D-FDAA-derivatized hydrolysates were 19.0 and 22.9 min, respectively. Compounds **6**-**9** were prepared and analyzed using the same procedure. The results demonstrated that all of the amino acids in compounds **5**-**9** were in the L-form.

Biological Assays. The cytotoxicity assays were performed in accordance with protocols reported in the literature.[39] Antimicrobial assays and Na^+/K^+-ATPase,[57] were performed according to previously reported methods.

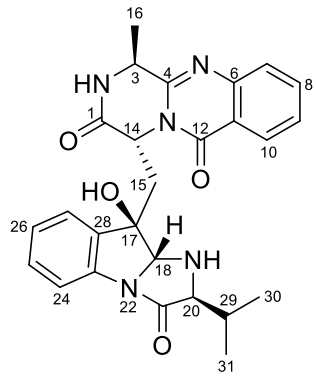

Table 3. ^{13}C and ^{1}H NMR assignment for compound **5** in DMSO-d_6

No.	δ_C	δ_H
1	168.9, C	
3	48.6, C	4.95, q (6.5)
4	153.3, C	
6	146.6, C	
7	126.9, CH	7.66, dd (8.3, 0.8)
8	134.5, CH	7.82, ddd (8.3, 7.5, 1.3)
9	126.7, CH	8.12, dd (8.1, 1.3)
10	126.5, CH	7.53, ddd (8.1, 7.5, 0.8)
11	120.0, C	
12	160.2, C	
14	51.8, CH	5.58, d (9.6, 4.5)
15	35.4, CH_2	2.58, dd (14.9, 9.6); 1.82, dd (14.9, 4.5)
16	16.6, CH_3	1.58, d (6.5)
17	80.1, C	
18	88.2, CH	5.26, dd (6.8, 1.7)
20	69.2, CH	3.54, m

21	172.1, C	
23	137.2, C	
24	115.1, CH	7.34, dd (7.9, 1.0)
25	128.8, CH	7.25, ddd (7.9, 7.5, 1.3)
26	124.6, CH	7.09, ddd (7.5, 7.5, 1.0)
27	125.5, CH	7.80, dd (7.5, 1.3)
28	138.7, C	
29	31.1, CH	1.98, m
30	18.6, CH_3	0.96, d (6.9)
31	17.6, CH_3	0.93, d (6.9)
2-NH		8.61, s
17-OH		5.70, brs
19-NH		3.51, m

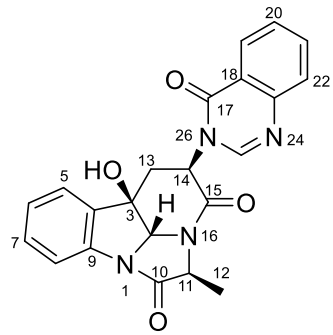

Table 4. ^{13}C and ^{1}H NMR assignment for compound **6** in DMSO-d_6

No.	δ_C	δ_H
2	82.9, CH	5.88, s
3	74.1, C	
4	135.8, C	
5	124.6, CH	7.40, dd (8.0, 1.0)
6	125.2, CH	7.20, ddd (8.0, 8.0, 1.3)
7	130.1, CH	7.38, ddd (8.0, 8.0, 1.0)
8	114.1, CH	7.47, dd (8.0, 1.3)
9	139.7, C	
10	174.4, C	
11	59.7, CH	4.58, q (7.3)
12	13.8, CH_3	1.57, d (7.3)
13	34.7, CH_2	2.92, dd (14.3, 7.0); 2.65, dd (14.3, 5.1)
14	55.6, CH	4.88, dd (7.0, 5.1)
15	164.2, C	
17	159.9, C	
18	121.4, C	
19	126.2, CH	8.14, dd (8.0, 1.3)
20	127.4, CH	7.56, ddd (8.0, 8.0, 1.0)
21	134.7, CH	7.84, ddd (8.0, 8.0, 1.3)

22	127.2, CH	7.67, dd (8.0, 1.0)
23	147.5, C	
25	146.7, CH	8.25, s
3-OH		6.25, brs

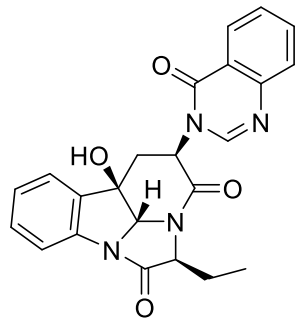

Table 5. ^{13}C and ^{1}H NMR assignment for compound **7** in DMSO-d_6

No.	δ_C	δ_H
2	83.3, CH	5.85, s
3	74.0, C	
4	135.4, C	
5	124.6, CH	7.52, dd (7.4, 1.0)
6	125.2, CH	7.24, ddd (7.5, 7.4, 1.4)
7	130.0, CH	7.42, ddd (7.6, 7.5, 1.0)
8	114.1, CH	7.43, dd (7.6, 1.4)
9	139.9, C	
10	175.2, C	
11	65.3, CH	4.45, dd (9.4, 5.9)
12	21.7, CH_2	2.06, m; 2.00, m
13	34.4, CH_2	2.97, dd (14.2, 7.2); 2.72, dd (14.2, 5.2)
14	55.7, CH	4.89, dd (7.2, 5.2)
15	164.6, C	
17	159.8, C	
18	121.5, C	
19	126.2, CH	8.17, dd (7.9, 1.2)
20	127.4, CH	7.59, ddd (7.9, 7.9, 1.0)
21	134.7, CH	7.87, ddd (7.9, 7.9, 1.2)
22	127.2, CH	7.71, dd (7.9, 1.0)

23	147.5, C	
25	146.7, CH	8.29, s
27	10.9, CH_3	1.11, t (7.3)
3-OH		6.28, brs

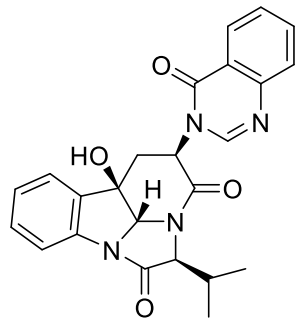

Table 6. ^{13}C and ^{1}H NMR assignment for compound **8** in DMSO-d_6

No.	δ_C	δ_H
2	83.7, CH	5.81, s
3	73.9, C	
4	134.9, C	
5	124.6, CH	7.54, dd (7.5, 1.3)
6	125.2, CH	7.26, ddd (7.8, 7.5, 1.3)
7	130.1, CH	7.43, ddd (7.8, 7.5, 1.3)
8	114.2, CH	7.46, dd (7.5, 1.3)
9	140.3, C	
10	173.9, C	
11	69.4, CH	4.21, d (9.3)
12	28.2, CH	2.44, m
13	34.1, CH_2	3.01, dd (14.0, 7.9); 2.77, dd (14.0, 5.3)
14	55.7, CH	4.86, dd (7.9, 5.3)
15	164.9, C	
17	159.8, C	
18	121.5, C	
19	126.2, CH	8.18, dd (7.9, 1.3)
20	127.4, CH	7.59, ddd (7.9, 7.5, 1.0)
21	134.7, CH	7.87, ddd (7.7, 7.5, 1.3)
22	127.2, CH	7.71, dd (7.7, 1.0)

23	147.5, C	
25	146.9, CH	8.30, s
27	20.2, CH_3	1.12, d (6.7)
28	18.7, CH_3	1.15, d (6.7)
3-OH		6.30, brs

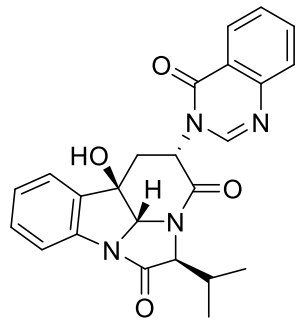

Table 7. ^{13}C and ^{1}H NMR assignment for compound **9** in DMSO-d_6

No.	δ_C	δ_H
2	84.5, CH	5.78, s
3	76.7, C	
4	137.5, C	
5	124.6, CH	7.47, dd (7.4, 0.9)
6	125.5, CH	7.24, ddd (7.4, 7.4, 1.2)
7	129.7, CH	7.41, ddd (7.8, 7.4, 0.9)
8	114.7, CH	7.49, dd (7.8, 1.2)
9	137.6, C	
10	169.7, C	
11	69.6, CH	4.37, d (6.7)
12	30.3, CH	2.26, m
13	38.2, CH_2	2.93, dd (13.0, 13.0); 2.49, dd (13.0, 3.5)
14	49.1, CH	5.98, dd (13.0, 3.5)
15	167.2, C	
17	159.9, C	
18	121.0, C	
19	126.4, CH	8.20, dd (7.9, 1.3)
20	127.2, CH	7.58, ddd (7.9, 7.6, 0.9)
21	134.7, CH	7.86, ddd (7.8, 7.6, 1.3)
22	127.1, CH	7.70, dd (7.8, 0.9)

23	147.2, C	
25	146.7, CH	8.23, s
27	19.1, CH_3	1.09, d (6.7)
28	19.0, CH_3	1.05, d (6.7)
3-OH		6.77, brs

IV. Asperphenins A and B, as anticancer agents from a Marine-Derived *Aspergillus* sp. Fungus

Asperphenins A (**17**) and B (**18**), two new lipopeptide containing aromatic compounds were isolated from the marine-derived fungus *Aspergillus* sp.. Based upon the results of combined spectroscopic analyses, these compounds were structurally elucidated to be lipopeptide containing the benzophenone function group, the first example of this type. The new compounds were significantly active toward HCT116, and moderately avtive against SNU638 SK-HEP1, MDA-MB 231, and weak toward the A549 cell line. Compound **18** also was studied the vivo test and elicited a significant antitumor on RKO cell-implanted xenografts.

4-1. Introduction

Marine microorganism has been widely recognized as the prolific sources of natural products with biological activities and unique structures.[2-6] Marine-derived fungi, as one of the three major dominated phylogenetic groups, have produed more than 400 novel compounds since 1997, of which exhibited potent and diverse bioactivities.[3,7-8]

During the course of searching for bioactive metabolites from

marine-derived fungi, one strain *Aspergillus* sp. was isolated from marine-submerged decaying wood from Korea based on the LC-ESIMS profile of crude extract, from which several fumiquinazoline-related and chatominine derivatives were isolated and structural determination as previous report.[69] Recently, another twe new compounds were isolated and structural determinated as lipopeptide type containing the benzophenone functional group. These two new compounds have the similar character with fellutamides possessing 3-hydroxydodecanoic acid, aspergine, and glutamine which have been reported in the literature.[70-72] However this is the first example of the lipoppeptide connected with the benzophenone functional group.[73] Both compounds possessed the significantly bioactivity toward the HCT116, moderately active toward the SNU638, SK-HEP1, and MDA-MB 231, and weak activity toward the A549. Compound **18** was studied the vivo test as well and showed the acute antitumor activity on RKO cell-implated xenografts.

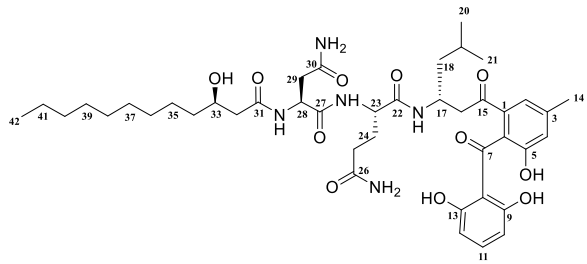

17

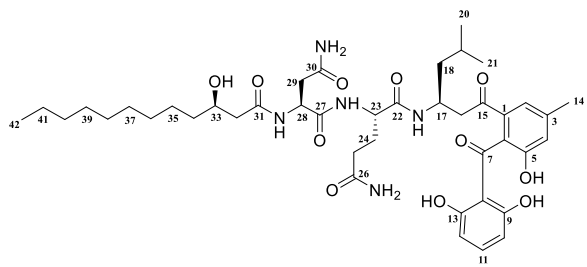

18

Figure 15. The chemical structures of compounds **17-18**

4-2. Results and discussion

The molecular formula of asperphenin A (**17**) was deduced as $C_{42}H_{61}N_5O_{11}$ by the HRFABMS analysis. The ^{13}C NMR data of this compound showed two ketones signals at δ_C 201.8 and 198.3, four carbonyl carbons at δ_C 171.8, 171.2, 170.9, and 170.2, respectively (Table 8). Additionly, two NH_2 groups were observed as two pairs of broad singlets at δ_H 7.14 and 6.70, 7.39 and 6.91 (Table 8) implied two units of primary amines. In ^1H NMR data three amine protons were observed as doublets using DMSO-d_6 as solvent at δ_H 8.04, 7.92, and 7.66, and three α-NH protons were detected

at δ_H 4.44, 4.13, and 4.02 as well. This information revealed the presence of three amino units in compound **17**, which was implied by the resonances at δ_H 52.6, 49.8, and 43.4 in ^{13}C NMR. The overlapped signals (δ_H 1.19-1.30) in ^{1}H NMR and methylenes (δ_C 37.0-22.1) in ^{13}C NMR indicated the fatty acid chain. And the presence of 12 carbon signals in the aromatic region (δ_C 161.6-106.8) in ^{13}C NMR data, along with the corresponding proton signals (δ_H 6.19-7.21) in the ^{1}H NMR data and aromatic absorptions (322 and 268 nm) in UV spectrum, was indicative of two benzene rings in **17**. Hence, the compound **17** was a system including fatty acid, three units of peptide, and two aromatic rings. The IR strong absorption at 3309 and 1671 cm^{-1} also supported it.

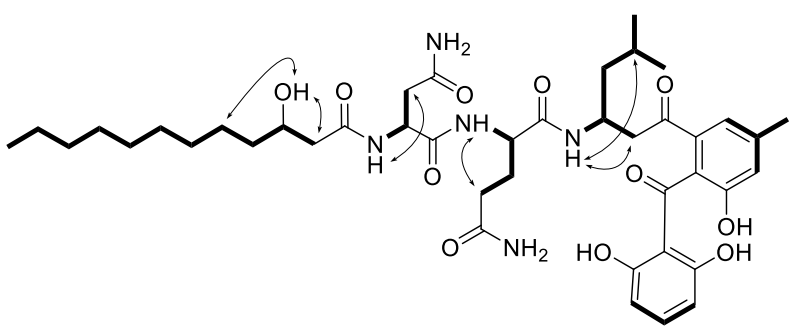

Figure 16. The COSY (bold line) and TOCSY (arrows) correlations of compound **17**.

The planar structure of compound **17** was determined by the combination of ^{1}H-^{1}H COSY, HSQC, and HMBC experiments. First, two aromatic protons (δ_H 7.21, H-2, and 6.84, H-4) appeared as broad siglets, and the ^{1}H-^{1}H COSY correlations between these two protons and the methyl group (δ_C 20.8 and δ_H 2.29) indicated the H-2 and H-4 had to be in the *meta*-positon to one another (Figure 16). The linear spin system of three aromatic protons resonating at δ_H 7.15, 6.19, and 6.19 implied three protons were adjacent in the other aromatic ring. All the carbons were assigned by the HSQC and HMBC data. Three downfield carbon signals at δ_C 161.6 (C-9, 13) and 153.4 (C-5) indicated the oxygenated ones.Two aromatic rings were connected with each other via the 15-keone at δ_C 198.3 based on the long-range correlation in the HMBC data, which was identical as monodictyphenone except the 7-ketone substitute in **17** instead of 1-carboxylic acid in monodictyphenone.[70] From the TOCSY, ^{1}H-^{1}H COSY, HSQC, and HMBC correlations, the fatty acid was determined as hydroxytetradecanoic acid and three amino uints were defined as aspergine, glutamine, and 1-methlene-3-methylbutyl-amine, which is quite similar to that of fellutamide C.[71] The linkage of these segments were deduced by the long-range HMBC (H-17/C-22, NH-17/C-22, NH-23/C-27, and NH-28/C-31). And the 1-methlene-3-methylbutyl-amine was connected to the

monodictyphenone via the 7-ketone at δ_C 201.8 in the long-range HMBC data (H-17/C-7 and H-16/C-7) (Figure 17). Thus, the planar structure of asperphenin A (**17**) was unambiguously determined.

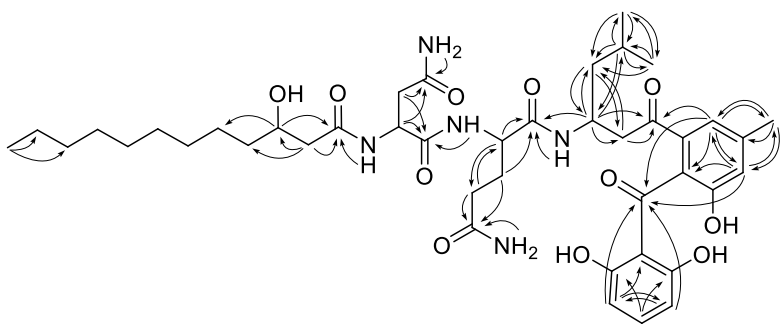

Figure 17. The selective HMBC (arrows) correlations of compound **17**.

Asperphenin A possesses asymmetric carbon centers at C-17, C-23, C-28, and C-33. The absolte configuration of the Gln-derived and Asn-derived residues at the C-23 and C-28 were determined as L by advanced Marfey's analysis as described in the references reported.[70-72] And the absolute chemistry of hydroxyl in C-33 was determined as *R* by Mosher method from the $\Delta\delta$ values between the MTPA esters (Figure 18). Dued to the unstability of compound **17** in basic condition, the cyclization of compound **17** was designed between C-7 and C-16 to make five member ring based on the aldol condensation mechanism[74] and compound **19** was obtained. And then all the phenolic hydroxyl group were protected by acetylation using

$(Ac)_2O$ as the reagent. *R*/*S*-MTPA ester of compound **19** (**19S** and **19R**) were obtained (schem 2). And the absolute chemistry of C-33 was unambiguously assigned as *R*.

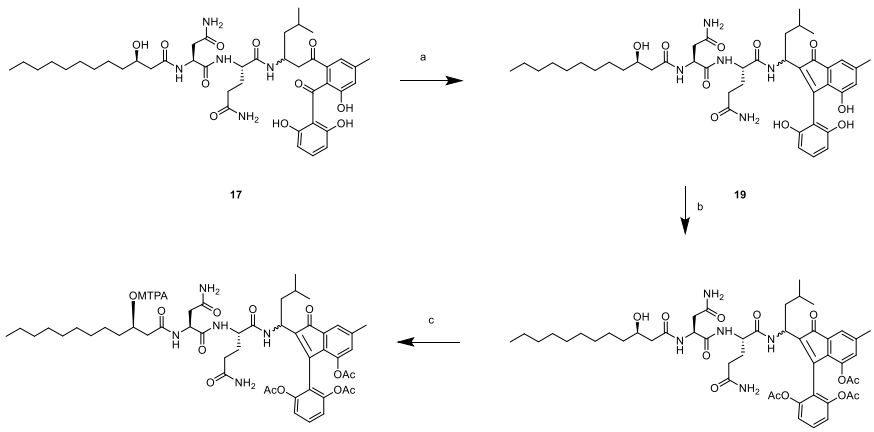

Schem 2. a. DMF, K_2CO_3; b. $(Ac)_2O$ in pyridine; c. MTPA-Cl in pyridine

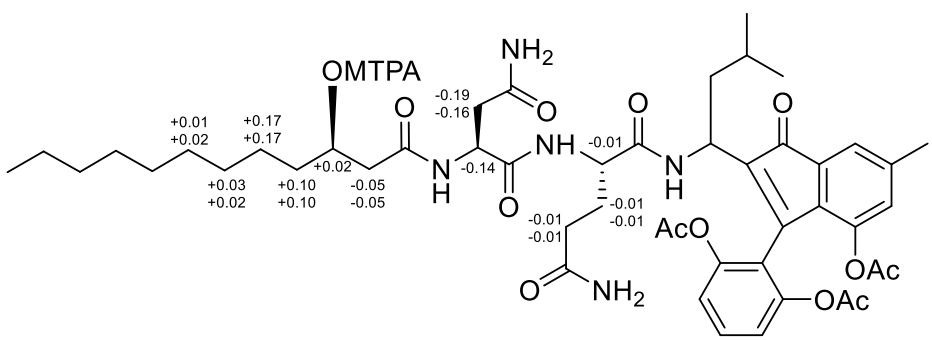

Figure 18. The Δδ ($\delta_{(S\text{-ester})}$-$\delta_{(R\text{-ester})}$) values of MTPA esterification for compound **19** acetylation.

To figure out the relative stereochemsity of C-17, we designed the ketone reduction of asperphenin A. As the 7-ketone located between two aromatic ring, it played more active character than 15-ketone. To get the 15-ketone reduction, 7-ketone was reduced firstly and produed two reduction products (comounds **21** and **22)**. As the reduction went further, the 15-ketone of compound **21** was reduced and produced two products, compounds **25** and **26**, respectively. However, the compound **22** was decomposed during the reduction procedure. As a result, two products (compounds **25** and **26**) of 7,15-diketone reduction of asperphenin A were produced using the $NaBH_4$ as reduction reagent (schem 3). Then we utilized *J*-based configuration[75] analysis with vicinal ^{1}H-^{1}H and 3-bond ^{1}H-^{13}C coupling constants and ROESY corrlations.

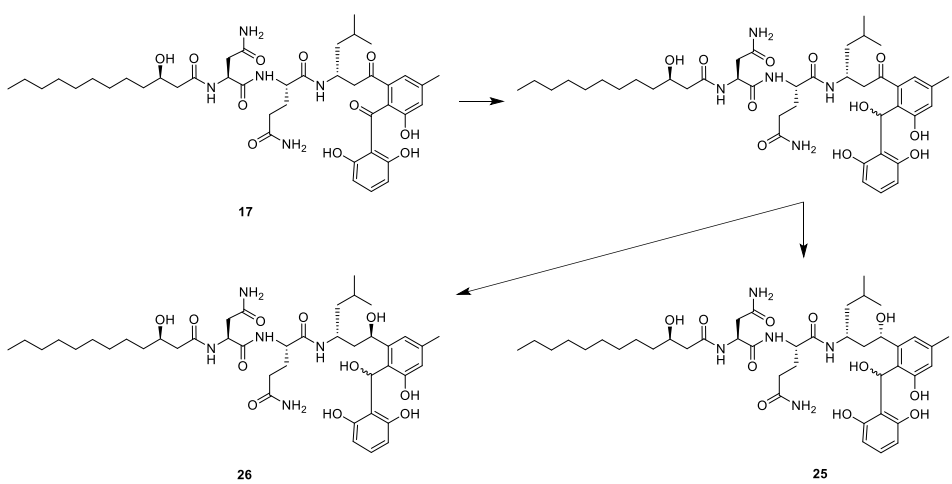

Schem 3. Reagent: $NaBH_4$, dry MeOH

The ^{1}H-^{1}H coupling constants were measured in the ^{1}H and ^{1}H homodecoupling NMR spectra, and long-range heteronuclear coupling constants were acquired via a hetero half-filtered TOCSY (HETLOC) NMR experiment.[75] For compound **25**, the $^{3}J_{H15/H16b}$ value (10.0 Hz) suggested an *anti* relationship between H-15 and H-16b. The small value of $^{3}J_{C17/H15}$ (2.2 Hz) indicated a relative *gauche* relationship between C-17 and H-15. The small value of $^{2}J_{C15/H16a}$ (-1.8 Hz) implied an *anti* relationship between 15-OH and H-16a. Futher analysis of the ^{1}H-^{1}H and ^{1}H-^{13}C coupling constants strongly suggested the rotamer depicted in Figure 19. The ROESY correlations of H-15 to H-16a and H-17 completely supported the configuration shown in Figure 19.

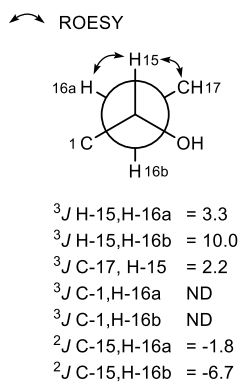

Figure 19. *J*-based configuration analysis of 7,15-diketone reduction of asperphenin A (**25**) at C-15 and C-16.

The intermediate value of $^{3}J_{H17/H16a}$ (7.3 Hz) and $^{3}J_{H17/H16b}$ (6.9 Hz) indicated the rotational changes occurred between two rotamers as the Figure 20b. The large value of $^{2}J_{C17/H16b}$ (-5.1 Hz) implied the gauche relationship between 17-NH and H-16b. The relative stereochemistry of C-15 and C-17 were assigned as *15S**, *17R**. For compound **26**, the relative stereochemistry between C-15 and C-17 were assigned as *15R**, *17R** based on the ^{1}H-^{1}H and ^{1}H-^{13}C coupling constants as shown in Figure 21, respectively.

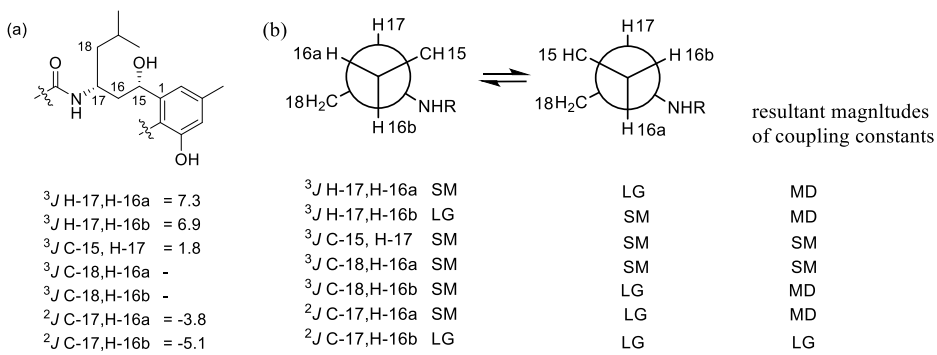

Figure 20. *J*-based configuration analysis of 7,15-diketone reduction of asperphenin A (**25**) at C-16 and C-17.

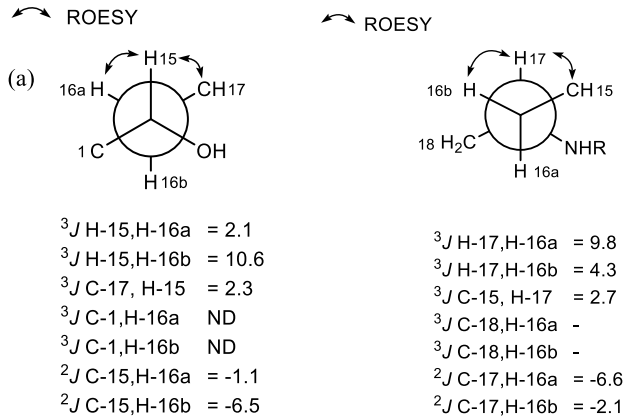

Figure 21. *J*-based configuration analysis of 7,15-diketone reduction of asperphenin A (**26**) at (a) C-15 and C-16, and (b) C-16 and C-17.

The molecular formula of asperphenin B (**18**) was deduced as $C_{42}H_{61}N_5O_{11}$ by the HRFABMS analysis, the same molecular formula with asperphenin A. The IR, UV spectrum were identical with asperphenin A. And the 1D and 2D NMR were quite similar with asperphenin A as well (Table 9). However, these two compounds eluted in different retension time in HPLC.

Futher analysis of asperphenin B, we found both compounds possessed the same planar structure and identical chirality in C-23, C-28, and C-33 using the same method as decribed in asperphenin A. Compound **20** was the cylization product of asperphenin B. To determine the stereochemistry of C-17 in asperphenin B, 7,15-diketone reduction products (compounds **27** and **28**) were designed and HETLOC analysis was applied for the products as

shown in the Figures 22, 23 and 24. The relative chemistry of C-15 and C-17 were assigned *15R** and *17S**, *15S** and *17S** in **27** and **28**, respectively. Asperphenins A and B possess the different chirality in C-17. This conclusion explained well the different retension time for these two compounds in the HPLC with the same condition. Unfortunately, the absolute chemistry of C-15 couldn't be assigned due to the decomposition of MTPA esterification of compounds **25**, **26, 27,** and **28** using the MTPA-chloride as reagent in pyridine.

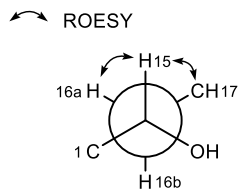

^{3}J H-15,H-16a	= 4.4
^{3}J H-15,H-16b	= 9.2
^{3}J C-17, H-15	= 2.7
^{3}J C-1,H-16a	ND
^{3}J C-1,H-16b	ND
^{2}J C-15,H-16a	= -2.0
^{2}J C-15,H-16b	= -6.3

Figure 22. *J*-based configuration analysis of 7,15-diketone reduction of asperphenin B (**27**) at C-15 and C-16.

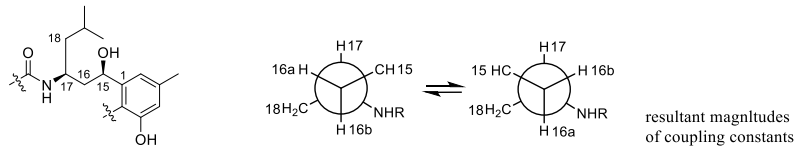

^3J H-17,H-16a = 6.8	^3J H-17,H-16a SM	LG	MD
^3J H-17,H-16b = 7.2	^3J H-17,H-16b LG	SM	MD
^3J C-15, H-17 = 2.7	^3J C-15, H-17 SM	SM	SM
^3J C-18,H-16a = 1.8	^3J C-18,H-16a SM	SM	SM
^3J C-18,H-16b -	^3J C-18,H-16b SM	LG	MD
^2J C-17,H-16a = -3.7	^2J C-17,H-16a SM	LG	MD
^2J C-17,H-16b = -5.6	^2J C-17,H-16b LG	LG	LG

Figure 23. *J*-based configuration analysis of 7,15-diketone reduction of asperphenin B (**27**) at C-16 and C-17.

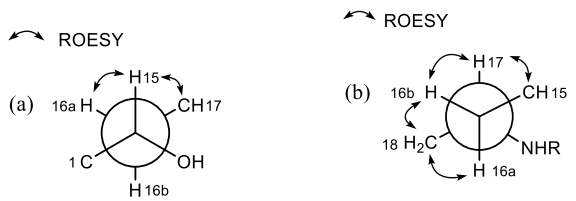

^3J H-15,H-16a = 2.1	^3J H-17,H-16a = 9.4
^3J H-15,H-16b = 10.7	^3J H-17,H-16b = 4.2
^3J C-17, H-15 = 2.8	^3J C-15, H-17 = 2.8
^3J C-1,H-16a ND	^3J C-18,H-16a = 2.5
^3J C-1,H-16b ND	^3J C-18,H-16b = 2.7
^2J C-15,H-16a = -1.4	^2J C-17,H-16a = -6.2
^2J C-15,H-16b = -5.8	^2J C-17,H-16b = -0.8

Figure 24. *J*-based configuration analysis of 7,15-diketone reduction of asperphenin B (**28**) at (a) C-15 and C-16, and (b) C-16 and C-17.

Then the recently proposed CD and ECD calculation was employed, which has been used to unambiguously assign both relative and absolute configurations for many natural products[76]. The first CD spectrum of asperphenins A and B is asymmetric and the similar optical rotation with -

24.7 and -18.4 for A and B, maybe due to the conjugated system is far away from the C-17 and free rotation with linear side chain. Interestingly, the cylization products of asperphenins A and B (comounds **19** and **20**) showed the symmetric CD spectrum and opposite optical rotation with +56.5 and -85.5 for **19** and **20**, repectively. Then the unit of C-1~C-21~17-NH was selected as unit to be applied the ECD calculation. From the ECD spectrum, we assigned the absolute chemistry of C-17 as *R* for asperphenin A and *S* for asperphenin B, respectively (Figure 25). Thus, all the stereochemistry were successfully determined as *17R*, *23S*, *28S*, and *33R* for asperphenin A, *17S*, *23S*, *28S*, and *33R* for asperphenin B.

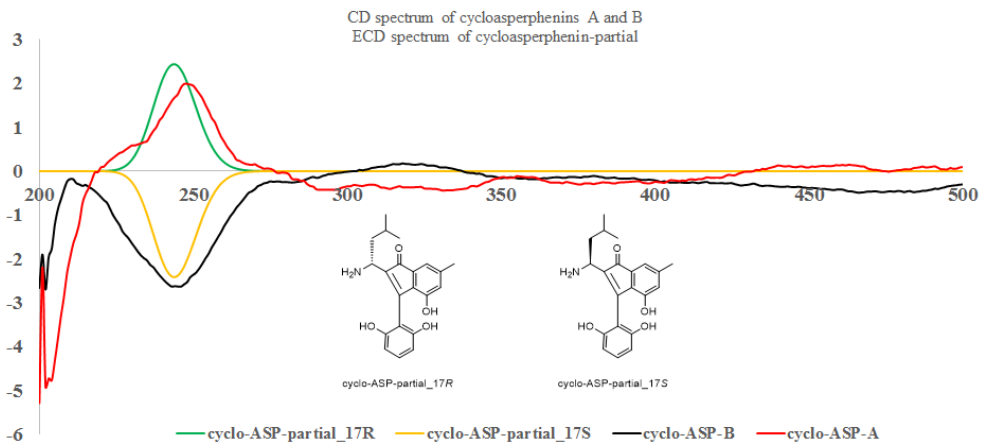

Figure 25. The CD spectrum of cycloasperphenins A and B, ECD spectrum of cyclo-ASP-partial_17*R* and cyclo-ASP-partial_17*S*.

In our bioactivity measurement, compounds **17**-**28** were studied toward the A549, HCT116, SNU638, SK-HEP1, and MDA-MB 231. Asperphenins A (**17**) and B (**18**) were significantly ative against HCT116, moderately active toward the SNU638, SK-HEP1, and MDA-MB 231, and weak activity toward the A549 (Table 10). However, the cycloasperphenins A (**19**) and B (**20**) were inactive toward all the cell lines, and 7-ketone reduction of asperphenins A (**21**, **22**) and B (**23**) were inactive toward the A549 and MDA-MB 231, and weak toward HCT116, SNU638 and SK-HEP1. And 7-ketone reduction of asperphenin B (**24**) and 7,15-diketone reduction of asperphenins A (**26**) and B (**27**, **28**) were inactive toward all the cell lines. The results implied that the 7-ketone and 15-ketone played the important role for activities against A549, HCT116, SNU638, SK-HEP1, and MDA-MB 231 (Table 10). Morever, the asperphenin B (**18**) was studied as the antitumor agent on RKO cell-implated xenografts. Asperphenin B exhibited significant inhibition of colon cancer. At a concentration of 8mg/kg, the inhibition rate was 68.7%, which was approached the inhibition rate of irinotecan with the 4 mg/kg. And the combination of asperphenin B and irinotecan improved the inhibition to 86.9% (Figure 26). Therefore, the significant inhibition toward the colon cancer by asperphenin B may be suggestive of a potential role in anticancer drug. The mechanism of anti-colon

cancer of asperphenin B is futher being studied.

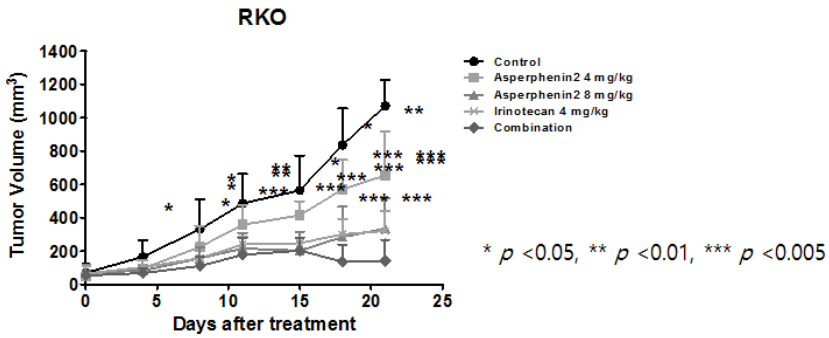

Group	Asperphenin B 4 mg/kg	Asperphenin B 8 mg/kg	Irinotecan 4 mg/kg	Combination
Inhibition rate (%)	38.9	68.7	70.0	86.9
FTV Asperphenin B (4 mg/kg)	FTV Irinotecan (4 mg/kg)	Expected FTV	Observed FTV	Combination ratio
0.61	0.30	0.18	0.13	1.39

Figure 26. The antitumor effects of asperphenin B (**18**) on RKO cell-implated xenografts.

4-3. Experimental section

General Experimental Procedures. The optical rotations were measured on a JASCO P-2000 polarimeter using a 1 cm cell. The UV spectra were acquired with a Hitachi U-3010 spectrophotometer. ECD spectra were recorded using an Applied Photophysic Chirasscan-plus circular dichroism detector. The IR spectra were recorded on a JASCO 4200 FT-IR spectrometer,

using a ZnSe cell. The NMR spectra were recorded on Bruker Avance 600 MHz spectrometer at the NCIRF (National Center for Interuniversity Research Facilities at Seoul National University), and on Bruker Avance II 800 MHz and 900 MHz at the KBSI (Korea Basic Science Institute at Ochang). HRFABMS data were acquired using a Jeol JMS 700 mass spectrometer with *meta*-nitrobenzyl alcohol (NBA) as the matrix at the Korea Basic Science Institute (Daegu, Korea). The HPLC analyses were performed on a Spectrasystem p2000 equipped with a refractive index detector (Spectrasystem RI-150). All of the solvents used were spectroscopic grade or distilled from glass prior to use.

Isolation and Identification of the Fungal Strain. The fungal strain *Aspergillus* sp. (strain number F452) was isolated from submerged decaying wood off of the shore of Jeju Island, Korea, in November 2011. The strain was identified using standard molecular biological protocols by DNA amplification and sequencing of the ITS region. The genomic DNA extraction was performed using Intron's i-genomic BYF DNA Extraction Mini Kit according to the manufacturer's protocol. The nucleotide sequence of F452 has been deposited in the GenBank database under the accession number KF384188. The 18S rDNA sequence of this strain showed a 99% identity with *Aspergillus versicolor* Ppf48 (GenBank accession number GU586852).

Fermentation and Isolation. The isolated strain was cultivated on a YPG agar plate (5 g yeast extract, 5 g peptone, 10 g glucose, and 16.0 g agar in 1 L artificial seawater) for 4 days. The agar plugs (1 cm × 1 cm, 5 pieces each) were inoculated into 100 mL of the YPG media in a 250 mL Erlenmeyer flask for 5 days, then separately transferred to 2.8 L glass Fernbach flasks with rice media (2 g peptone, 2 g yeast extract, 200 g rice with 200 mL artificial seawater in each flask, boiled in an autoclave for 20 min at 120 ℃; 24 flasks in total). The fermentation in the rice media was conducted under static conditions for 6 weeks and then was extracted by MeOH (1 L × 3) and CH_2Cl_2 (1 L × 3). The solvent was evaporated to obtain an organic extract. The combined extracts (102.6 g) were successively partitioned between *n*-BuOH (72.5 g) and H_2O (30.1 g); the former fraction was repartitioned using H_2O-MeOH (15:85) (44.3 g) and *n*-hexane (31.2 g). The fraction of H_2O-MeOH (15:85) was separated by C_{18} reversed-phase vacuum flash chromatography using a sequential mixture of MeCN and H_2O as eluents (five fractions in gradient, H_2O–MeCN, from 80:20 to 0:100), MeOH, acetone, and finally EtOAc. On the basis of the results of LC-MS analysis, the fractions eluted with H_2O–MeCN (40:60) (11.3 g) was separated by C_{18} reversed-phase vacuum flash chromatography again using a sequential mixture of MeCN and H_2O as eluents (six fractions in gradient, H_2O–MeCN,

from 50:50 to 0:100), and 100% MeOH. The fraction eluted with H_2O–MeCN (40:60) (2.1 g) was separated by semi-preparative reversed-phase HPLC (H_2O–MeOH, 30:70, 2.0 mL/min) to afford compound **17** (103.2 mg) and compound 1**8** (106.7 mg).

Asperphenin A (**17**): pale yellow amorphous solid, $[\alpha]_D^{25}$ –24.7 (*c* 0.1, MeOH); UV (MeOH) λ_{max} (log ε) 211 (4.65), 268 (4.25), 322 (3.95) nm; CD (MeOH) λ (Δε) 217 (+2.26), 235 (-1.79), 331 (-0.30) nm; IR (ZnSe) ν_{max} 3309, 1671 cm^{-1}; ^1H and ^{13}C NMR data, see Table 8; HRFABMS, *m/z* 812.4430 $[M+H]^+$ (Calcd for $C_{42}H_{62}N_5O_{11}$, 812.4440).

Asperphenin B (**18**): pale yellow amorphous solid, $[\alpha]_D^{25}$ –18.4 (*c* 0.1, MeOH); UV (MeOH) λ_{max} (log ε) 211 (4.65), 268 (4.25), 322 (3.95) nm; CD (MeOH) λ (Δε) 224 (-0.80), 242 (-1.10), 280 (+0.66), 337 (-0.08), 448 (+0.10) nm; IR (ZnSe) ν_{max} 3309, 1670 cm^{-1}; ^1H and ^{13}C NMR data, see Table 8; HRFABMS, *m/z* 812.4431 $[M+H]^+$ (Calcd for $C_{42}H_{62}N_5O_{11}$, 812.4440).

Cyclization of Compounds 17 and 18. Compound **17** (21.2 mg) was dissolved in DMF (3 ml) containing K_2CO_3 (4.3 mg) and was stirred for 7 h. The solution was extracted by EA and evaporated under vacuum and the residue of the reaction was purified by reverse-phase HPLC (YMC-ODS

column, 4.6 × 250 mm; H_2O–MeCN, 50:50, 1.0 mL/min) to afford **19** (4.2 mg) (retention time in HPLC: 17.5min). **20** (4.3 mg) was prepared in the same procedure from the compound **18** (22.8 mg).

Compound 19 (**19**)**:** ^{1}H NMR (600 MHz, MeOD-d_4) δ 7.03 (1 H, t, J = 8.3 Hz, H-11), 6.77 (1 H, s, H-2), 6.57 (1 H, s, H-4), 6.45 (1 H, J = 8.3 Hz, H-10), 6.41 (1 H, J = 8.3 Hz, H-12), 4.70 (1 H, dd, J = 7.2, 5.4 Hz, H-28), 4.65 (1 H, t, J = 7.8 Hz, H-17), 4.25 (1 H, dd, J = 9.5, 4.4 Hz, H-23), 3.97 (1 H, m, H-33), 2.81 (1 H, dd, J = 15.4, 5.4 Hz, H-29), 2.75 (1 H, dd, J = 15.4, 7.2 Hz, H-29), 2.45 (1 H, dd, J = 14.3, 4.1 Hz, H-32), 2.32 (1 H, dd, J = 14.3, 8.4 Hz, H-32), 2.26 (2 H, overlap, H-25), 2.23 (3 H, s, H-14), 2.10 (1 H, m, H-24), 1.84 (1 H, m, H-24), 1.56 (1 H, m, H-19), 1.47 (3 H, m, H-18, H-34), 1.28 (15 H, m, H-34–H-41), 0.88 (3 H, t, J = 6.8 Hz, H-42), 0.71 (3 H, d, J = 6.8 Hz, H-20), 0.70 (3 H, d, J = 6.8 Hz, H-21); ^{13}C NMR (600 MHz, MeOD-d_4) δ 199.3 (C-15), 178.2 (C-26), 175.2 (C-27), 174.7 (C-4), 173.4 (C-5), 172.0 (C-22), 156.7 (C-9), 156.4 9C-13), 156.1 (C-5), 153.4 (C-7), 141.7 (C-3), 134.3 (C-1), 132.9 (C-16), 131.0 (C-11), 126.8 (C-6), 125.2 (C-4), 116.5 (C-2), 111.5 (C-8), 108.4 (C-12), 108.0 (C-10), 69.8 (C-33), 54.4 (C-23), 51.7 (C-28), 45.5 (C-17), 44.6 (C-32), 43.5 (C-18), 38.3 (C-34), 37.3 (C-29), 33.1 (C-40), 32.5 (C-25), 30.8 (C-36), 30.7 (C-37), 30.7 (C-38), 30.5 (C-39), 28.9 (C-24), 26.8 (C-35), 25.6 (C-19), 23.8 (C-41), 23.2 (C-21), 22.5 (C-20), 21.2

(C-14), 14.5 (C-42); $[\alpha]_D^{25}$ +56.5 (*c* 1.0, MeOH); CD (MeOH) λ (Δε) 248 (+1.99), 334 (-0.44), 448 (+0.10) nm (Figure 20); LRESIMS *m/z* 794.4, $[M-H_2O+H]^+$ (Calcd for $C_{42}H_{60}N_5O_{10}$).

Compound 20 (20): ^{1}H NMR (600 MHz, MeOD-d_4) δ 7.03 (1 H, t, *J* = 8.3 Hz, H-11), 6.77 (1 H, s, H-2), 6.57 (1 H, s, H-4), 6.46 (1 H, *J* = 8.3 Hz, H-10), 6.40 (1 H, *J* = 8.3 Hz, H-12), 4.71 (1 H, dd, *J* = 5.6, 6.4 Hz, H-28), 4.65 (1 H, t, *J* = 7.8 Hz, H-17), 4.26 (1 H, dd, *J* = 9.5, 4.5 Hz, H-23), 3.98 (1 H, m, H-33), 2.75 (2 H, overlap, H-29), 2.47 (1 H, dd, *J* = 14.3, 4.1 Hz, H-32), 2.34 (1 H, dd, *J* = 14.3, 8.7 Hz, H-32), 2.26 (2 H, overlap, H-25), 2.23 (3 H, s, H-14), 2.14 (1 H, m, H-24), 1.85 (1 H, m, H-24), 1.56 (1 H, m, H-19), 1.49 (3 H, m, H-18, H-34), 1.28 (15 H, m, H-34–H-41), 0.89 (3 H, t, *J* = 6.8 Hz, H-42), 0.71 (3 H, d, *J* = 6.8 Hz, H-20), 0.69 (3 H, d, *J* = 6.8 Hz, H-21); ^{13}C NMR (600 MHz, MeOD-d_4) δ 199.4 (C-15), 178.1 (C-26), 175.1 (C-27), 174.8 (C-4), 173.5 (C-5), 172.1 (C-22), 156.8 (C-9), 156.4 (C-13), 156.1 (C-5), 153.4 (C-7), 141.7 (C-3), 134.3 (C-1), 132.9 (C-16), 131.0 (C-11), 126.8 (C-6), 125.3 (C-4), 116.6 (C-2), 111.6 (C-8), 108.4 (C-12), 108.0 (C-10), 69.8 (C-33), 54.5 (C-23), 51.9 (C-28), 45.7 (C-17), 44.6 (C-32), 43.5 (C-18), 38.3 (C-34), 37.4 (C-29), 33.1 (C-40), 32.5 (C-25), 30.8 (C-36), 30.7 (C-37), 30.7 (C-38), 30.5 (C-39), 28.9 (C-24), 26.7 (C-35), 25.7 (C-19), 23.8 (C-41), 23.1

(C-21), 22.5 (C-20), 21.2 (C-14), 14.5 (C-42); $[\alpha]_D^{25}$ –85.5 (*c* 1.0, MeOH); CD (MeOH) λ (Δε) 241 (-2.53), 318 (+0.18), 470 (-0.47) nm (Figure 20); LRESIMS *m/z* 794.3, $[M\text{-}H_2O+H]^+$ (Calcd for $C_{42}H_{60}N_5O_{10}$).

Esterifications of Compounds 19 and 20. Compound **19** (2.5 mg) was dissolved in pyridine (0.5 ml), then acetic anhydride (3 μl) was added in ice cooling water bath. After 2 h in room temperature, the reaction was quenched by adding ice water and evaporated the solvent using evaporator. And the residue was divided to 1.5 mg and 1.4 mg, respectively. To a solution of 1.5 mg in 1.0 mL of pyridine (distilled over CaH_2), were added 0.5 mg DMAP, and 10 μL of (-)-(*R*)-MTPA chloride. The mixture was stirred under N_2 for 2 h at room temperature. After the consumption of the starting material was confirmed by HPLC-DAD, the solvent was removed under vacuum and the residue was purified by reverse-phase HPLC (YMC-ODS column, 4.6 × 250 mm; H_2O–MeCN, 20:80, 1.0 mL/min) to afford **19S**, the (*S*)-MTPA ester of **19** acetylation (***S*** of **19** acetylation). **19R**, the corresponding (*R*)-MTPA ester of **19** acetylation (***R*** of **19** acetylation) was also obtained from the same esterification reaction with (+)-(*S*)-MTPA chloride. **20S** (***S*** of **20** acetylation) and **20R** (***R*** of **20** acetylation**)** were obtained from **20** using the same procedure.

Compound 19S (21): ^{1}H NMR (600 MHz, MeOD-d_4) δ 7.53 (1 H, t, J = 8.3 Hz, H-11), 7.53-7.42 (5 H, m, aromatic, MPTA), 7.30 (1 H, d, J = 8.3 Hz, H-12), 7.29 (1 H, d, J = 8.3 Hz, H-10), 7.18 (1 H, s, H-2), 6.96 (1 H, s, H-4), 5.55 (1 H, dddd, J = 12.4, 6.2, 6.2, 6.2 Hz, H-33), 4.65 (1 H, dd, J = 10.2, 4.3 Hz, H-17), 4.49 (1 H, dd, J = 6.8, 6.0 Hz, H-28), 4.32 (1 H, dd, J = 9.6, 4.2 Hz, H-23), 3.51 (3 H, s, OMe, MTPA), 2.76 (1 H, dd, J = 16.9, 6.0 Hz, H-29), 2.72 (1 H, dd, J = 16.9, 6.0 Hz, H-29), 2.65 (2 H, t, J = 6.2 Hz, H-32), 2.46 (2 H, t, J = 7.9 Hz, H-25), 2.34 (3 H, s, H-14), 2.15 (1 H, m, H-24), 2.04 (3 H, s, 9-OAc), 2.02 (3 H, s, 13-OAc), 1.85 (1 H, m, H-24), 1.76 (1 H, m, H-18), 1.73 (2 H, overlap, H-34), 1.55 (3 H, s, 5-OAc), 1.50 (1 H, m, H-19), 1.36 (2 H, overlap, H-35), 1.32 (1 H, m, H-18), 1.30-1.25 (12 H, overlap, H-36─H-41), 0.89 (3 H, t, J = 7.1 Hz, H-42), 0.79 (3 H, d, J = 6.9 Hz, H-20), 0.73 (3 H, d, J = 6.5 Hz, H-21); ESI-MS *m/z* 1136.40, $[M+H]^+$ (Calcd for $C_{58}H_{73}F_3N_5O_{15}$ 1136.50).

Compound 19R (22): ^{1}H NMR (600 MHz, MeOD-d_4) δ 7.53 (1 H, t, J = 8.3 Hz, H-11), 7.53-7.42 (5 H, m, aromatic, MPTA), 7.30 (1 H, d, J = 8.3 Hz, H-12), 7.29 (1 H, d, J = 8.3 Hz, H-10), 7.18 (1 H, s, H-2), 6.96 (1 H, s, H-4), 5.53 (1 H, dddd, J = 12.4, 6.4, 6.4, 6.3 Hz, H-33), 4.65 (1 H, dd, J = 10.2, 4.3 Hz, H-17), 4.63 (1 H, dd, J = 7.6, 5.6 Hz, H-28), 4.33 (1 H, dd, J = 9.6, 4.2 Hz, H-23), 3.55 (3 H, s, OMe, MTPA), 2.95 (1 H, dd, J = 17.2, 5.6

Hz, H-29), 2.88 (1 H, dd, *J* = 17.2, 7.6 Hz, H-29), 2.70 (2 H, t, *J* = 6.4 Hz, H-32), 2.47 (2 H, t, *J* = 7.9 Hz, H-25), 2.34 (3 H, s, H-14), 2.15 (1 H, m, H-24), 2.04 (3 H, s, 9-OAc), 2.02 (3 H, s, 13-OAc), 1.86 (1 H, m, H-24), 1.76 (1 H, m, H-18), 1.63 (2 H, overlap, H-34), 1.55 (3 H, s, 5-OAc), 1.50 (1 H, m, H-19), 1.32 (1 H, m, H-18), 1.28-1.21 (12 H, overlap, H-36─H-41), 1.19 (2 H, overlap, H-35), 0.89 (3 H, t, *J* = 7.1 Hz, H-42), 0.79 (3 H, d, *J* = 6.9 Hz, H-20), 0.73 (3 H, d, *J* = 6.5 Hz, H-21); LRESIMS *m/z* 1136.4, $[M+H]^+$ (Calcd for $C_{58}H_{73}F_3N_5O_{15}$ 1136.4).

Compound 20S (23): ^{1}H NMR (600 MHz, MeOD-d_4) δ 7.53 (1 H, t, *J* = 8.3 Hz, H-11), 7.53-7.42 (5 H, m, aromatic, MPTA), 7.30 (1 H, d, *J* = 8.3 Hz, H-12), 7.30 (1 H, d, *J* = 8.3 Hz, H-10), 7.19 (1 H, s, H-2), 6.96 (1 H, s, H-4), 5.55 (1 H, m, H-33), 4.64 (1 H, dd, *J* = 10.1, 4.4 Hz, H-17), 4.50 (1 H, dd, *J* = 7.2, 5.9 Hz, H-28), 4.31 (1 H, dd, *J* = 9.7, 4.6 Hz, H-23), 3.50 (3 H, s, OMe, MTPA), 2.74 (1 H, dd, *J* = 17.0, 5.9 Hz, H-29), 2.67 (1 H, dd, *J* = 17.0, 7.2 Hz, H-29), 2.64 (1 H, dd, *J* = 15.2, 5.0 Hz, H-32), 2.58 (1 H, dd, *J* = 15.2, 8.4 Hz, H-32), 2.46 (2 H, m, H-25), 2.34 (3 H, s, H-14), 2.13 (1 H, m, H-24), 2.05 (3 H, s, 9-OAc), 2.03 (3 H, s, 13-OAc), 1.86 (1 H, m, H-24), 1.73 (1 H, m, H-18), 1.73 (2 H, overlap, H-34), 1.56 (3 H, s, 5-OAc), 1.50 (1 H, m, H-19), 1.35 (2 H, overlap, H-35), 1.33 (1 H, m, H-18), 1.35-1.28 (12 H, overlap, H-36─H-41), 0.89 (3 H, t, *J* = 7.0 Hz, H-42), 0.77 (3 H, d, *J* = 6.8 Hz, H-20),

0.73 (3 H, d, *J* = 6.6 Hz, H-21); ESI-MS *m/z* 1136.41, $[M+H]^+$ (Calcd for $C_{58}H_{73}F_3N_5O_{15}$ 1136.50).

Compound 20R (24): ^{1}H NMR (600 MHz, MeOD-d_4) δ 7.53 (1 H, t, *J* = 8.3 Hz, H-11), 7.53-7.42 (5 H, m, aromatic, MPTA), 7.30 (1 H, d, *J* = 8.3 Hz, H-12), 7.30 (1 H, d, *J* = 8.3 Hz, H-10), 7.19 (1 H, s, H-2), 6.96 (1 H, s, H-4), 5.51 (1 H, m, H-33), 4.65 (1 H, dd, *J* = 10.1, 4.4 Hz, H-17), 4.63 (1 H, dd, *J* = 8.0, 5.6 Hz, H-28), 4.31 (1 H, dd, *J* = 9.7, 4.6 Hz, H-23), 3.56 (3 H, s, OMe, MTPA), 2.91 (1 H, dd, *J* = 17.2, 5.6 Hz, H-29), 2.82 (1 H, dd, *J* = 17.2, 8.0 Hz, H-29), 2.69 (1 H, dd, *J* = 15.4, 8.4 Hz, H-32), 2.62 (1 H, dd, *J* = 15.4, 5.0 Hz, H-32), 2.47 (2 H, m, H-25), 2.33 (3 H, s, H-14), 2.14 (1 H, m, H-24), 2.05 (3 H, s, 9-OAc), 2.03 (3 H, s, 13-OAc), 1.87 (1 H, m, H-24), 1.73 (1 H, m, H-18), 1.62 (2 H, overlap, H-34), 1.56 (3 H, s, 5-OAc), 1.50 (1 H, m, H-19), 1.32 (1 H, m, H-18), 1.30-1.18 (12 H, overlap, H-36─H-41), 1.18 (2 H, overlap, H-35), 0.89 (3 H, t, *J* = 7.0 Hz, H-42), 0.77 (3 H, d, *J* = 6.8 Hz, H-20), 0.72 (3 H, d, *J* = 6.6 Hz, H-21); LRESIMS *m/z* 1136.4, $[M+H]^+$ (Calcd for $C_{58}H_{73}F_3N_5O_{15}$ 1136.5).

Advanced Marfey's Analysis of Compounds 17 and 18. Compound **17** (1.0 mg) was dissolved in 6 N HCl (0.5 ml) and heated at 110 ^{o}C for 12 h. The solution was evaporated with distilled water three times to

remove the trace of HCl under vacuum. The divided hydrolysate (0.5 mg) was treated with 100 μL of 1N $NaHCO_3$ followed by 50 μL of 1% L- or D- FDAA in acetone. The mixture was stirred at 80 ^oC for 5 min. After the reaction was quenched by the addition of 50 μL 2N HCl, the mixture was analyzed by ESI-LC/MS to assign the chirality of the amino acids. The retention times of the L- and D-FDAA-derivatized hydrolysates were 10.8 and 11.4 min for L- and D-aspartic acid, respectively; and the retention times of the L- and D-FDAA-derivatized hydrolysates were 12.0 and 13.2 min for L- and D-glutamic acid, respectively. Compound **18** was prepared and analyzed using the same procedure. The results demonstrated that all the amino acids in compounds **17** and **18** were L-form.

7-ketone reduction of Compounds 17 and 18. Compound **17** (22.1 mg) was dissolved in MeOH (2 ml) and $NaBH_4$ (1.2 mg) was added to the solution in 0 ^oC. Then the reaction was stirred for 30 min and quenched by adding 1 N HCl, the solution was purified by reverse-phase HPLC (YMC-ODS column, 4.6 × 250 mm; H_2O–MeOH, 45:55, 1.0 mL/min) to afford compounds **21** (8.1 mg) and **22** (8.7 mg). Compounds **23** (8.2 mg) and **24** (8.0 mg) were prepared in the same procedure from compound 1**8** (24.5 mg).

Compound 21 (25): ^{1}H NMR (600 MHz, MeOD-d_4) δ 6.75 (1 H, t,

J = 8.0 Hz, H-11), 6.67 (1 H, s, H-2), 6.63 (1 H, s, H-4), 6.43 (1 H, s, H-7), 6.21 (1 H, d, *J* = 7.9 Hz, H-12), 6.07 (1 H, d, *J* = 7.9 Hz, H-10), 4.61 (1 H, t, *J* = 6.4 Hz, H-28), 4.44 (1 H, dd, *J* = 10.2, 3.7 Hz, H-17), 4.27 (1 H, dd, *J* = 9.6, 4.3 Hz, H-23), 3.94 (1 H, m, H-33), 2.74 (1 H, dd, *J* = 15.7, 6.4 Hz, H-29), 2.70 (1 H, dd, *J* = 15.7, 6.4 Hz, H-29), 2.40 (1 H, dd, *J* = 14.4, 4.3 Hz, H-32), 2.31 (2 H, m, H-25), 2.29 (1 H, dd, *J* = 14.4, 6.8 Hz, H-32), 2.21 (3 H, s, H-14), 2.17 (1 H, m, H-24), 1.92 (1 H, m, H-24), 1.68 (1 H, m, H-16), 1.60 (1 H, m, H-16), 1.49 (1 H, m, H-19), 1.44 (3 H, m, H-18, H-34), 1.29 (1 H, overlap, H-34), 1.34-1.23 (14 H, overlap, H-35─H-41), 0.96 (3 H, d, *J* = 6.9 Hz, H-20), 0.93 (3 H, d, *J* = 6.9 Hz, H-21), 0.88 (3 H, t, *J* = 7.1 Hz, H-42); LRESIMS *m/z* 796.2, $[M\text{-}H_2O+H]^+$ (Calcd for $C_{42}H_{62}N_5O_{10}$ 796.4).

Compound 22 (26): ^{1}H NMR (600 MHz, MeOD-d_4) δ 6.83 (1 H, s, H-4), 6.75 (1 H, t, *J* = 8.0 Hz, H-11), 6.67 (1 H, s, H-2), 6.44 (1 H, s, H-7), 6.22 (1 H, d, *J* = 7.9 Hz, H-12), 6.09 (1 H, d, *J* = 7.9 Hz, H-10), 4.62 (1 H, t, *J* = 6.4 Hz, H-28), 4.52 (1 H, dd, *J* = 10.2, 3.7 Hz, H-17), 4.26 (1 H, dd, *J* = 9.6, 4.3 Hz, H-23), 3.94 (1 H, m, H-33), 2.75 (1 H, dd, *J* = 15.7, 6.4 Hz, H-29), 2.66 (1 H, dd, *J* = 15.7, 6.4 Hz, H-29), 2.38 (1 H, dd, *J* = 14.4, 4.3 Hz, H-32), 2.31 (2 H, m, H-25), 2.29 (1 H, dd, *J* = 14.4, 6.8 Hz, H-32), 2.24 (3 H, s, H-14), 2.18 (1 H, m, H-24), 1.94 (1 H, m, H-24), 1.64 (1 H, m, H-16), 1.60 (1 H, m, H-16), 1.44 (3 H, m, H-18, H-34), 1.36 (1 H, m, H-19), 1.29 (1 H,

overlap, H-34), 1.34-1.23 (14 H, overlap, H-35─H-41), 0.96 (3 H, d, *J* = 6.9 Hz, H-20), 0.94 (3 H, d, *J* = 6.9 Hz, H-21), 0.82 (3 H, t, *J* = 7.1 Hz, H-42); LRESIMS *m/z* 796.2, $[M\text{-}H_2O+H]^+$ (Calcd for $C_{42}H_{62}N_5O_{10}$ 796.4).

Compound 23 (27): ^{1}H NMR (600 MHz, MeOD-d_4) δ 6.74 (1 H, t, *J* = 8.0 Hz, H-11), 6.65 (1 H, s, H-2), 6.63 (1 H, s, H-4), 6.43 (1 H, s, H-7), 6.21 (1 H, d, *J* = 7.9 Hz, H-12), 6.08 (1 H, d, *J* = 7.9 Hz, H-10), 4.64 (1 H, t, *J* = 6.4 Hz, H-28), 4.45 (1 H, dd, *J* = 10.2, 3.7 Hz, H-17), 4.25 (1 H, dd, *J* = 9.6, 4.3 Hz, H-23), 3.96 (1 H, m, H-33), 2.78 (1 H, dd, *J* = 15.7, 6.4 Hz, H-29), 2.70 (1 H, dd, *J* = 15.7, 6.4 Hz, H-29), 2.41 (1 H, dd, *J* = 14.4, 4.3 Hz, H-32), 2.32 (1 H, dd, *J* = 14.4, 6.8 Hz, H-32), 2.30 (2 H, m, H-25), 2.21 (3 H, s, H-14), 2.18 (1 H, m, H-24), 1.92 (1 H, m, H-24), 1.68 (1 H, m, H-16), 1.63 (1 H, m, H-16), 1.51 (1 H, m, H-19), 1.45 (3 H, m, H-18, H-34), 1.32 (1 H, overlap, H-34), 1.31-1.23 (14 H, overlap, H-35─H-41), 0.97 (3 H, d, *J* = 6.9 Hz, H-20), 0.95 (3 H, d, *J* = 6.9 Hz, H-21), 0.87 (3 H, t, *J* = 7.1 Hz, H-42); LRESIMS *m/z* 796.2, $[M\text{-}H_2O+H]^+$ (Calcd for $C_{42}H_{62}N_5O_{10}$ 796.4).

Compound 24 (28): ^{1}H NMR (600 MHz, MeOD-d_4) δ 6.81 (1 H, s, H-4), 6.75 (1 H, t, *J* = 8.0 Hz, H-11), 6.66 (1 H, s, H-2), 6.43 (1 H, s, H-7), 6.23 (1 H, d, *J* = 7.9 Hz, H-12), 6.07 (1 H, d, *J* = 7.9 Hz, H-10), 4.66 (1 H, t, *J* = 6.4 Hz, H-28), 4.46 (1 H, dd, *J* = 10.2, 3.7 Hz, H-17), 4.26 (1 H, dd, *J* =

9.6, 4.3 Hz, H-23), 3.95 (1 H, m, H-33), 2.80 (1 H, dd, *J* = 15.7, 6.4 Hz, H-29), 2.71 (1 H, dd, *J* = 15.7, 6.4 Hz, H-29), 2.40 (1 H, dd, *J* = 14.2, 4.2 Hz, H-32), 2.31 (1 H, dd, *J* = 14.2, 8.3 Hz, H-32), 2.25 (2 H, overlap, H-32), 2.24 (3 H, s, H-14), 2.13 (1 H, m, H-24), 1.80 (1 H, m, H-24), 1.62 (2 H, overlap, H-16), 1.45 (3 H, m, H-18, H-34), 1.39 (1 H, m, H-19), 1.31 (1 H, overlap, H-34), 1.31-1.23 (14 H, overlap, H-35─H-41), 0.94 (3 H, d, *J* = 6.9 Hz, H-20), 0.93 (3 H, d, *J* = 6.9 Hz, H-21), 0.89 (3 H, t, *J* = 7.1 Hz, H-42); LRESIMS *m/z* 796.2, $[M\text{-}H_2O+H]^+$ (Calcd for $C_{42}H_{62}N_5O_{10}$ 796.4).

15-ketone reduction of Compounds 21 and 22. Compound **21** (8.1 mg) was dissolved in MeOH (2 ml) and $NaBH_4$ (0.6 mg) was added to the solution in 0 ^oC. Then the reaction was kept in room temperature for 1 h and quenched by adding 1 N HCl to adjust PH = 7.0, the solution was purified by reverse-phase HPLC (YMC-ODS column, 4.6 × 250 mm; H_2O–MeCN, 70:30 to 50:50, 0-20 min, 1.0 mL/min) to afford compounds **25** (2.1 mg) and **26** (2.2 mg). Compounds **27** (2.5 mg) and **28** (2.4 mg) were prepared in the same procedure from compound **23** (8.2 mg).

Compound 25 (29): ^1H NMR (800 MHz, MeOD-d_4) δ 6.77 (1 H, t, *J* = 8.0 Hz, H-11), 6.61 (1 H, s, H-2), 6.46 (1 H, s, H-4), 6.29 (1 H, s, H-7), 6.24 (1 H, d, *J* = 8.0 Hz, H-12), 6.13 (1 H, d, *J* = 8.0 Hz, H-10), 5.52 (1 H, dd,

J = 9.2, 4.4, H-15), 4.64 (1 H, t, *J* = 6.4 Hz, H-28), 4.29 (1 H, dd, *J* = 10.0, 4.1 Hz, H-23), 4.23 (1 H, dddd, *J* = 10.5, 7.3, 6.9, 4.0 Hz, H-17), 3.96 (1 H, m, H-33), 2.80 (1 H, dd, *J* = 15.8, 6.4 Hz, H-29), 2.75 (1 H, dd, *J* = 15.8, 6.4 Hz, H-29), 2.45 (1 H, dd, *J* = 14.1, 4.3 Hz, H-32), 2.33 (2 H, m, H-25), 2.32 (1 H, dd, *J* = 14.1, 6.8 Hz, H-32), 2.23 (1 H, m, H-24), 2.18 (3 H, s, H-14), 2.02 (1 H, ddd, *J* = 14.1, 10.0, 6.9, H-16), 1.94 (1 H, m, H-24), 1.75 (1 H, ddd, *J* = 14.1, 7.3, 3.3, H-16), 1.50 (1 H, ddd, *J* = 14.1, 10.5, 4.5, H-18), 1.39 (1 H, ddd, *J* = 14.1, 9.7, 4.0, H-18), 1.45 (2 H, m, H-34), 1.29 (1 H, m, H-19), 1.31-1.22 (14 H, overlap, H-35─H-41), 0.93 (3 H, t, *J* = 7.1 Hz, H-42), 0.88 (3 H, d, *J* = 6.9 Hz, H-20), 0.87 (3 H, d, *J* = 6.9 Hz, H-21); LRESIMS *m/z* 798.3, $[M\text{-}H_2O+H]^+$ (Calcd for $C_{42}H_{64}N_5O_{10}$ 798.4).

Compound 26 (30): ^{1}H NMR (900 MHz, MeOD-d_4) δ 6.77 (1 H, t, *J* = 8.0 Hz, H-11), 6.63 (1 H, s, H-2), 6.45 (1 H, s, H-4), 6.27 (1 H, s, H-7), 6.24 (1 H, d, *J* = 8.0 Hz, H-12), 6.11 (1 H, d, *J* = 8.0 Hz, H-10), 5.38 (1 H, dd, *J* = 10.6, 2.1, H-15), 4.65 (1 H, dd, *J* = 7.2, 6.3 Hz, H-28), 4.32 (1 H, dd, *J* = 9.4, 4.3 Hz, H-23), 4.29 (1 H, dddd, *J* = 9.8, 9.8, 4.3, 4.3 Hz, H-17), 3.94 (1 H, m, H-33), 2.79 (1 H, dd, *J* = 15.9, 7.2 Hz, H-29), 2.68 (1 H, dd, *J* = 15.9, 6.3 Hz, H-29), 2.40 (1 H, dd, *J* = 14.4, 4.2 Hz, H-32), 2.39 (2 H, overlap, H-25), 2.30 (1 H, dd, *J* = 14.4, 8.6 Hz, H-32), 2.23 (1 H, m, H-24), 2.18 (3 H, s, H-14), 2.03 (1 H, m, H-24), 1.94 (1 H, ddd, *J* = 14.3, 10.6, 4.3, H-16), 1.72

(1 H, ddd, *J* = 14.3, 9.8, 2.1, H-16), 1.66 (1 H, m, H-19), 1.54 (1 H, ddd, *J* = 14.4, 10.4, 4.3, H-18), 1.41 (1 H, ddd, *J* = 14.4, 9.8, 4.4, H-18), 1.45 (2 H, m, H-34), 1.33-1.25 (14 H, overlap, H-35─H-41), 0.92 (3 H, d, *J* = 6.7 Hz, H-20), 0.91 (3 H, d, *J* = 6.7 Hz, H-21), 0.89 (3 H, t, *J* = 7.2 Hz, H-42); LRESIMS *m/z* 798.3, $[M\text{-}H_2O+H]^+$ (Calcd for $C_{42}H_{64}N_5O_{10}$ 798.4).

Compound 27 (31): ^{1}H NMR (900 MHz, MeOD-d_4) δ 6.77 (1 H, t, *J* = 8.0 Hz, H-11), 6.61 (1 H, s, H-2), 6.46 (1 H, s, H-4), 6.31 (1 H, s, H-7), 6.24 (1 H, d, *J* = 8.0 Hz, H-12), 6.13 (1 H, d, *J* = 8.0 Hz, H-10), 5.50 (1 H, dd, *J* = 9.2, 4.4, H-15), 4.65 (1 H, t, *J* = 6.4 Hz, H-28), 4.26 (1 H, dd, *J* = 9.8, 4.2 Hz, H-23), 4.15 (1 H, dddd, *J* = 10.1, 7.2, 6.8, 4.7 Hz, H-17), 3.98 (1 H, m, H-33), 2.79 (1 H, dd, *J* = 15.8, 6.4 Hz, H-29), 2.73 (1 H, dd, *J* = 15.8, 6.4 Hz, H-29), 2.44 (1 H, dd, *J* = 14.3, 4.1 Hz, H-32), 2.33 (1 H, dd, *J* = 14.3, 8.6 Hz, H-32), 2.31 (2 H, m, H-25), 2.19 (1 H, overlap, H-24), 2.18 (3 H, s, H-14), 2.03 (1 H, ddd, *J* = 14.2, 9.2, 7.2, H-16), 1.91 (1 H, m, H-24), 1.81 (1 H, ddd, *J* = 14.2, 6.8, 4.4, H-16), 1.59 (1 H, m, H-19), 1.50 (1 H, overlap, H-18), 1.40 (1 H, ddd, *J* = 13.7, 9.1, 4.7, H-18), 1.48 (1 H, m, H-34), 1.44 (1 H, m, H-34), 1.35-1.25 (14 H, overlap, H-35─H-41), 0.89 (3 H, t, *J* = 6.5 Hz, H-42), 0.89 (3 H, d, *J* = 6.5 Hz, H-20), 0.86 (3 H, d, *J* = 6.5 Hz, H-21); LRESIMS *m/z* 798.2, $[M\text{-}H_2O+H]^+$ (Calcd for $C_{42}H_{64}N_5O_{10}$ 798.4).

Compound 28 (32): ^{1}H NMR (900 MHz, MeOD-d_4) δ 6.76 (1 H, t, J = 8.1 Hz, H-11), 6.60 (1 H, s, H-2), 6.45 (1 H, s, H-4), 6.28 (1 H, s, H-7), 6.23 (1 H, d, J = 8.1 Hz, H-12), 6.18 (1 H, d, J = 8.1 Hz, H-10), 5.50 (1 H, dd, J = 10.7, 2.1, H-15), 4.66 (1 H, t, J = 6.4 Hz, H-28), 4.38 (1 H, dd, J = 10.2, 3.6 Hz, H-23), 4.28 (1 H, dddd, J = 9.5, 9.4, 4.9, 4.2 Hz, H-17), 3.98 (1 H, m, H-33), 2.80 (1 H, dd, J = 15.7, 6.4 Hz, H-29), 2.74 (1 H, dd, J = 15.7, 6.4 Hz, H-29), 2.43 (1 H, dd, J = 14.3, 4.1 Hz, H-32), 2.33 (1 H, dd, J = 14.3, 8.6 Hz, H-32), 2.31 (2 H, m, H-25), 2.31 (1 H, overlap, H-24), 2.18 (3 H, s, H-14), 1.97 (1 H, ddd, J = 14.7, 10.7, 4.2, H-16), 1.95 (1 H, m, H-24), 1.69 (1 H, ddd, J = 14.7, 9.4, 2.1, H-16), 1.68 (1 H, m, H-19), 1.64 (1 H, J = 14.2, 10.4, 4.9, H-18), 1.48 (2 H, m, H-34), 1.44 (1 H, ddd, J = 14.2, 9.5, 4.5, H-18), 1.35-1.25 (14 H, overlap, H-35─H-41), 0.94 (3 H, d, J = 6.5 Hz, H-20), 0.91 (3 H, d, J = 6.5 Hz, H-21), 0.89 (3 H, t, J = 6.5 Hz, H-42); LRESIMS *m/z* 798.3, $[M\text{-}H_2O+H]^+$ (Calcd for $C_{42}H_{64}N_5O_{10}$ 798.4).

Computational Analysis. The ground-state geometries were optimized with density functional theory (DFT) calculations using Turbomole 6.5 with the basis set def-SV(P) for all atoms at the DFT level, using the B3LYP functional; the ground states were further confirmed by a harmonic frequency calculation. The calculated ECD data corresponding to the optimized structures were obtained using TDDFT with the basis set def2-

TZVPP for all atoms at the DFT level, using the B3LYP functional. The ECD spectra were simulated by overlapping for each traction, where σ is the width of the band at 1/e height. Δ*Ei* and *Ri* are the excitation energies and rotatory strengths for transition *i*, respectively

Biological assays. Five human cancer cell lines (A549, HCT116, SNU638, SK-HEP1, and MDA-MB231; 3.5×10^4 cells/mL) were treated with asperphenins A, B, and cycloasperhenins A, B, and other several reduction products of asperphenins A, B for 3 days. After treatment, cells were fixed with a 10% TCA solution, and cell viability was determined using a sulforhodamine B (SRB) assay. The results were expressed as percentages relative to solvent-treated control incubations, and IC50 values were calculated using nonlinear regression analysis (percent survival versus concentration).

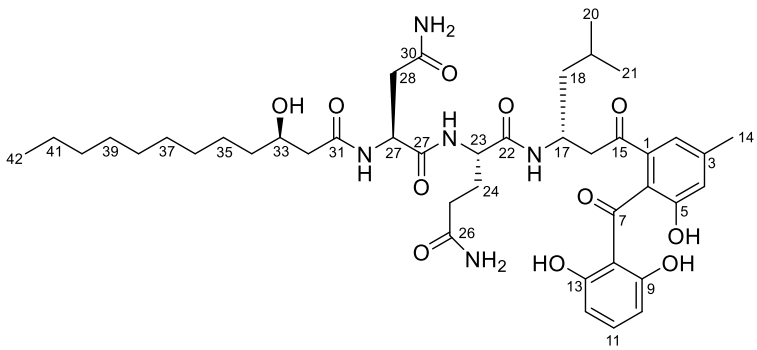

Table 8. ^{13}C and ^{1}H NMR assignment for compound **17** in DMSO-d_6[a]

Position	δ_C	δ_H
1	136.0, C	
2	120.4, CH	7.21, s
3	138.5, C	
4	120.2, CH	6.84, s
5	153.4, C	
6	128.6, C	
7	201.8, C	
8	111.1, C	
9	161.6, C	
10	106.8, CH	6.19, d (8.3)
11	135.7, CH	7.15, t (8.3)
12	106.8, CH	6.19, d (8.3)
13	161.6, C	
14	20.8, CH_3	2.29, s
15	198.3, C	
16	44.7, CH_2	3.00, dd (16.5, 4.5); 2.85, dd (16.5, 8.7)
17	43.4, CH	4.13, m
17-NH		7.66, d (8.3)
18	42.4, CH_2	1.28, m[b]; 0.98, ddd (13.7, 9.4, 3.4)

19	24.1, CH	1.45, m
20	21.3, CH_3	0.66, d (6.7)
21	23.3, CH_3	0.71, d (6.7)
22	170.2, C	
23	52.6, CH	4.02, m
23-NH		7.92, d (7.7)
24	27.6, CH_2	1.87, m; 1.65, m
25	31.4, CH_2	2.02, t (7.9); 2.02, t (7.9)
26	173.9, C	
26-NH_2		7.14, brs; 6.70, brs
27	170.9, C	
28	49.8, CH	4.44, m
28-NH		8.04, d (7.5)
29	36.9, CH_2	2.40, m[b]
30	171.8, C	
30-NH_2		7.39, brs; 6.91, brs
31	171.2, C	
32	43.7, CH_2	2.18, m[b]
33	67.5, CH	3.75, m
33-OH		4.59, brs
34	37.0, CH_2	1.30, m[b]; 1.30, m[b]
35	25.1, CH_2	1.19, m[b]; 1.19, m[b]
36	31.3, CH_2	1.19, m[b]; 1.19, m[b]
37	29.1, CH_2	1.19, m[b]; 1.19, m[b]
38	29.1, CH_2	1.19, m[b]; 1.19, m[b]
39	29.0, CH_2	1.19, m[b]; 1.19, m[b]
40	28.7, CH_2	1.19, m[b]; 1.19, m[b]
41	22.1, CH_2	1.21, m[b]; 1.21, m[b]
42	13.9, CH_3	0.81, t (7.0)

[a] ^1H and ^{13}C NMR data were recorded at 600 and 150 MHz, respectively; [b]Overlapped signals

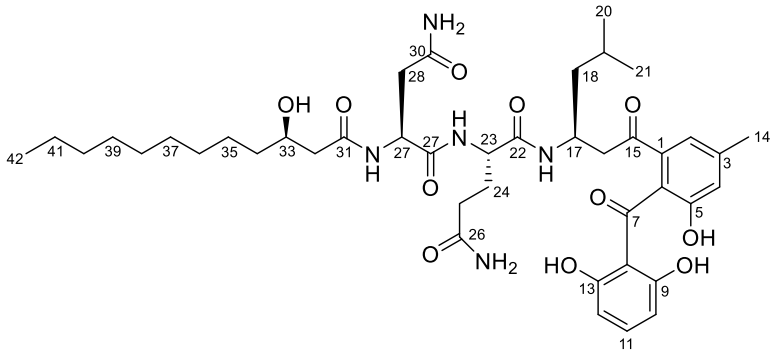

Table 9. ^{13}C and ^{1}H NMR assignment for compound **18** in DMSO-d_6[a]

Position	δ_C	δ_H
1	136.0, C	
2	120.3, CH	7.21, s
3	138.6, C	
4	120.5, CH	6.84, s
5	153.4, C	
6	128.7, C	
7	201.8, C	
8	111.1, C	
9	161.6, C	
10	106.8, CH	6.19, d (8.1)
11	135.7, CH	7.15, t (8.1)
12	106.8, CH	6.19, d (8.1)
13	161.6, C	
14	20.8, CH_3	2.29, s
15	198.4, C	
16	44.6, CH_2	2.97, dd (16.4, 4.2); 2.85, dd (16.4, 8.5)
17	43.5, CH	4.13, brs
17-NH		7.63, d (8.2)
18	42.6, CH_2	1.34, m[b]; 1.01, m[b]
19	24.2, CH	1.46, m

20	21.4, CH_3	0.69, d (6.4)
21	23.4, CH_3	0.74, d (6.4)
22	170.4, C	
23	52.7, CH	4.02, brs
23-NH		8.03, d (8.4)
24	27.5, CH_2	1.87, m; 1.65, m
25	31.5, CH_2	2.02, m[b]; 2.02, m[b]
26	174.1, C	
26-NH_2		7.16, brs; 6.74, brs
27	171.0, C	
28	49.9, CH	4.46, ddd (6.9, 6.9, 5.1)
28-NH		8.05, d (7.5)
29	36.9, CH_2	2.53, dd (15.6, 6.9); 2.42, dd (15.6, 6.9)
30	171.9, C	
30-NH_2		7.41, brs; 6.95, brs
31	171.3, C	
32	43.7, CH_2	2.18, m[b]; 2.18, m[b]
33	67.5, CH	3.75, m
33-OH		4.60, brs
34	37.0, CH_2	1.30, m[b]; 1.30, m[b]
35	25.1, CH_2	1.30, m[b]; 1.19, m[b]
36	31.3, CH_2	1.19, m[b]; 1.19, m[b]
37	29.1, CH_2	1.19, m[b]; 1.19, m[b]
38	29.1, CH_2	1.19, m[b]; 1.19, m[b]
39	29.0, CH_2	1.19, m[b]; 1.19, m[b]
40	28.8, CH_2	1.19, m[b]; 1.19, m[b]
41	22.1, CH_2	1.19, m[b]; 1.19, m[b]
42	14.0, CH_3	0.81, t (6.7)

[a] ^{1}H and ^{13}C NMR data were recorded at 600 and 150 MHz, respectively; [b]Overlapped signals

Table 10. Results of bioactivity tests (compounds **17-24, 26-28**).

>50	IC_{50}				
	A549	HCT116	SNU638	SK-HEP1	MDA-MB231
17	25.7	29.5	4.8	2.9	1.9
18	38.7	2.2	8.0	3.5	4.3
19	>50	>50	>50	>50	>50
20	>50	35.0	35.0	31.5	42.4
21	>50	29.5	39.3	36.9	45.4
22	>50	48.2	48.6	41.4	>50
23	>50	36.8	43.3	48.1	>50
24	>50	>50	>50	>50	>50
26	>50	>50	>50	>50	>50
27	>50	>50	>50	>50	>50
28	>50	>50	>50	>50	>50
Doxorubicin	0.4	1.8	0.3	0.4	0.6

V. Conclusion

The purpose of this work is the investigation of new bioactive metabolites from marine-derived fungi. Based upon chemical analysis and bioassay, novel substances from marine-derived fungi have been isolated and demonstrated the biomedical potential as new drug candidates.

LC-ESIMS analysis and bioactivity studies of selected two fungal strains lead to isolation of 9 novel compounds and 9 known compounds. These compounds have been structurally elucidated by combined spectroscopic methods and chemical analysis. The structures of these 18 compounds are belonged to various structural classes and have been derived from various biogenetic origins.

Diverse bioassay tests related to anticancer, antimicrobial, enzyme-inhibitory, and quinone reductase activities have been performed. Some of the isolated compounds showed potent bioactivities anticancer and quinone reductase. Structure-activity relationships were also deduced.

Part B.

Simultaneous Analysis of Herbal Medicines by HPLC-DAD-ELSD-MS

I. Introduction

Traditional herbal medicines have been practiced to maintain health and treat diseases especially in the Asia communities for more than 2,000 years. Herbal medicines are a comprehensive and holistic approach of medical practice with their own principles, diagnosis, and treatment system that balancing body function. They consider that human body is related to its own physical, natural and social environment.[76] Recently, herbal medicines were used increasingly not only complement of conventional medical care but also functional food and dietary supplements in worldwide. According to U.S. national surveys conducted in 2002, over 75% of Asian-Americans and 20% of adults had used herbal therapies in the past year.[77]

Herbal medicines are prescribed alone for the treatment of various chronic diseases as well as in combination with other herbal ingredients in traditional herbal prescriptions.[78] The combined use or processing of plants is thought to have favorable effects such as reduction of toxicity and side effects, potentiation of biological effects, alteration of properties or functions, microbiological prevention, correction of unpleasant tastes and an increase in purity by reduction of contaminants.[79]

Increment of worldwide attention and concomitant pharmaceutical

research has made it essential to carry out the quality control measurement for the herbal medicines. However, serious hindrance has been attributed to the lack of recognition and regulation of professions, qualified practitioners, quality-controlled herbal medicines, and evidence-based clinical studies.[80] Thus it is urgently needed to establish a comprehensive qualified evaluation method that could accurately reflect the quality of herbal medicines.

The purpose of this study is developing simultaneous analysis methods of bioactive compounds in herbal medicines. Two widely used herbal medicines, which are Kalopanacis Cortex (the dried stem bark of *Kalopanax pictus*) and semen Ziziphus jujuba were subjected to the current study. In herbal medicines, it is hard to consider that single or a few compounds would determine the overall pharmacological activities. Rather, it is more likely that multiple compounds act simultaneously and attribute to the therapeutic function of the herbal medicine. For this reason, every bioactive metabolites in the selected herbal medicines were analyzed and determined. In particular, three phenolics and nine hedergenin saponins were selected for the analysis of Kalopanacis Cortex. Moreover, one alkaloid, five flavonoid saponins and three jujuboside saponins from semen Ziziphus jujuba were also analyzed.

The methods based on HPLC-DAD-ELSD-MS was established for

the quantitative and qualitative analysis of a selected folk medicines. Various validation parameters, such as linearity, limit of detection, limit of quantification, recovery, accuracy, and precision, were successfully obtained. In addition, the efficiencies of diverse extraction methods were compared for the development of a standard analytic method. The verified methods were successfully applied to the quantitative determination of representative metabolites in commercial samples from Korea, Myanmar and China.

II. Quantification and Identification of Bioactive Metabolites from Kalopanacis Cortex by HPLC with Evaporative Light Scattering Detection and ESI Quadrupole TOF MS

A method based on HPLC-ELSD-Q-TOF-MS was established for the simultaneous determination of twelve bioactive metabolites from the Kalopanacis Cortex. Validation parameters, such as linearity, limit of detection, limit of quantification, recovery, accuracy, and precision, were successfully obtained. In addition, the efficiencies of diverse extraction methods were compared for the development of a standard analytic method. The verified method was successfully applied to the quantitative determination of twelve representative metabolites in sixty-one Kalopanacis Cortex samples from Korea and China. The quantitation results demonstrated that six compounds, coniferin (**33**), kalopanaxsaponin C (**40**), septemlosides II (**38**), III (**36**), C (**39**), and D (**37**), which exhibited distinct regional patterns in KC samples, could serve as marker compounds to distinguish KC from Korea and China.

2-1. Introduction

Kalopanax pictus, which belongs to the Araliaceae family, is a deciduous tree that is widely distributed in east Asian countries. Kalopanacis

Cortex, the dried stem bark of *Kalopanax pictus*, has been used as a traditional medicine to treat diverse conditions, such as diabetes mellitus, lumbago, neurotic pain, paralysis, and rheumatic arthritis.[81,82]

Chemical investigations have revealed that the major constituents of this plant are triterpene saponins of the hederagenin class,[83-85] with other constituents including phenolics [81] and lignans.[86]

The crude extract of the stem bark of *K. pictus* has been reported to possess diverse bioactivities, such as antinociceptive,[87,88] antidiabetic,[89] anti-inflammatory[90-92] and cytotoxic activities.[93,94] Kalopanaxsaponin B, a hederagenin bisdesmosidic saponin and one of the major constituents of KC, showed potent antimutagenic activity against aflatoxin.[93] Kalopanaxsaponin A and I, monodesmosides, showed anti-inflammatory and anti-rheumatoidal activities.[95] Additionally, the phenolic compounds such as liriodendrin and syringin exhibited significant hepatoprotective effect.[96]

To date, diverse efforts have been reported to develop HPLC-UV methods to analyze these therapeutical constituents in KC. However, these methods have been restricted to limited marker compounds, such as one triterpene saponin [96] or only phenolic constituents.[97,98] This is mainly attributed to the lack of chromophore in triterpene saponins, the major components of KC, which significantly hinders their analysis by UV

detection due to the high level of baseline noise and poor sensitivity. Furthermore, a complex mixture of many different compounds is responsible for all of the pharmacological activities in herbal medicines.[99] Therefore, it is necessary to develop a new method for the simultaneous analysis of the overall chemical components of KC.

The present study aimed to develop a simple and reliable HPLC method involving evaporative light scattering detector (ELSD) and electrospray ionization quadrupole time-of-flight (ESI-QTOF) mass detectors to quantify and identify triterpene saponins and phenolics in KC. ELSD was selected as the detector due to its capacity for the sensitive detection of nonvolatile analytes regardless of the presence of chromophores.[100,101] HPLC-ESI-QTOF-MS was also used to confirm peak identification by comparing the high resolution molecular mass and molecular formulas of the constituents.

The efficiency of the developed HPLC-ELSD methods was successfully verified by diverse validation parameters such as the linearity, limits of detection and quantification, accuracy, precision, repeatability, and stability. In addition, the efficiencies of different extraction methods were compared. Using the developed methods, the contents of marker compounds in sixty-one commercial KC samples from Korea and China were

quantitatively analyzed and compared.

During this study, one new hederagenin saponin, designated to be septemloside D, was isolated and included as one of the representative metabolites for the development of the analytical method. The structure of this compound was unambiguously elucidated by a combination of spectroscopic methods including IR, MS, and 1D and 2D NMR analyses.

Significant differences between the concentrations of the phenolic compound coniferin, triterpene saponins septemlosides II and III, septemlosides C and D, and kalopanaxsaponin C from Korean and Chinese KC samples demonstrated their potential to serve as marker compounds for the quality control and geographical discrimination of KC samples upon the validation of their biological activities.

2-2. Experimental section

Plant materials - Sixty-one KC samples were collected and identified from various locations in Korea and China, and were provided by Prof. Je-Hyun Lee, Dongguk University, Korea thorough the National Center for Standardization of Herbal Medicine, Korea. Of the KC samples, eighteen (K-01~K-18) were collected from Korea, and forty-three (C-01~C-43) were collected from China. Voucher specimens of all of the KC samples were

deposited at the Natural Products Research Institute, Seoul National University (Table S1).

Extraction, isolation, and structure determination - KC (C-16: 280 g for extraction) was repeatedly extracted with methanol (1 L × 3). The crude extract was partitioned between H_2O and *n*-BuOH. The *n*-BuOH extract was subjected to reverse-phase vacuum flash chromatography using sequential mixtures of H_2O and MeOH (elution order: 50%, 40%, 30%, 20%, 10% aqueous MeOH and 100% MeOH) and acetone as eluents. For the HPLC-ELSD analysis, the fractions that eluted with 50:50 H_2O-MeOH and 40:60 H_2O-MeOH were chosen for separation. The 50:50 H_2O-MeOH fraction was separated by semi-preparative reverse-phase HPLC (10 × 250 mm, 5.0 μm) using H_2O-MeOH (65:35) as the eluent followed by purification with reverse-phase HPLC (4.6 × 250 mm, 5.0 μm) using H_2O-MeCN (85:15) to yield compound **33** (65.3 mg).

The fraction that eluted with H_2O-MeOH (40:60) was separated by semi-preparative reverse-phase HPLC (10 × 250 mm, 5.0 μm) using H_2O-MeOH (50:50) as the eluent to yield, in order of elution, compounds **34** (40.1 mg), **35** (32.4 mg), **36** (20.6 mg) and **37** (21.3 mg). Comparison of the NMR and MS data with reported values led to the identification of the structures of

the known compounds **34**, **36**, **38**, **39** as chlorogenic acid (**34**), septemloside III (**36**),[102] septemloside II (**38**),[103] (http://www.dissertationtopic.net/doc/1588727), septemloside C (**39**),[103] respectively, while compound **37** was determined as a new hederagenin saponin.

Compound **37** was obtained as a white, amorphous powder. The molecular formula was determined to be $C_{74}H_{120}O_{38}$ from the pseudomolecular ion peak $[M+H]^+$ at *m/z* 1616.7458 (calcd for $C_{74}H_{120}O_{38,}$ 1616.7528) in the HR-ESI-QTOF-MS. The aglycone moiety of **37** was determined to be the same as in the other hedegrin triterpenoids by 2D NMR analyses as well as comparison of the spectroscopic data with literature data.[103] The proton-proton COSY, HSQC and HMBC experiments successfully assigned all of the protons and carbons in the aglycone moiety (Table 11).

The anomeric proton signals at δ_H 6.41 (1 H, d, *J* = 2.5 Hz), 6.28 (1 H, br s), 6.09 (1 H, d, *J* = 8.5 Hz), 5.83 (1 H, s), 5.29 (1 H, d, *J* = 7.6 Hz), 5.06 (1 H, d, *J* = 6.7 Hz), 4.98 (1 H, d, *J* = 8.2 Hz), and 4.84 (1 H, d, *J* = 7.8 Hz) showed HMQC correlations with the carbon signals at δ_C 109.0, 101.5, 94.4, 102.8, 107.2, 104.6, 104.8 and 103.8, respectively, indicating the presence of eight sugar units in **37**. The downfield chemical shift of C-3 (δ_C

81.3) and upfield chemical shift of C-28 (δ_C 176.5) in the ^{13}C NMR spectrum of **37** (Table 11) indicated that this compound is a bisdesmosidic saponin.[103]

However, the acid hydrolysis of **37** yielded a sugar mixture consisting of only four sugar residues D-xylose, D-glucose, L-rhamnose and L-arabinose, which were identified by RP-HPLC-UV analysis using authentic samples as references. The peak intensity of each sugar unit in conjunction with the ^{1}H and ^{13}C-NMR analyses, indicated that the eight sugar units of **37** were indeed consisted of each two four-sugar units. The protons of each of the monosaccharide residues were assigned starting with the anomeric protons via 1D and 2D TOCSY experiments. The presence of a furanoarabinose was determined from its distinct proton-proton coupling constants (2.4 Hz for H-1; 4.6 Hz and 2.4 Hz for H-2) and carbon chemical shifts (δ_C 109.0, 82.7, 77.9, 85.7, 62.8) (Table 11), while the remaining seven sugars contained the same pyranose backbone as in septemloside II.[103]

Given this information, the bisdesmosidic nature of **37** as well as its full structure was determined by HMBC experiments. First, the sugar chain at C-3 was elucidated to be *β*-D-xylopyranosyl-(1→4)-*β*-D-xyloyranosyl-(1→3)-*α*-L-rhamnopyranosyl-(1→2)-*β*-D-arabinopyranosyl from the following HMBC correlations: H-1 of xylose-II with C-4 of xylose-I, H-1 of xylose-I with C-3 of rhamnose-I, H-1 of rhamnose-I with C-2 of arabinose-I,

H-1 of arabinose-I with C-3 of the aglycone. Similarly, the sugar chain at C-28 was also elucidated to be [*α*-L-arabinofuranosyl-(1→2)]-*α*-L-rhamnopyranosyl-(1→4)-*β*-D-glucopyranosyl-(1→6)-*β*-D-glucopyranosyl. The structure of *α*-L-arabinofuranose was also confirmed by the HMBC correlations of the H-1 anomeric proton with the C-4 carbon at δ_C 77.9 in the same sugar residue. Hence, the structure of **37** was identified as 3-O-*β*-D-xylopyranosyl-(1→4)-*β*-D-xyloyranosyl-(1→3)-*α*-L-rhamnopyranosyl-(1→2)-*β*-D-arabinopyranosyl hederagenin 28-O-[*α*-L-arabinofuranosyl-(1→2)]-*α*-L-rhamnopyranosyl-(1→4)-*β*-D-glucopyranosyl-(1→6)-*β*-D-glucopyranosyl ester, and designated to be septemloside D.

Acid hydrolysis and HPLC analysis of compound 37. A solution of **37** (2.0 mg) in 4 N TFA (0.5 mL) was stirred at 110 ^{o}C for 4 h. After it was cooled to room temperature, the solution was concentrated by rotary evaporation and kept under high vacuum for 12 h. The residue was dissolved in pyridine (0.5 mL) containing L-cysteine methyl ester hydrochloride (0.5 mg) and heated at 60 ^{o}C for 1 h. A 0.1 mL solution of *o*-tolyl isothiocyanate (0.5 mg) in pyridine (0.5 mL) was added to the mixture, which was then heated at 60 ^{o}C for 1 h. The reaction mixture was directly analyzed by reverse-phase HPLC.[104] Peaks of hydrolysate derivatives were detected at 21.52, 24.59, 25.57, and 38.19 min. The retention times of the authentic sugar

samples after treating simultaneously with L-cysteine methyl ester hydrochloride and *o*-tolyl isothiocyanate were 19.66 (L-glucose), 21.56 (D-glucose), 23.75 (L-xylose), 24.55 (L-arabinose), 25.56 (D-xylose), 26.67 (D-arabinose) and 38.15 (L-rhamnose) min. Co-injection of the hydrolysate derivatives with authentic samples of D-glucose, L-arabinose, D-xylose, and L-rhamnose gave single peaks at 21.54, 24.62, 25.54 and 38.23 min, respectively.

Chemicals and reagents. Coniferin (**33**), liriodendrin (**35**), kalopanaxsaponin C (**40**), sieboldianoside A (**41**), kalopanaxsaponin B (**42**), cussonoside A (**43**), and kalopanaxsaponin A (**44**) were provided from the National Center for Standardization of Herbal Medicine, Korea. Chlorogenic acid (**34**), septemloside III (**36**), septemloside D (**37**), septemloside II (**38**), and septemloside C (**39**) were isolated and purified from KC using a series of chromatographic procedures. Glycyrrhizin was used as an internal standard compound and was obtained from Sigma-Aldrich (USA). Methanol, acetonitrile, and water were HPLC grade and purchased from Burdick & Jackson (USA), and analytical grade ethanol was purchased from Duksan (Korea).

Instrumentation and chromatographic conditions. The HPLC system consisted of Agilent 1200 series equipped with an autosampler, a column oven, a binary pump, an ELSD detector (Agilent Technologies, 1260 Infinity), and a degasser (Agilent Technologies, Avondale, CA, USA). Separation was performed on an OptimaPak C18 (4.6 × 250 mm, 5.0 μm) analytical column. A gradient elution of A (water, 0.1% formic acid) and B (acetonitrile, 0.1% formic acid) was used (0 min, 15% B; 25 min, 25% B; 55 min, 30% B; 60 min, 40% B; 65 min, 45% B; 75 min, 70% B; 80 min, 100% B in A v/v). The analytes were monitored with ELSD. Standard or sample solutions (10 μL) were directly injected to the HPLC system. The mobile phase flow rate was 0.3 mL/min and the column temperature was set to 25 ^{o}C.

The ESI-QTOF-MS was performed with an Agilent 1260 series HPLC equipped with a binary pump (Agilent Technologies, 1290 Infinity) and coupled to an Accurate-Mass Q-TOF LC/MS (Agilent Technologies, 6530). All of the mass data were obtained in positive ion mode $[M + Na]^+$ with an ESI source and the mass range set to *m/z* 100 – 2000. The conditions of the ESI source were as follows: capillary voltage, 4000 V; nebulizing gas (N_2) pressure, 30 psig; drying gas (N_2) flow rate, 10.0 L/min; drying gas temperature, 350 ^{o}C; spectra rate, 1.03 Hz; sheath gas temperature, 350 ^{o}C; sheath gas flow 12 L/min. The operations and data analysis were performed

using the Agilent LC-MS-Q-TOF Mass Hunter Data Acquisition Software Ver. A.01.00 (Agilent Technologies) and the Agilent Mass Hunter Qualitative Analysis Software B.02.01, respectively.

Preparation of standard solution. Stock solution (1 mg/mL) of the coniferin (**33**), chlorogenic acid (**34**), liriodendrin (**35**), septemloside III (**36**), septemloside D (**37**), septemloside II (**38**), septemloside C (**39**), kalopanaxsaponin C (**40**), sieboldianoside A (**41**), kalopanaxsaponin B (**42**), cussonoside A (**43**), and kalopanaxsaponin A (**44**) (Figure 27) isolated from KC were prepared individually in methanol. An appropriate amount of each standard solution was mixed and diluted to a series of concentrations as indicated for calibration.

Preparation of test samples. 200 mg of KC and 1 mg of an internal standard compound were accurately weighed and extracted with 10 mL of 50% aqueous methanol by sonication at room temperature for 30 min. The solution was filtered through a 0.45 μm membrane filter prior to use. A 10 μL aliquot was injected for analysis.

Calibration curves, limit of detection and limit of quantification. A methanol stock solution that contained the twelve analytes was prepared and diluted to a series of appropriate concentrations for the construction of

calibration curves. Mixed standard solutions at six different concentrations were loaded onto the HPLC in triplicate. The calibration function of each individual compound was calculated by plotting the logarithms of the peak areas versus the logarithms of the concentrations for each analyte. The limit of detection (LOD) and limit of quantification (LOQ) values under the chromatographic conditions used were determined separately at S/N values of 3 and 10, respectively.

Precision, repeatability and stability. Intra- and inter-day variations were chosen to determine the precision of the developed method. Using three different concentrations of the twelve standard compounds, the intra-day precision was determined by performing the analysis three times within one day, while the inter-day precision was examined by performing the analysis on three consecutive days. To evaluate the repeatability of the developed method, five independently prepared KC samples were extracted and analyzed using identical conditions. The stability was tested by repeated analysis of KC samples every 4 h within a 24 h time period at room temperature. The relative standard deviation (RSD) was used as a measure of precision, repeatability and stability.

Accuracy. Recovery was used to evaluate the accuracy of the method.

Standard addition was performed with a pre-analyzed standard solution. Three different standard mixtures were added to the KC sample. Spiked samples were prepared in triplicate and three determinations were performed. The recovery was determined according to the following formula: recovery (%) = (detected amount – original amount)/amount spiked × 100%.

5-4. Results and discussion

Optimization of HPLC conditions. The chromatographic conditions were first optimized for the simultaneous determination of representative KC metabolites belonging to two different chemical classes, phenolics and triterpene saponins. Various mixtures of acetonitrile, methanol and water were tested as the mobile phase. The mobile phase composed of acetonitrile (0.1% formic acid) and water (0.1% formic acid) achieved the best separation of the KC metabolites. To obtain the chromatographic benefit by suppressing silanol activity and provide an excess of cations in mass spectrometric analysis in positive mode, formic acid was added. The detection temperature was optimized by testing at 25, 30, 35, and 40 ^{o}C. The optimal detection temperature was determined to be 25 ^{o}C, where the baseline was stable and all of the compounds had good capacity factors, separation factors and resolutions. The ELSD parameters, such as the nebulizing gas flow rate

and drift tube temperature, were optimized to obtain the highest signals at the lowest nebulizer gas flow rate. The optimum ELSD parameters used to analyze the twelve compounds were as follows: drift tube temperature, 85 ^{o}C; nebulizing gas flow rate, 45 psig. As a result, a gradient system composed of acetonitrile (0.1% formic acid) – water (0.1% formic acid) solvent system gave the desired separation at 25 ^{o}C within a running time of 85 min (Figure 28).

Optimization of extraction conditions. To obtain a quantitative analytical method, the extraction conditions, including the extraction method, extraction solvent and extraction time, were optimized. Sonication, vortex and reflux extraction methods were compared for the selection of the optimal extraction method (Table S2) in 50% aqueous methanol as the solvent for 30 min. Aqueous methanol or ethanol solutions were also texted as the extraction solvent (Table S3) using sonication for 30 min. The yields were also compared for the extraction time of 10, 20, 30, 60, and 90 min of sonication in 50% aqueous methanol to determine the optimal extraction time (Table S4). The results indicated that most of the marker compounds showed significantly higher yields with extraction in 50% aqueous methanol for 30 min of extraction by sonication than under any of the other tested conditions.

Validation of methodology. The calibration curves showed good linearity and the correlation coefficients were found to be in the range of 0.996 – 0.999 for all of the tested compounds. The LODs and LOQs for the nine triterpene saponins were 2.5 – 4.6 and 8.5 – 15.7 μg/mL, respectively, whereas the LODs and LOQs for phenolics were 6.2 – 10.0 and 21.0 – 34.5 μg/mL, respectively (Table 12). The relative standard deviation (RSD) was used as a measurement of precision. The RSD of the intra-day and inter-day variability was less than 3.80% (Table 13). The variations in overall stability over 24 h and repeatability variations were no more than 2.24% and 3.38%, respectively. The recoveries (Table 14) of the twelve analytes were in the range of 104.21% – 95.02%. Overall, these results demonstrate that the developed method has enough accuracy, precision and sensitivity for the simultaneously quantitative analysis of the twelve representative compounds in KC extract.

HPLC-DAD-ELSD-QTOF-MS analysis of the metabolites. Because the identification of chromatographic peaks by retention time and ELSD spectrum alone may be ambiguous, HPLC-ESI-QTOF-MS was used to identify each compound by comparison of high resolution molecular mass and molecular formula in addition to the HPLC-ELSD analysis. The spectroscopic conditions were optimized in positive ion mode, and each

compound exhibited distinct quasi-molecular ions $[M + Na]^+$ in this mode (Table 15). The molecular ion and molecular formula of each compound were well matched with the chemical structures in the HPLC-ESI-QTOF-MS spectra (Table 15). In summary, twelve bioactive compounds were identified in KC extract, and the identity of each peak as **33** – **44** was clearly demonstrated.

Quantitative analysis. The developed method was applied for the measurement the concentration of marker compounds in the commercial KC samples. Sixty-one KC samples from various areas of Korea and China were prepared as described for the development of analytical method and analyzed in triplicate. The results are summarized in Table 16. Among the tested compounds, kalopanaxsaponin B, kalopanaxsaponin C, sieboldianoside A, and liriodendrin were detected in all of the KC samples, while the concentrations of the remaining eight compounds were variable and often below the detecting limits (10.0, 10.0, 3.2, 2.5, 3.4, 3.2, 3.5, and 3.4 μg/mL for chlorogenic acid, coniferin, cussonoside A, kalopanaxsaponin A, and septemlosides II, III, C and D, respectively).

Among the triterpene saponins, kalopanaxsaponin B and sieboldianoside A showed significantly higher average content levels in

Korean KC samples (28.16 ± 10.04, 18.07 ± 14.03 mg/g, respectively) than in Chinese KC samples (6.88 ± 8.93, 7.49 ± 10.23 mg/g, respectively). In contrast, kalopanaxsaponin C showed a higher concentration in Chinese KC samples (37.23 ± 15.45 mg/g) than in Korean samples (0.78 ± 0.66 mg/g). Chinese samples also contained moderate concentrations of septemlosides II (**38**) (7.94 ± 4.68 mg/g), III (**36**) (7.57 ± 4.65 mg/g), C (**39**) (3.19 ± 1.61 mg/g,), and D (**37**) (7.09 ± 3.66 mg/g), but these compounds were not detected in Korean samples. Finally, cussonoside A (**43**) and kalopanaxsaponin A (**44**) were detected at low concentration in both Korean (0.35 ± 0.20, 0.40 ± 0.22 mg/g, respectively) and Chinese KC (0.31 ± 0.16, 0.36 ± 0.26 mg/g, respectively) samples. Among the phenolics, liriodendrin (**35**) was found at a higher concentration in Korean KC samples (12.08 ± 6.22 mg/g) than Chinese samples (5.65 ± 2.61 mg/g). In contrast, chlorogenic acid (**34**) was found at a higher concentration in Chinese KC samples (3.92 ± 3.36 mg/g) than in Korean samples (1.03 ± 2.01 mg/g). Coniferin (**33**), which was detectable in all Korean, but only in a few Chinese KC samples showed one order of magnitude difference between the Korean (1.55 ± 0.65 mg/g) and Chinese (0.16 ± 0.30 mg/g) KC samples.

These results clearly demonstrated that the composition of metabolites differs significantly between the Korean and Chinese KC samples.

The variations may be due to their geographical environment. This type of trend has been widely observed in recent analyses of other herbal medicines, such as the roots of *Scrophularia buergeriana*[105] and the seed of *Cassia obtusifolia* L.[106]

The quantitation results demonstrated that six compounds, coniferin (**33**), kalopanaxsaponin C (**40**), septemlosides II (**38**), III (**36**), C (**39**), and D (**37**), which exhibited distinct regional patterns in KC samples, could serve as marker compounds to distinguish KC from Korea and China. In addition, these results clearly demonstrated that the developed HPLC-ELSD-ESI-QTOF-MS method used for the quantification and identification of several standard compounds, including both triterpene saponins and phenolics, has potential as a valuable tool for the quality control of Kalopanacis Cortex and may be applicable to the other parts of the *Kalopanax pictus* plant.

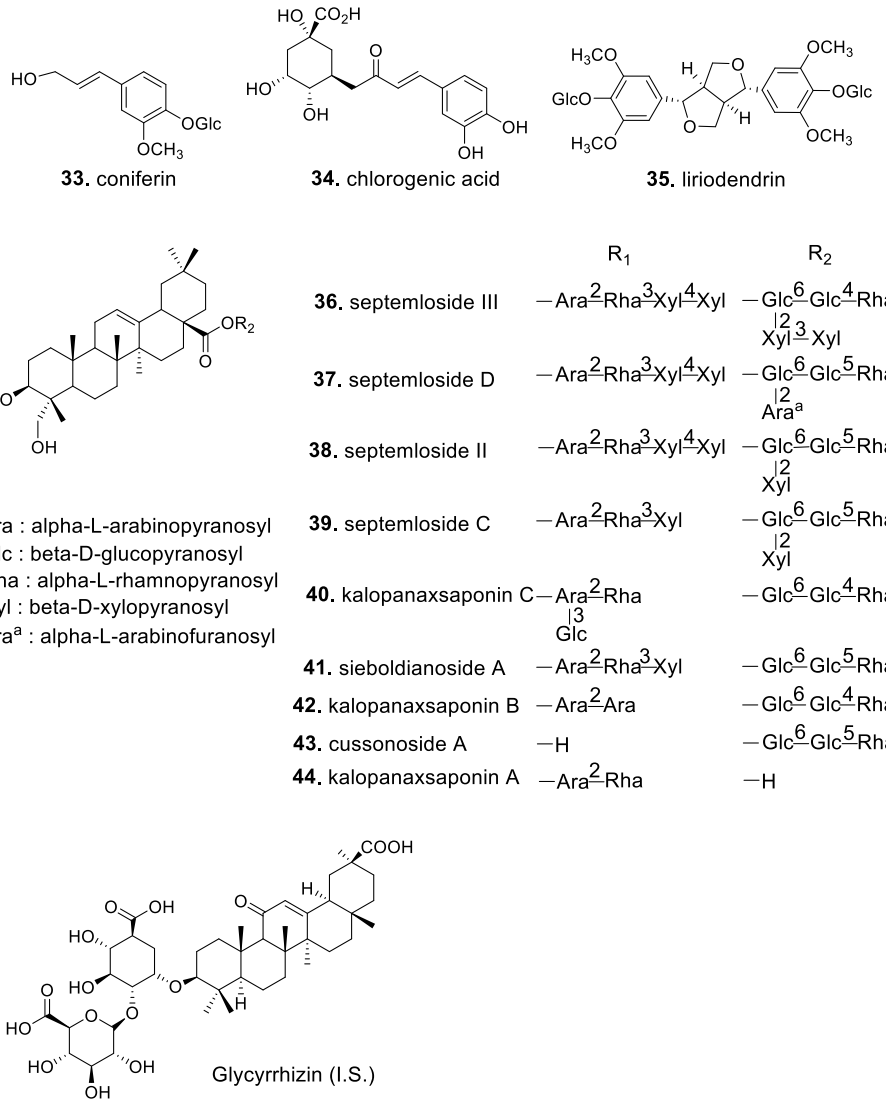

Figure 27. Chemical structures of representative compounds in KC and glycyrrhizin as an internal standard compound.

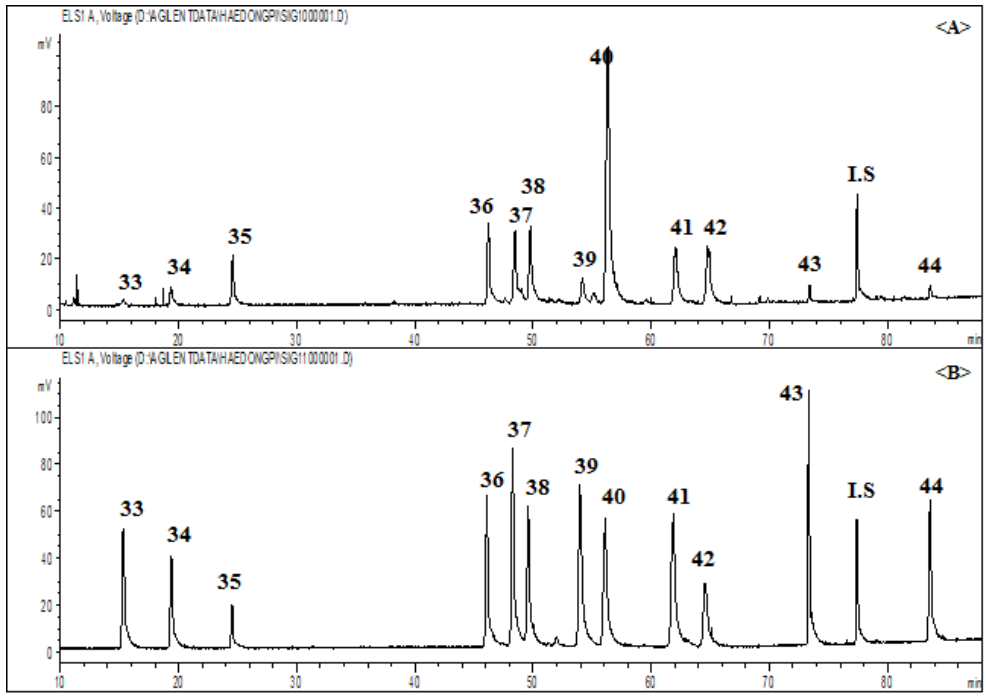

Figure 28. HPLC-ELSD chromatograms of extracts of KC (A) and standard mixture (B)

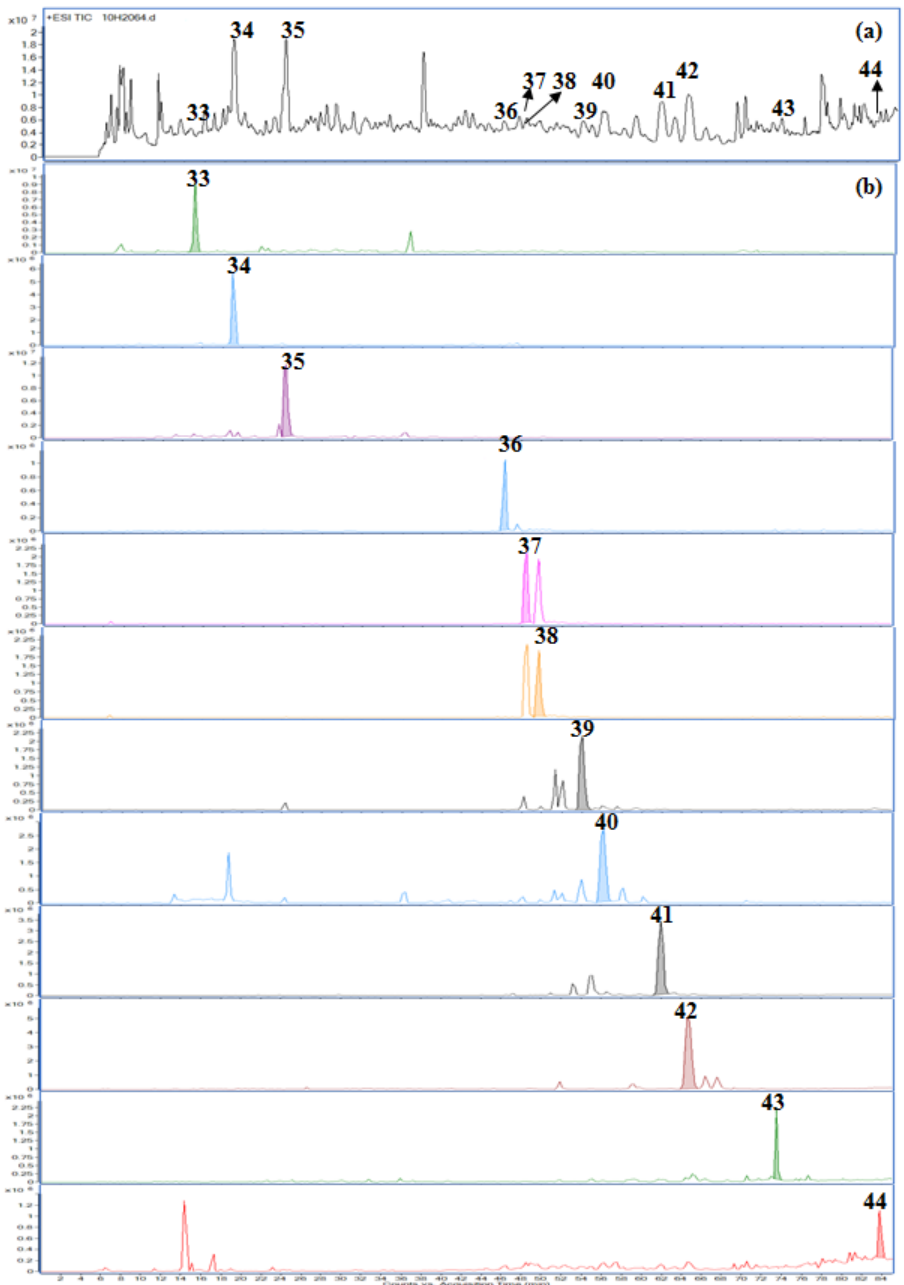

Figure 29. The total ion chromatogram (a) and extract ion chromatograms (b) of KC

Table 11. ^{1}H (600 MHz) and ^{13}C (150 MHz) data for septemloside D (**37**) (in pyridine-d_5)

Position	δ_C	δ_H	Position	δ_C	δ_H
1	39.2, CH_2	1.57, m; 1.08, m	C-3		
2	28.7, CH_2	2.19, m; 1.43, d (13.3)	Ara-I-1	104.6, CH	5.06, d (6.3)
3	81.3, CH	4.29, m	2	75.5, CH	4.56, t (7.4)
4	43.7, C		3	75.1, CH	4.03, m
5	48.3, CH	1.76, m	4	69.7, CH	4.14, m
6	18.3, CH_2	1.84, m; 1.31, m	5	66.1, CH_2	4.26, m; 3.69, m
7	32.3, CH_2	1.89, m; 1.77, m	Rha-I-1	101.5, CH	6.28, br s
8	40.1, C		2	71.9, CH	4.87, br s
9	47.8, CH	1.73, m	3	83.1, CH	4.72, m
10	37.0, C		4	73.1, CH	4.47, t (9.3)
11	23.9, CH_2	1.97, m; 1.93, m	5	69.6, CH	4.70, m
12	123.1, CH	5.43, br s	6	18.4, CH_3	1.58, d (6.0)
13	144.2, C		Xyl-I-1	107.2, CH	5.29, d (7.6)
14	42.3, C		2	75.4, CH	4.03, m
15	26.4, CH_2	2.24, m; 2.03, m	3	76.0, CH	4.24, m
16	23.4, CH_2	1.98, m; 1.92, m	4	76.8, CH	4.14, m
17	47.1, C		5	64.9, CH_2	4.33, m; 3.60, m
18	41.9, CH	3.13, dd (13.6, 4.0)	Xyl-II-1	103.8, CH	4.84, d (7.6)
19	46.2, CH_2	1.70, m; 1.20, m	2	74.0, CH	3.97, m
20	30.7, C		3	78.0, CH	4.07, m
21	34.1, CH_2	1.29, m; 1.05, m	4	71.0, CH	4.14, m
22	33.2, CH_2	1.76, m; 1.69, m	5	67.4, CH_2	4.28, m; 3.63, m
23	64.0, CH	4.23, m; 3.83, d (10.4)	C-28		
24	14.1, CH_3	1.08, s	Glc-I-1	94.4, CH	6.09, d (8.0)

25	16.3, CH_3	0.97, s	2	76.2, CH	4.31, m
26	17.5, CH_3	1.08, s	3	77.8, CH	4.07, m
27	26.0, CH_3	1.19, s	4	71.0, CH	4.21, m
28	176.5, C		5	78.5, CH	4.38, m
29	32.9, CH_3	0.85, s	6	69.0, CH	4.61, d (10.6)
30	23.8, CH_3	1.19, s	Glc-II-1	104.8, CH	4.98, d (8.2)
			2	75.4, CH	3.94, m
			3	76.6, CH	4.14, m
			4	78.8, CH	4.38, m
			5	77.2, CH	3.66, m
			6	61.4, CH_2	4.21, m; 4.08, m
			Rha-II-1	102.8, CH	5.83, s
			2	72.6, CH	4.66, br s
			3	72.8, CH	4.54,dd (8.9, 2.8)
			4	73.9, CH	4.31, m
			5	70.4, CH	4.93, dd (6.5, 2.8)
			6	18.5, CH_3	1.70, d (6.0)
			Ara-II-1	109.0, CH	6.41, d (2.4)
			2	82.7, CH	4.96,dd (4.6, 2.4)
			3	77.9, CH	4.87, m
			4	85.7, CH	4.81, m
			5	62.8, CH_2	4.41, m; 4.29, m

a) Protons are overlapped, unless otherwise stated (s: singlet; d: doublet; t: triplet)

Table 12. Calibration curves, LODs and LOQ of standard compounds

Comp.	Range (μg/mL)	Regression equation [a)]	r^2 [b)]	LOD (μg)	LOQ (μg)
33	20-200	Y=1.63609X-3.73191	0.998	10.0	34.2
34	20-200	Y=1.65378X-4.12177	0.998	10.0	34.5
35	20-200	Y=1.56300X-3.56005	0.996	6.2	21.0
36	20-200	Y=1.57909X-3.42611	0.999	3.2	10.4
37	20-200	Y=1.61341X-3.52106	0.999	3.4	11.4
38	20-200	Y=1.60897X-3.51462	0.998	3.4	11.6
39	20-200	Y=1.66117X-3.68748	0.999	3.5	12.0
40	20-200	Y=1.57408X-3.16422	0.998	4.3	14.5
41	30-300	Y=1.51018X-2.99213	0.996	4.5	15.3
42	20-200	Y=1.45481X-2.79906	0.998	4.6	15.7
43	20-200	Y=1.45252X-2.86573	0.998	3.2	10.9
44	20-200	Y=1.72059X-3.32448	0.996	2.5	8.5

a) Y: logarithmic value of peak area, X: logarithmic value of concentration of the analyte (μg/mL)

b) r^2: correlation coefficient

Table 13. Precision [a], repeatability [b] and stability [b] of twelve analytes

Comp.	Spiked amount	Intra-day		Inter-day		Repeatability	Stablility
	(μg)	Recovery (%)	RSD (%)	Recovery (%)	RSD (%)	RSD (%)	RSD (%)
33	20	97.49	0.39	97.51	1.04	2.30	1.35
	40	99.74	0.75	99.92	0.25		
	80	99.79	0.44	100.46	0.63		
34	20	97.49	0.32	97.55	1.06	1.86	1.23
	40	104.59	1.06	105.13	1.49		
	80	99.23	1.09	99.25	1.15		
35	20	95.09	2.58	95.11	0.95	2.23	1.06
	40	100.05	0.67	99.65	1.74		
	80	98.85	1.08	96.19	2.43		
36	40	100.12	1.05	100.18	1.05	1.19	1.20
	80	105.81	1.12	105.83	1.03		
	120	99.72	1.04	99.86	1.12		
37	40	100.36	0.22	100.66	0.75	1.50	0.93
	80	105.75	1.14	106.21	1.40		
	120	101.36	0.90	101.38	1.23		
38	40	103.65	1.24	103.84	1.15	3.38	2.20
	80	103.23	0.93	103.34	0.99		
	120	101.07	1.19	101.13	1.06		
39	40	101.79	1.51	102.53	0.62	1.31	1.21
	80	101.38	1.15	101.42	1.10		
	120	98.21	1.17	98.39	1.17		
40	40	97.92	2.79	97.45	1.16	1.87	0.89
	80	99.36	2.18	99.98	0.72		
	120	98.62	2.06	98.36	0.31		
41	40	99.88	1.89	100.47	1.07	1.59	2.24
	80	97.36	1.22	97.38	0.94		

	120	99.34	0.96	98.69	0.67		
42	40	101.39	1.18	101.13	0.46	2.34	1.11
	80	97.92	2.34	97.83	0.64		
	120	99.59	1.19	100.51	0.79		
43	20	101.69	3.61	102.77	3.14	1.71	1.52
	40	95.99	2.96	95.02	0.89		
	80	97.41	3.80	96.19	1.34		
44	20	99.54	1.96	98.96	0.55	1.40	2.01
	40	99.09	1.50	99.15	1.07		
	80	98.18	1.23	98.91	0.68		

[a)] standard compounds

[b)] crude sample

Table 14. Recovery assay of twelve analytes in KC (*n=3*, mean ± SD)

Comp.	Contained (μg)	Added (μg)	Found (μg)	Recovery (%)	RSD (%)
33	69.07 ± 2.14	25.00	94.23 ± 1.18	100.64	1.25
		50.00	119.03 ± 2.27	99.92	2.31
		100.00	169.53 ± 2.61	100.46	1.54
34	57.50 ± 0.71	25.00	82.00 ± 1.13	97.98	1.38
		50.00	109.06 ± 2.06	103.13	1.89
		100.00	156.75 ± 1.52	99.25	0.97
35	366.22 ± 9.30	100.00	464.92 ± 4.93	98.71	1.06
		150.00	515.70 ± 10.00	99.65	1.94
		200.00	510.50 ± 15.37	96.19	3.01
36	202.63 ± 4.01	100.00	305.01 ± 6.56	102.38	2.15
		150.00	355.38 ± 3.52	101.83	0.99
		200.00	402.34 ± 8.53	99.86	2.12
37	301.80 ± 4.80	100.00	398.43 ± 3.79	96.63	0.95
		150.00	458.12 ± 7.06	104.21	1.54
		200.00	504.56 ± 11.15	101.38	2.21
38	245.25 ± 5.15	100.00	348.79 ± 6.10	103.54	1.75
		150.00	400.26 ± 7.96	103.34	1.99
		200.00	447.51 ± 9.22	101.13	2.06
39	230.01 ± 5.11	100.00	331.23 ± 5.37	101.22	1.62
		150.00	382.15 ± 3.44	101.42	0.90
		200.00	426.78 ± 3.71	98.39	0.87
40	652.34 ± 13.11	100.00	750.69 ± 8.78	98.35	1.17
		150.00	802.31 ± 21.82	99.98	2.72
		300.00	947.41 ± 9.57	98.36	1.01
41	305.32 ± 5.14	100.00	404.79 ± 4.29	99.47	1.06
		150.00	451.38 ± 4.42	97.38	0.98
		200.00	502.70 ± 4.22	98.69	0.84
42	153.56 ± 1.89	100.00	254.29 ± 3.43	100.73	1.35

		150.00	300.31 ± 5.35	97.83	1.78
		200.00	364.58 ± 6.53	100.51	1.79
43	79.76 ± 1.01	25.00	105.07 ± 3.73	101.25	3.55
		50.00	127.27 ± 2.41	95.02	1.89
		100.00	175.95 ± 1.02	96.19	0.58
44	106.55 ± 2.03	25.00	131.16 ± 1.11	98.45	0.85
		50.00	156.13 ± 1.98	99.15	1.27
		100.00	205.46 ± 2.01	98.91	0.98

Table 15. HPLC-ESI-QTOF-MS Data of standard compounds

Comp.	t_R (min)	Identification	Formula	*m/z* (calculated)	*m/z* (observed)	Error (ppm)
33	15.025	coniferin	$C_{16}H_{22}O_8$	342.1301	342.1315	-3.98
34	18.925	chlorogenic acid	$C_{16}H_{18}O_9$	354.0924	354.0951	-7.48
35	24.353	liriodendrin	$C_{34}H_{46}O_{18}$	742.2687	742.2684	0.31
36	46.200	septemlosideIII	$C_{79}H_{128}O_{42}$	1748.8042	1748.7880	9.27
37	48.409	septemloside D	$C_{74}H_{120}O_{38}$	1616.7528	1616.7458	4.37
38	49.635	septemloside II	$C_{74}H_{120}O_{38}$	1616.7583	1616.7358	7.76
39	56.267	septemloside C	$C_{69}H_{112}O_{34}$	1484.7103	1484.7035	4.59
40	59.458	kalopanax saponin C	$C_{65}H_{106}O_{31}$	1382.6792	1382.6718	5.32
41	61.913	sieboldianoside A	$C_{64}H_{104}O_{30}$	1352.6680	1352.6612	5.00
42	64.613	kalopanax saponin B	$C_{59}H_{96}O_{26}$	1220.6239	1220.6190	4.05
43	73.462	cussonoside A	$C_{48}H_{78}O_{18}$	942.5194	942.5188	0.64
44	83.772	kalopanax saponin A	$C_{41}H_{66}O_{12}$	750.4558	750.4554	0.54

Table 16. The results of quantitative analysis of KC from Korea and China (mg/g, *n=3*, mean ± SD)

NO.	29	30	31	32	33	34	35	36	37	38	39	40
K-01	1.33 ± 0.05	0.15 ± 0.00	17.91 ± 0.56	N/D	N/D	N/D	N/D	0.58 ± 0.00	29.55 ± 0.11	23.74 ± 0.09	0.54 ± 0.00	N/D
K-02	1.17 ± 0.05	N/D	16.05 ± 0.10	N/D	N/D	N/D	N/D	0.36 ± 0.00	0.50 ± 0.00	16.53 ± 0.02	0.42 ± 0.00	0.48 ± 0.00
K-03	2.25 ± 0.04	N/D	23.19 ± 0.71	N/D	N/D	N/D	N/D	0.59 ± 0.00	37.45 ± 0.09	30.81 ± 0.11	0.51 ± 0.00	0.48 ± 0.00
K-04	0.67 ± 0.01	N/D	4.79 ± 0.01	N/D	N/D	N/D	N/D	0.40 ± 0.00	19.45 ± 0.00	20.83 ± 0.01	0.45 ± 0.00	0.50 ± 0.00
K-05	1.91 ± 0.03	N/D	11.18 ± 0.12	N/D	N/D	N/D	N/D	0.69 ± 0.01	31.33 ± 1.56	35.03 ± 1.12	0.42 ± 0.00	0.51 ± 0.00
K-06	1.93 ± 0.06	N/D	13.55 ± 0.23	N/D	N/D	N/D	N/D	2.60 ± 0.01	0.84 ± 0.00	55.05 ± 1.23	N/D	0.51 ± 0.00
K-07	1.68 ± 0.03	N/D	8.06 ± 0.32	N/D	N/D	N/D	N/D	0.36 ± 0.00	1.79 ± 0.00	24.83 ± 1.03	0.42 ± 0.00	0.49 ± 0.00
K-08	0.88 ± 0.01	N/D	4.75 ± 0.10	N/D	N/D	N/D	N/D	0.47 ± 0.00	0.64 ± 0.00	28.18 ± 1.34	0.10 ± 0.00	0.49 ± 0.00
K-09	0.86 ± 0.01	N/D	4.55 ± 0.20	N/D	N/D	N/D	N/D	0.50 ± 0.00	0.99 ± 0.00	34.21 ± 1.45	0.41 ± 0.00	0.52 ± 0.00
K-10	1.48 ± 0.02	N/D	17.54 ± 0.33	N/D	N/D	N/D	N/D	0.42 ± 0.00	32.95 ± 1.06	19.26 ± 0.94	0.42 ± 0.00	N/D
K-11	3.07 ± 0.05	N/D	18.64 ± 0.22	N/D	N/D	N/D	N/D	0.66 ± 0.00	11.95 ± 0.92	23.87 ± 0.92	0.40 ± 0.00	N/D
K-12	0.95 ± 0.00	5.89 ± 0.08	2.40 ± 0.04	N/D	N/D	N/D	N/D	0.39 ± 0.00	14.97 ± 0.61	28.48 ± 0.83	N/D	0.49 ± 0.00
K-13	0.81 ± 0.00	N/D	7.27 ± 0.35	N/D	N/D	N/D	N/D	0.39 ± 0.00	19.23 ± 0.86	12.73 ± 0.89	0.47 ± 0.00	0.49 ± 0.00
K-14	1.29 ± 0.04	N/D	11.37 ± 0.22	N/D	N/D	N/D	N/D	0.60 ± 0.00	16.92 ± 0.75	27.74 ± 0.78	0.43 ± 0.00	0.53 ± 0.00
K-15	2.47 ± 0.07	4.37 ± 0.09	8.12 ± 0.10	N/D	N/D	N/D	N/D	2.11 ± 0.09	35.20 ± 1.05	17.00 ± 0.45	0.54 ± 0.00	0.50 ± 0.00
K-16	2.17 ± 0.08	N/D	13.70 ± 0.52	N/D	N/D	N/D	N/D	0.68 ± 0.00	6.04 ± 0.89	32.48 ± 1.33	0.39 ± 0.00	0.48 ± 0.00
K-17	1.28 ± 0.05	3.88 ± 0.03	12.71 ± 0.69	N/D	N/D	N/D	N/D	1.76 ± 0.08	27.49 ± 1.03	39.70 ± 2.03	0.42 ± 0.00	0.67 ± 0.00
K-18	1.61 ± 0.08	4.35 ± 0.02	21.71 ± 0.51	N/D	N/D	N/D	N/D	0.51 ± 0.00	37.95 ± 1.50	36.47 ± 1.89	N/D	N/D
C-01	N/D	3.54 ± 0.17	5.47 ± 0.05	7.95 ± 0.31	7.19 ± 0.09	7.58 ± 0.15	3.07 ± 0.16	6.88 ± 0.10	12.10 ± 0.61	0.33 ± 0.00	0.39 ± 0.00	0.50 ± 0.00
C-02	0.63 ± 0.00	N/D	4.80 ± 0.12	6.61 ± 0.34	5.79 ± 0.05	7.29 ± 0.12	3.11 ± 0.13	18.86 ± 0.22	4.07 ± 0.45	11.07 ± 0.19	N/D	0.49 ± 0.00
C-03	0.66 ± 0.00	N/D	7.26 ± 0.15	3.78 ± 0.40	4.41 ± 0.05	5.85 ± 0.12	2.60 ± 0.08	44.67 ± 1.02	2.48 ± 0.06	0.54 ± 0.00	0.39 ± 0.00	N/D
C-04	0.63 ± 0.00	4.87 ± 0.10	6.00 ± 0.14	12.88 ± 0.45	11.77 ± 0.10	16.31 ± 0.42	4.55 ± 0.25	47.03 ± 1.09	3.20 ± 0.04	1.76 ± 0.00	0.39 ± 0.00	0.50 ± 0.00
C-05	N/D	2.74 ± 0.05	4.78 ± 0.14	2.86 ± 0.05	3.38 ± 0.08	3.95 ± 0.09	2.45 ± 0.13	8.69 ± 0.27	2.10 ± 0.01	1.28 ± 0.03	0.39 ± 0.00	0.48 ± 0.00
C-06	0.63 ± 0.00	N/D	5.61 ± 0.11	4.84 ± 0.12	6.01 ± 0.10	6.28 ± 0.11	2.89 ± 0.09	34.64 ± 0.33	3.61 ± 0.08	6.78 ± 0.22	0.39 ± 0.00	0.49 ± 0.00
C-07	0.62 ± 0.00	2.42 ± 0.02	4.54 ± 0.12	5.19 ± 0.13	4.94 ± 0.07	4.20 ± 0.12	1.25 ± 0.07	48.64 ± 0.99	2.06 ± 0.06	1.44 ± 0.00	0.39 ± 0.00	0.48 ± 0.00
C-08	N/D	2.20 ± 0.02	6.65 ± 0.20	5.00 ± 0.34	3.47 ± 0.04	4.36 ± 0.00	2.23 ± 0.04	47.85 ± 0.91	8.64 ± 0.14	3.46 ± 0.67	0.39 ± 0.00	0.10 ± 0.00
C-09	N/D	1.95 ± 0.02	4.16 ± 0.10	9.79 ± 0.43	11.33 ± 0.24	16.04 ± 0.33	5.85 ± 0.22	39.86 ± 1.04	3.24 ± 0.07	2.48 ± 0.01	0.39 ± 0.01	0.55 ± 0.00
C-10	N/D	2.21 ± 0.03	5.59 ± 0.15	6.82 ± 0.32	6.35 ± 0.02	8.77 ± 0.14	5.18 ± 0.14	43.21 ± 0.82	7.39 ± 0.11	2.27 ± 0.00	0.39 ± 0.00	N/D
C-11	N/D	10.13 ± 0.52	7.78 ± 0.13	11.40 ± 0.51	6.28 ± 0.13	10.09 ± 0.23	3.27 ± 0.12	50.43 ± 1.45	4.62 ± 0.12	7.48 ± 0.11	0.39 ± 0.00	0.49 ± 0.00
C-12	0.62 ± 0.00	5.54 ± 0.10	5.88 ± 0.14	9.82 ± 0.13	9.44 ± 0.23	11.01 ± 0.33	6.79 ± 0.26	27.94 ± 0.84	5.26 ± 0.09	5.12 ± 0.54	0.39 ± 0.00	0.78 ± 0.00
C-13	N/D	N/D	3.67 ± 0.10	18.99 ± 0.67	10.43 ± 0.15	9.65 ± 0.21	5.35 ± 0.10	50.94 ± 2.31	4.90 ± 0.10	38.06 ± 1.34	0.40 ± 0.00	0.57 ± 0.00
C-14	0.61 ± 0.00	4.68 ± 0.08	3.59 ± 0.09	3.29 ± 0.09	3.41 ± 0.02	4.65 ± 0.04	1.41 ± 0.09	58.30 ± 0.99	5.91 ± 0.09	9.11 ± 0.58	0.38 ± 0.00	N/D
C-15	N/D	1.89 ± 0.00	3.61 ± 0.11	13.63 ± 0.08	12.14 ± 0.14	16.79 ± 0.23	4.90 ± 0.20	47.06 ± 1.32	4.29 ± 0.09	2.68 ± 0.00	0.40 ± 0.00	0.61 ± 0.00
C-16	N/D	10.42 ± 0.30	6.41 ± 0.18	26.13 ± 0.89	18.86 ± 0.23	16.76 ± 0.32	7.58 ± 0.32	42.77 ± 0.87	10.71 ± 0.11	21.28 ± 1.09	0.38 ± 0.00	0.49 ± 0.00
C-17	N/D	3.15 ± 0.02	3.87 ± 0.09	20.59 ± 1.08	9.23 ± 0.90	5.35 ± 0.78	4.85 ± 0.89	16.68 ± 0.79	3.61 ± 0.09	12.65 ± 0.82	0.39 ± 0.00	0.50 ± 0.00
C-18	0.86 ± 0.00	5.10 ± 0.09	5.16 ± 0.19	4.04 ± 0.04	3.75 ± 0.05	3.78 ± 0.01	1.31 ± 0.06	42.16 ± 1.14	3.44 ± 0.08	21.22 ± 0.99	N/D	N/D
C-19	N/D	2.11 ± 0.02	4.34 ± 0.11	7.51 ± 0.06	8.01 ± 0.13	8.42 ± 0.12	4.21 ± 0.14	46.42 ± 2.02	9.09 ± 0.11	13.81 ± 0.72	0.39 ± 0.00	0.57 ± 0.00
C-20	N/D	1.95 ± 0.00	5.67 ± 0.08	5.44 ± 0.12	5.35 ± 0.12	7.36 ± 0.13	3.14 ± 0.10	44.74 ± 1.13	4.89 ± 0.21	4.42 ± 0.09	0.38 ± 0.00	0.50 ± 0.00
C-21	N/D	N/D	4.99 ± 0.12	6.13 ± 0.12	5.52 ± 0.12	5.67 ± 0.12	2.56 ± 0.07	26.11 ± 0.67	2.94 ± 0.08	2.16 ± 0.05	0.41 ± 0.00	0.68 ± 0.00

C-22	N/D	3.05 ± 0.09	4.02 ± 0.14	6.25 ± 0.23	4.37 ± 0.15	4.51 ± 0.19	1.15 ± 0.02	44.47 ± 0.82	5.20 ± 0.07	6.44 ± 0.06	0.39 ± 0.00	0.48 ± 0.00
C-23	N/D	3.56 ± 0.02	4.57 ± 0.09	8.37 ± 0.54	8.95 ± 0.49	8.15 ± 0.89	3.20 ± 0.09	41.48 ± 0.83	4.47 ± 0.10	3.40 ± 0.01	0.40 ± 0.00	0.48 ± 0.00
C-24	N/D	4.28 ± 0.02	3.52 ± 0.10	6.68 ± 0.23	7.52 ± 0.18	3.52 ± 0.04	3.86 ± 0.15	22.46 ± 0.71	3.77 ± 0.05	1.01 ± 0.00	N/D	N/D
C-25	N/D	N/D	4.44 ± 0.07	5.20 ± 0.21	5.34 ± 0.04	6.25 ± 0.11	3.61 ± 0.14	18.85 ± 0.62	2.47 ± 0.04	6.50 ± 0.40	0.41 ± 0.00	0.48 ± 0.00
C-26	N/D	2.05 ± 0.02	2.06 ± 0.02	9.83 ± 0.32	7.06 ± 0.09	8.82 ± 0.20	4.16 ± 0.21	48.76 ± 0.94	4.97 ± 0.02	6.70 ± 0.22	0.42 ± 0.00	0.49 ± 0.00
C-27	N/D	3.43 ± 0.15	2.75 ± 0.08	5.37 ± 0.95	5.78 ± 1.01	6.98 ± 0.83	1.89 ± 0.07	51.60 ± 0.96	2.34 ± 0.01	0.94 ± 0.01	0.38 ± 0.00	0.49 ± 0.00
C-28	N/D	6.32 ± 0.05	8.34 ± 0.20	6.84 ± 0.22	5.92 ± 0.13	8.31 ± 0.24	2.85 ± 0.05	19.78 ± 0.51	1.51 ± 0.00	1.03 ± 0.00	0.40 ± 0.00	N/D
C-29	N/D	4.30 ± 0.02	5.66 ± 0.15	7.23 ± 0.24	8.46 ± 0.25	8.38 ± 0.26	3.89 ± 0.14	47.08 ± 0.73	7.42 ± 0.91	4.20 ± 0.51	0.40 ± 0.00	0.50 ± 0.00
C-30	N/D	4.50 ± 0.02	5.88 ± 0.12	9.12 ± 0.31	12.79 ± 0.21	13.35 ± 0.47	5.39 ± 0.23	62.95 ± 1.65	14.45 ± 0.85	17.44 ± 0.99	N/D	0.49 ± 0.00
C-31	N/D	4.75 ± 0.19	4.54 ± 0.11	5.01 ± 0.78	7.05 ± 0.89	6.74 ± 0.55	1.53 ± 0.09	56.42 ± 2.05	11.43 ± 0.79	24.24 ± 1.35	N/D	0.62 ± 0.00
C-32	N/D	7.43 ± 0.05	8.74 ± 0.23	9.61 ± 0.29	9.02 ± 0.15	8.96 ± 0.22	3.46 ± 0.10	43.01 ± 1.05	3.23 ± 0.06	3.51 ± 0.01	0.39 ± 0.00	0.48 ± 0.00
C-33	N/D	5.66 ± 0.05	8.45 ± 0.19	8.63 ± 0.24	7.91 ± 0.12	7.54 ± 0.34	3.30 ± 0.06	45.58 ± 2.01	3.68 ± 0.02	4.43 ± 0.06	0.41 ± 0.00	N/D
C-34	N/D	3.46 ± 0.02	16.96 ± 0.50	5.34 ± 0.15	5.01 ± 0.12	4.64 ± 0.25	2.50 ± 0.04	23.00 ± 1.00	2.02 ± 0.01	0.74 ± 0.00	0.39 ± 0.00	N/D
C-35	N/D	N/D	5.17 ± 0.16	6.94 ± 0.11	4.23 ± 0.14	4.08 ± 0.09	2.07 ± 0.01	48.18 ± 0.73	6.31 ± 0.08	0.85 ± 0.00	0.39 ± 0.00	0.82 ± 0.00
C-36	N/D	3.00 ± 0.02	3.72 ± 0.09	1.29 ± 0.05	1.56 ± 0.01	2.11 ± 0.02	1.28 ± 0.01	23.10 ± 0.53	1.65 ± 0.01	0.90 ± 0.00	N/D	0.49 ± 0.00
C-37	N/D	13.86 ± 0.55	5.67 ± 0.09	10.99 ± 0.10	11.52 ± 0.22	16.12 ± 0.50	3.06 ± 0.07	38.50 ± 0.95	2.12 ± 0.04	0.49 ± 0.00	0.39 ± 0.00	N/D
C-38	N/D	2.70 ± 0.07	8.36 ± 0.12	4.35 ± 0.46	3.05 ± 0.09	3.24 ± 0.07	1.30 ± 0.00	32.68 ± 0.86	4.36 ± 0.05	2.16 ± 0.01	N/D	0.49 ± 0.00
C-39	0.92 ± 0.02	5.40 ± 0.08	6.13 ± 0.11	4.98 ± 0.14	6.47 ± 0.08	2.10 ± 0.00	0.53 ± 0.01	29.79 ± 0.51	8.25 ± 0.00	34.20 ± 1.22	0.41 ± 0.00	0.52 ± 0.00
C-40	N/D	3.54 ± 0.05	5.47 ± 0.34	7.95 ± 0.37	7.19 ± 0.43	7.58 ± 0.58	3.07 ± 0.09	6.88 ± 0.32	12.10 ± 0.65	0.33 ± 0.00	0.39 ± 0.00	0.49 ± 0.00
C-41	N/D	N/D	4.04 ± 0.38	5.71 ± 0.28	5.61 ± 0.24	7.22 ± 0.46	2.26 ± 0.08	32.27 ± 1.59	3.26 ± 0.06	6.38 ± 0.88	N/D	N/D
C-42	N/D	13.57 ± 0.98	2.26 ± 0.08	1.99 ± 0.00	3.35 ± 0.18	4.85 ± 0.24	3.50 ± 0.12	5.86 ± 0.07	3.91 ± 0.07	0.52 ± 0.00	0.40 ± 0.00	N/D
C-43	0.67	7.92 ± 0.56	12.22 ± 0.97	15.08 ± 0.79	15.54 ± 0.87	22.49 ± 1.08	4.86 ± 0.21	64.56 ± 2.08	12.89 ± 0.68	5.16 ± 0.50	N/D	N/D
Average K	1.55 ± 0.65	1.03 ± 2.01	12.08 ± 6.22	N/D	N/D	N/D	N/D	0.78 ± 0.66	18.07 ± 14.03	28.16 ± 10.04	0.35 ± 0.20	0.40 ± 0.22
Average C	0.16 ± 0.30	3.92 ± 3.36	5.65 ± 2.61	7.57 ± 4.65	7.09 ± 3.66	7.94 ± 4.68	3.19 ± 1.61	37.23 ± 15.45	7.49 ± 10.23	6.88 ± 8.93	0.31 ± 0.16	0.36 ± 0.26

Average K: the average of Korean samples (K-01 ~ K18); Average C: the average of Chinese samples (C-01 ~ C43)

N/D: Not detected

III. Simultaneous Analysis of Bioactive Metabolites from *Ziziphus jujube* byHPLC-DAD-ELSD-MS/MS

A method based on HPLC-DAD-ELSD-MS/MS was established for the simultaneous determination of nine representative metabolites from semen Ziziphus jujuba. Validation parameters, such as linearity, limit of detection, limit of quantification, recovery, accuracy, and precision, were successfully obtained. In addition, the efficiencies of diverse extraction methods were compared for the development of a standard analytic method. The verified method was successfully applied to the quantitative determination of nine representative metabolites in twenty-four commercial samples of *Z. jujuba var. spinosa* and *Z. mauritiana* from different markets in Korea, China and Myanmar were analyzed and compared to each other. The analytical results showed that the contents of the nine analytes vary significantly with two different species.

3-1. Introduction

The dried seed of *Ziziphus jujuba var. spinosa*, which belongs to the Rhamnaceae, is listed in Korea and China Pharmacopeia. This plant is widely used as folk medicine for the treatment of insomnia and anxiety in clinical practice.[107,108] However *Ziziphus mauritiana*, another species of this plant, not

listed in Pharmacopeia. But it is also used as herbal medicine. It is considered as counterfeit, because there are some differences in chemical constituent concentrations and pharmacological effects.[109]

Many studies have demonstrated that semen Ziziphus jujuba processes multiple bioactivities such as nervine tonic, hypnotic-sedative, hypotensive, antihypoxia, antihyperlipidemia and hypothermic effects.[107,108, 110-112] Moreover, semen Ziziphus jujuba is beneficial to purify the blood, aid digestion and inhibit the inflammatory cells.[113,114]

Up to now, there are many bioactive compounds have been reported such as cyclopeptide alkaloids, flavonoids, saponins, fatty acids.[115-119] From the prior researches, total saponins fraction including jujuboside A, jujuboside B, jujuboside D was the main pharmacological active compounds in the extracts of semen Ziziphus jujuba, which has been proved to prevent anoxemia of cardiac muscle, improve SOD activity,[110] increase sleep time and lower hypelipemia,[109] the cyclopeptide alkaloids, such as magnoflorine, has sedative activity,[115] and flavonoids are responsible for the sedative activity.[120-123] In Chinese pharmacopeia, spinosin and jujuboside A were chosen as markers to estimate the quality of semen Ziziphus jujuba (Pharmacopeia Commission of PRC, 2010). However the curative effect of traditional herbal

medicine is an integrative result of a number of bioactive compounds. A single or a few compounds could not be responsible for the overall pharmacological activities. Simultaneous determination of multiple components is therefore a better strategy for the comprehensive quality evaluation. In present study, a HPLC-DAD-ELSD-MS/MS method was developed and validated for comparison of two species and simultaneous determination of nine bioactive components of semen Ziziphus jujuba, including one cyclopeptide alkaloid namely magnoflorine (**45**), five flavonoids namely isospinosin (**46**), spinosin (**47**), 6'''-sinapoyl spinosin (**48**), 6'''-feruloyl spinosin (**49**), and 6'''-coumaroyl spinosin (**50**), three triterpenoic saponins namely jujuboside A (**51**), jujuboside A_2 (**52**), and jujuboside B (**53**) (Figure 30), The developed methods have been verified for their effectiveness against diverse validation parameters. In addition, the contents of bioactive compounds in twenty-four commercial samples of *Z. jujuba var. spinosa* and *Z. mauritiana* from different markets in Korea, China and Myanmar were analyzed and compared to each other.

3-2. Experimental section

Plant materials. Twenty-four samples of *Ziziphus var. spinosa* (Z-1~Z-12) and *Ziziphus mauritiana* (Z-13~Z-24) grown in different regions

were provided by the National Center for Standardization of Herbal Medicine, such as Z-1 (Shandong, China), Z-2~Z-6 (unidentified area, China), Z-7 (Hebei Province, Taiheng Mountain, China), Z-8 (Shanxi, China), Z-9 (Hebei, China), Z-10 (Liaoning, China), Z-11~Z-12 (unidentified area, Korea), Z-13~Z-16 (unidentified area, Korea), Z-17~Z-18 (unidentified area, China), and Z-19~Z-24 (unidentified area, Myanmar).

Reagents, chemicals and samples - Magnoflorine (**45**), spinosin (**46**), isospinosin (**47**), 6'''-sinapoyl spinosin (**48**), 6'''-feruloyl spinosin (**49**), 6'''-coumaroyl spinosin (**50**), jujuboside A (**51**), jujuboside A_2 (**52**), jujuboside B (**53**) isolated and purified from semen Ziziphus jujuba by a series of chromatographic procedures were provided from National Center for Standardization of Herbal Medicine, Korea and the structures were elucidated by comparison of spectral data (UV, IR, MS, 1H-NMR, 13C-NMR) with the literature data. The purities of these compounds were determined to be higher than 92 % by normalization of the peak area detection by HPLC-DAD-ELSD analysis. Naringin as an internal standard compound was obtained from Sigma-Aldrich (USA).

Methanol, acetonitrile, and water were HPLC grade purchased from Burdick & Jackson (USA) and ethanol (Duksan, Korea) was analytical grade.

Instrumentation and chromatographic conditions. The HPLC system was consisted of Agilent 1200 series equipped with an autosampler, a column oven, a binary pump, a diode array detector (Agilent Technologies, Waldbronn, Germany) , an ELSD detector (Agilent Technologies,1260 Infinity) and a degasser (Agilent Technologies, Tokyo, Japan). The Chemstation software (Agilent Technologies, Avondale, CA, USA) was used to operate this HPLC-DAD-ELSD system. Separation was performed on a Shiseido CAPCELL PAK C_{18} 5um (250 × 4.6 mm) analytical column. A gradient elution of A (water, 0.1% formic acid) and B (methanol, 0.1% formic acid) was used (0 min, 45% B; 25 min, 50% B; 40 min, 100% B; 50 min, 100% B; 55 min, 45% B in *v/v*). The analytes were monitored with DAD and ELSD. Standard or sample solutions of 10 μL were directly injected to the HPLC system and the mobile phase flow rate was 0.3 mL/min and the column temperature was set at 25 ℃.

All ESI-MS and ESI-MS^n spectra were acquired using a Finnigan MAT LCA ion-trap mass spectrometer (San Jose, CA, USA) equipped with a Finnigan electrospray source and capable of analyzing ions up to *m/z* 2000. Mass spectrometer conditions were firstly optimized using flow injection analysis of the standards without the HPLC column. The conditions were as follows: a sheath gas flow rate 60 arbitrary units, aux gas flow rate o arbitrary

units, capillary temperature 250 ℃, spray voltage 5kV, capillary voltage 39V, tube lens offset 55V.

Preparation of test sample. In order to achieve quantitative extraction method, variables involved in the procedure such as extraction method, solvent, and extraction time were optimized. Ultrasonication, vortex and reflux methods were compared to each other for the selection of the optimal extraction method (Table 17) at 50 % aqueous methanol solvent for 30 min. Aqueous methanol or ethanol solutions were tried as the extraction solvent (Table 18) using ultrasonication method at 30 min. Yields were also compared for the extraction times of 10, 20, 30, 60, and 90 min to determine the optimal extraction time (Table 19) using ultrasonication method at 50 % aqueous methanol. As a result, 50 % aqueous methanol for 30 min using ultrasonication was chosen for the best extraction condition for semen Ziziphus jujuba.

Accurately weighed plant powder of 200 mg were extracted with 10 mL of 50 % aqueous methanol, by means of sonication at room temperature for 30 min. After the filtration through 0.2 μm membrane filter, to an aliquot of 1 mL of the filtrate was added 10μg of internal standard compound, evaporated under vacuum, and then dissolved in 55 % aqueous methanol prior

to analysis.

Calibration. Stock solution (1 mg/mL) of the magnoflorine (**45**), spinosin (**46**), isospinosin (**47**), 6’’’-sinapoyl spinosin (**48**), 6’’’-feruloyl spinosin (**49**), 6’’’-coumaroyl spinosin (**50**), jujuboside A (**51**), jujuboside A_2 (**52**), jujuboside B (**53**) isolated from semen Ziziphus jujuba were prepared individually in methanol, and different concentration (1,2, 4, 8, 15 and 20 μg/mL) of these were loaded onto an HPLC for the preparation of the calibration function. The calibration function of individual compound was calculated with peak area (y), concentration (x, μg/mL), and mean values (n=3) ± standard deviation.

3-3. Results and discussion

For the simultaneously determination of nine bioactive compounds belonging to three kinds different chemical structures from alkaloid, flavonoid, and triterpenoid in semen Ziziphus jujuba, the chromatographic conditions were firstly investigated. Various mixtures of water, methanol and acetonitrile were tested as a mobile phase. The optimal wavelength for detection was tested at 210, 230, 250, 280, and 335 nm, respectively. Considering the significantly distinct UV maxima between the alkaloid and flavonoid chemical structure of analytes, optimum detection

wavelength was decided at 280 nm where of the six representative compounds showed relatively good absorptions. The parameters of ELSD such as nebulizing gas flow rate and drift tube temperature were optimized to obtain the best signals. In order to obtain highest signals at the lowest nebulizer gas flow rate, the optimized parameters of ELSD used to analyse three triterpenoic saponin were as follows: drift tube temperature , 50℃; nebulizing gas flow rate, 39 psi. The temperature for detection was tested at 25, 30, 35, 40, and 45℃. Optimum detection temperature was decided at 25 ℃, where the baseline was stable and all of the compounds had good theoretical plate, capacity factor, separation factor, and resolution (Table 20). The presences of magnoflorine (**45**), spinosin (**46**), isospinosin (**47**), 6'''-sinapoyl spinosin (**48**), 6'''-feruloyl spinosin (**49**), 6'''-coumaroyl spinosin (**50**), jujuboside A (**51**), jujuboside A_2 (**52**), jujuboside B (**53**) in semen Ziziphus jujuba were verified by comparing each retention time , UV and ELSD spectrum with those of each standard compound and spiking with authentic standards. As a result, a gradient methanol (0.1% formic acid) – water (0.1% formic acid) solvent system at 280 nm and 25 ^{o}C gave the desired separation within the running time of 50 min (Figure 31).

A methanol stock solution, containing nine standard compounds, was prepared and diluted to a series of appropriate concentrations for the

construction of calibration curves. The curves showed good linearity and the correlation coefficients were found to be in the range of 0.995- 0.999 for all the compounds, over the concentration ranges 1 - 20 µg/mL. Limits of detection and limits of quantitation were determined by means of serial dilution based on a signal-to-noise (S/N) ratio of 3:1 and 10:1, respectively. LOD and LOQ were less than 0.895 and 2.712 µg/mL, respectively (Table 21).

The accuracy and precision tests were carried out by measurement of the intra-day and inter-day variability and recovery of these constituents. The measurement of intra-day and inter-day variability was utilized to determine the precision of this method. The intra-day variation was determined by analyzing in the triplicate same mixed standard methanol solution for three times within 1 day while for the inter-day variability test, the solution was examined in triplicate for consecutive 3 days. The average percentage recoveries were evaluated by calculating the ratio of detected amount versus the added amount and the mean recovery of each compound was 92.76 - 104.32 %. The relative standard deviation (RSD) was taken as a tool of precision. The RSD of intra-day and inter-day variability was less than 3.20 % (Table 22).

Since the chromatographic peaks could not be identified unambiguously only by retention time and UV spectra in HPLC, HPLC - DAD - MS/MS was used as a supplement for confirmation of peak identification, by comparing the retention time, molecular ion and fragment pattern. In this experiment, mass spectral conditions were optimized in positive-ion mode and nine compounds exhibited distinct quasi-molecular ions ($[M+Na^+]$, $[M^+]$) in this mode (Table 23). In HPLC-ESI- MS spectra, molecular ion and fragmentation pattern of each compound were well matched with chemical structures (Figure 32). Throughout these results, nine standard compounds were identified in the extract of *Z. semen* and the specificity of each peak for **45-53** was clearly demonstrated.

The developed method was applied for the measurement of concentration of standard components in commercial semen Ziziphus jujuba. Twelve samples of *Ziziphus var. spinosa* from various areas of China and Korea, and twelve samples of *Ziziphus. mauritiana* from China, Korea and Myanmar were analyzed. The test samples were prepared as described for the development of analytical method and injected in triplicate. The results are summarized in Table 24. It was found that contents of standard compounds in various regional samples vary significantly by sources. Jujuboside A_2, which could be well detected in *Z. var. spinosa* (0.010 ± 0.006), could not be detected

in *Z. mauritiana*. The contents of magnoflorine (0.461 ± 0.183 %), jujuboside A (0.063 ± 0.033 %) and jujuboside B (0.043 ± 0.017 %) in *Z. var. spinosa* were much higher than magnoflorine (0.217 ± 0.023 %), jujuboside A (0.001 ± 0.004 %), and jujuboside B (0.015 ± 0.260 %) in *Z. mauritiana*. However, the contents of spinosin (0.146 ± 0.025 %), 6’’’-sinapoyl spinosin (0.006 ± 0.009 %) and 6’’’-feruloyl spinosin (0.065 ± 0.015 %) in *Z. var. spinosa* were much lower than spinosin (0.210 ± 0.034 %), 6’’’-sinapoyl spinosin (0.029 ± 0.030 %) and 6’’’-feruloyl spinosin (0.091 ± 0.021) in *Z. mauritiana.* The contents of isospinosin and 6’’’-coumaroyl spinosin from the two sources differentiated, but unremarkably. These results clearly demonstrated the significant differences in bioactive components between two different species. There was no big difference between Chinese and Korean regions from the same source. Overall, based on nine standard compounds, HPLC-DAD-ELSD methods we developed can confirm two species easily and swiftly. Therefore it will be effectively used to screen and discriminate a great number of samples.

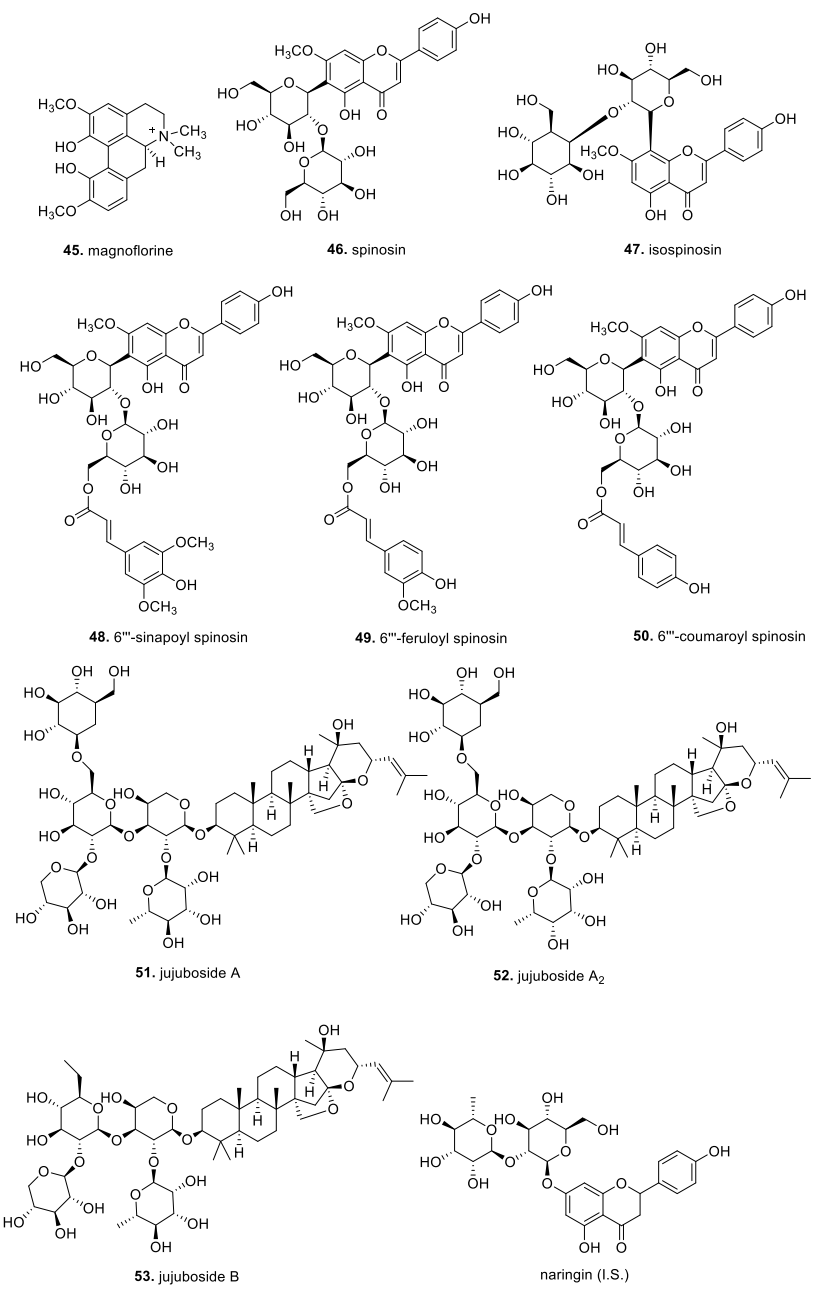

Figure 30. Chemical structures of representive compounds in semen Ziziphus jujuba.

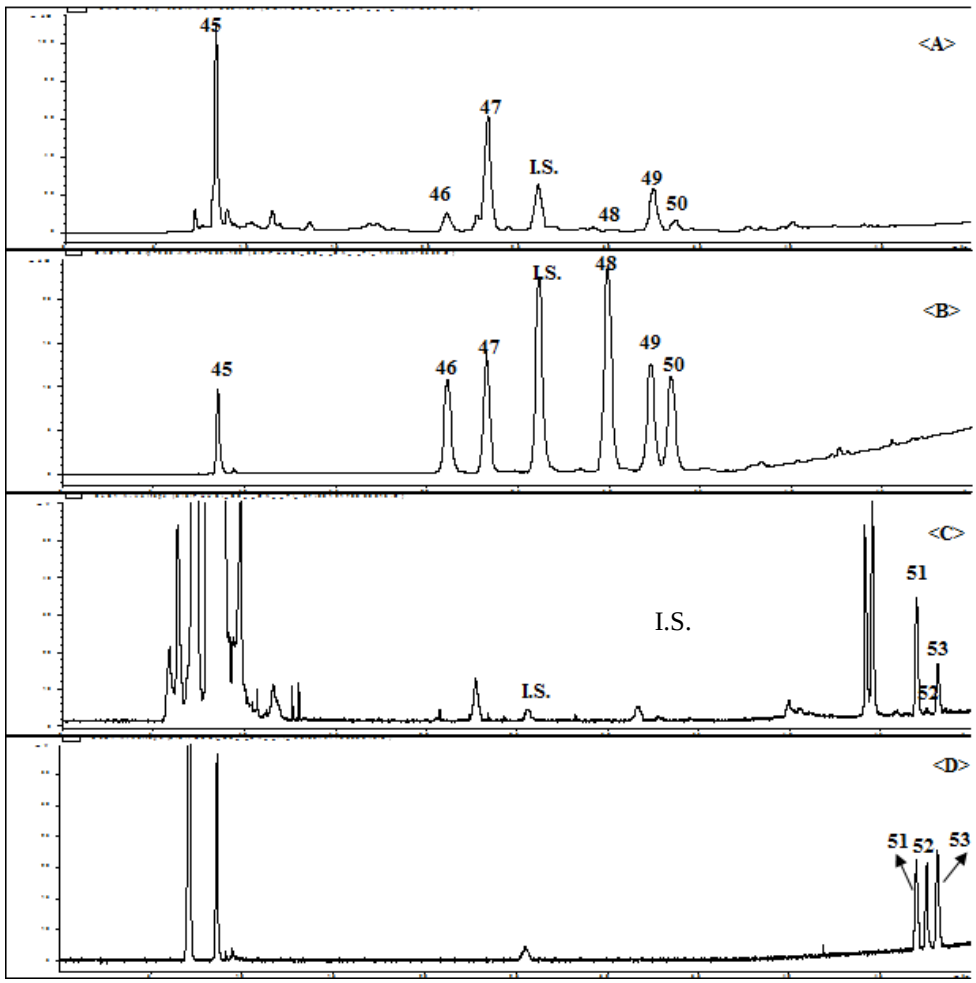

Figure 31. HPLC chromatograms of extract of crude sample and standard mixture in HPLC-DAD (A, B) and in HPLC-ELSD (C, D).

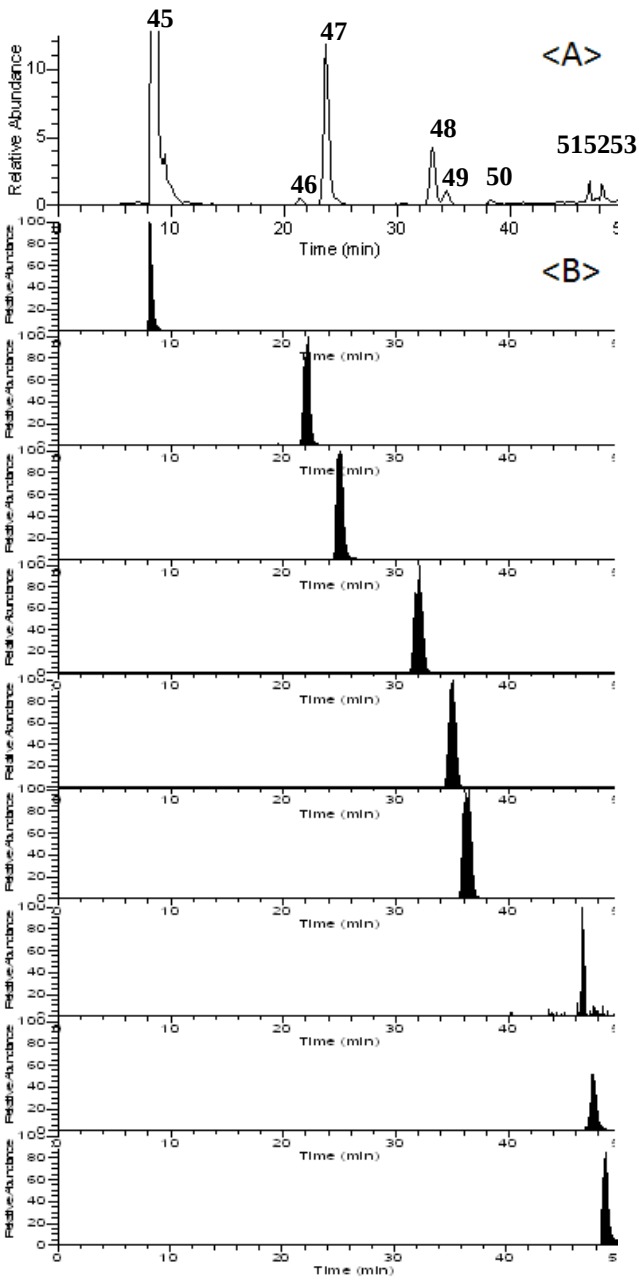

Figure 32. Total ion chromatograms of semen Ziziphus jujuba in SIM mode (A) and SRM mode (B).

Table 17. Comparison of effectiveness by extraction method (w/w, %, n=3)

Compounds	Vortex	Reflux	Sonication
45	0.611 ± 0.000	0.645 ± 0.002	0.678 ± 0.001
46	0.025 ± 0.000	0.023 ± 0.000	0.025 ± 0.000
47	0.151 ± 0.000	0.147 ± 0.000	0.146 ± 0.000
48	0.002 ± 0.000	0.002 ± 0.000	0.002 ± 0.000
49	0.056 ± 0.000	0.051 ± 0.000	0.060 ± 0.000
50	0.028 ± 0.000	0.028 ± 0.000	0.026 ± 0.000
51	0.074 ± 0.000	0.085 ± 0.000	0.078 ± 0.003
52	0.013 ± 0.000	0.013 ± 0.000	0.013 ± 0.000
53	0.048 ± 0.001	0.047 ± 0.001	0.048 ± 0.001

Table 18. Comparison of effectiveness by extraction solvent (w/w, %, n=3)

Compounds	70%Methanol	50%Methanol	70%Ethanol	50%Ethanol
45	0.532 ± 0.000	0.678 ± 0.001	0.643 ± 0.001	0.505 ± 0.001
46	0.023 ± 0.000	0.025 ± 0.000	0.022 ± 0.000	0.021 ± 0.000
47	0.142 ± 0.000	0.146 ± 0.000	0.144 ± 0.000	0.134 ± 0.000
48	0.002 ± 0.000	0.002 ± 0.000	0.002 ± 0.000	0.002 ± 0.000
49	0.053 ± 0.000	0.060 ± 0.000	0.056 ± 0.000	0.054 ± 0.000
50	0.027 ± 0.000	0.026 ± 0.000	0.028 ± 0.000	0.023 ± 0.000
51	0.060 ± 0.001	0.078 ± 0.003	0.068 ± 0.002	0.073 ± 0.000
52	0.011 ± 0.000	0.013 ± 0.000	0.012 ± 0.000	0.012 ± 0.000
53	0.032 ± 0.001	0.048 ± 0.001	0.040 ± 0.001	0.046 ± 0.001

Table 19. Comparison of effectiveness by extraction time (w/w, %, n=3)

Compounds	10 min	20 min	30 min	60 min	90 min
45	0.594 ± 0.001	0.661 ± 0.001	0.676 ± 0.001	0.653 ± 0.001	0.594 ± 0.001
46	0.022 ± 0.000	0.024 ± 0.000	0.025 ± 0.000	0.021 ± 0.000	0.022 ± 0.000
47	0.140 ± 0.000	0.155 ± 0.000	0.145 ± 0.000	0.130 ± 0.000	0.140 ± 0.000
48	0.002 ± 0.000	0.002 ± 0.000	0.002 ± 0.000	0.002 ± 0.000	0.002 ± 0.000
49	0.055 ± 0.000	0.059 ± 0.000	0.055 ± 0.000	0.046 ± 0.000	0.055 ± 0.000
50	0.022 ± 0.000	0.021 ± 0.000	0.025 ± 0.000	0.028 ± 0.000	0.022 ± 0.000
51	0.067 ± 0.000	0.077 ± 0.001	0.075 ± 0.002	0.067 ± 0.003	0.067 ± 0.003
52	0.012 ± 0.000	0.012 ± 0.000	0.013 ± 0.000	0.011 ± 0.000	0.012 ± 0.000
53	0.047 ± 0.001	0.047 ± 0.001	0.048 ± 0.002	0.037 ± 0.000	0.047 ± 0.001

Table 20. Compared with temperature of column oven

Temperature (°C)	Analytes 45	46	47	48	49	50	51	52	53
Theoretical plates (N)									
25	10991.67 ±253.60	14771.00 ±308.21	22423.00 ±399.03	24943.33 ±308.23	27680.00 ±308.64	25437.34 ±345.67	795003.00 ±7390.06	751251.30 ±486.75	758846.70 ±19643.71
30	12300.33 ±1152.73	17018.67 ±354.80	23432.33 ±1020.65	26436.33 ±976.63	28554.67 ±1145.70	24784.35 ±1034.56	776265.00 ±29461.08	746364.70 ±12800.66	700632.30 ±11300.37
35	12366.00 ±43.49	18743.33 ±128.94	23730.33 ±807.87	26461.00 ±727.50	28730.67 ±930.68	25349.06 ±850.76	751224.30 ±25839.51	709814.00 ±6337.09	750275.30 ±14291.09
40	12281.00 ±300.38	19932.00 ±401.00	23629.00 ±727.22	26548.67 ±648.31	27908.67 ±791.36	27360.65 ±785.66	729425.30 ±42711.61	668044.00 ±7160.33	787865.70 ±5837.62
45	12388.33 ±223.04	20603.00 ±876.91	23523.00 ±1106.78	26434.00 ±1417.47	27813.33 ±1561.18	26275.89 ±563.88	775806.70 ±16296.38	714951.30 ±12225.74	807067.00 ±18889.27
Capacity factor (k')									
25	5.08±0.00	14.24±0.04	15.82±0.04	20.75±0.05	22.48±0.05	24.45±0.23	32.97±0.03	33.39±0.07	33.81±0.03
30	5.01±0.06	13.36±0.25	14.70±0.28	19.22±0.27	20.77±0.28	22.37±0.26	32.77±0.00	33.17±0.00	33.61±0.00
35	4.87±0.04	12.39±0.21	13.50±0.25	17.63±0.25	18.99±0.26	20.35±0.25	32.58±0.01	33.00±0.00	33.42±0.00
40	4.76±0.03	11.57±0.20	12.48±0.23	16.25±0.25	17.45±0.26	19.17±0.34	32.40±0.01	32.84±0.02	33.26±0.01
45	4.64±0.03	10.84±0.17	11.59±0.20	15.03±0.23	16.08±0.24	18.76±0.29	32.19±0.01	32.66±0.00	33.07±0.00
Separation factor (α)									
25	-	2.80±0.01	1.11±0.00	1.16±0.01	1.08±0.00	1.08±0.00	1.85±0.01	1.01±0.00	1.01±0.00
30	-	2.67±0.02	1.11±0.00	1.15±0.00	1.08±0.00	1.08±0.00	1.98±0.02	1.01±0.00	1.01±0.00
35	-	2.54±0.02	1.09±0.00	1.14±0.00	1.08±0.00	1.09±0.00	2.13±0.02	1.01±0.00	1.01±0.00
40	-	2.43±0.02	1.08±0.00	1.14±0.00	1.07±0.00	1.09±0.00	2.29±0.03	1.01±0.00	1.01±0.00
45	-	2.34±0.02	1.07±0.00	1.13±0.00	1.07±0.00	1.08±0.00	2.40±0.01	1.01±0.00	1.01±0.00
Resolution factor (Rs)									

25	-	24.94±0.21	3.31±0.02	5.16±0.02	3.11±0.01	3.21±0.02	50.23±0.04	2.09±0.04	2.67±0.01
30	-	25.39±0.72	3.14±0.07	5.01±0.06	3.04±0.03	3.19±0.04	58.94±0.02	2.23±0.04	2.40±0.04
35	-	24.92±0.32	2.86±0.08	4.74±0.05	2.92±0.02	2.85±0.03	62.15±0.05	2.41±0.08	2.25±0.01
40	-	24.12±0.48	2.56±0.08	4.47±0.05	2.75±0.03	2.69±0.02	72.65±0.02	2.42±0.01	2.36±0.03
45	-	23.25±0.61	2.27±0.10	4.24±0.10	2.60±0.06	2.63±0.01	79.71±0.03	2.65±0.03	2.42±0.01

Table 21. Calibration curves, LOD and LOQ of nine standard compounds

Compounds	Range (μg/ml)	Regression equation[a)]	r^2	LOD [b)] (μg/ml)	LOQ[c)] (μg/ml)
45	1~20	Y=0.02713X - 0.00701	0.9995	0.064	0.195
46	1~20	Y=0.05764X - 0.00891	0.9999	0.046	0.141
47	1~20	Y=0.06347X - 0.02215	0.9992	0.027	0.083
48	1~20	Y=0.15388X - 0.03322	0.9997	0.019	0.059
49	1~20	Y=0.07367X - 0.01395	0.9999	0.023	0.071
50	1~20	Y=0.06247X - 0.02431	0.9994	0.030	0.092
51	1~20	Y=0.33170X - 0.57136	0.996	0.895	2.712
52	1~20	Y=0.33922X - 0.59272	0.995	0.787	2.383
53	1~20	Y=0.29968X - 0.50443	0.996	0.833	2.526

a)y: peak area, x: concentration of the analyte (μg/mL).

b)LOD, limit of detection.

c)LOQ, limit of quantification.

Table 22. Precision and accuracy of the nine standard compounds

Compounds	Spiked amount (μg)	Intra-day (n = 3)		Inter-day (n = 3)	
		Recovery (%)	RSD (%)	Recovery (%)	RSD (%)
	10	97.77	0.37	98.07	1.30
45	14	98.43	0.41	98.38	0.61
	17	98.41	0.09	98.51	0.47
	2	92.99	2.38	92.76	3.20
46	4	95.11	0.82	94.41	0.31
	8	95.48	0.34	95.63	0.75
	4	98.42	0.10	98.35	0.61
47	8	98.04	0.69	97.94	0.67
	12	98.89	0.59	98.37	0.54
	2	96.54	1.47	96.08	1.23
48	4	95.89	0.84	96.73	0.96
	8	96.21	0.35	96.53	0.52
	2	102.44	1.55	100.35	1.11
49	4	101.65	1.36	100.32	1.38
	8	99.37	0.82	98.76	0.42
	2	98.35	0.95	99.34	0.35
50	4	96.43	0.56	98.12	0.55
	8	99.23	0.43	94.19	0.47
	20	99.29	2.66	100.59	1.48
51	40	99.61	2.55	98.19	1.89
	80	96.47	0.49	97.88	1.25
	10	100.17	1.39	102.55	2.00
52	20	102.17	2.64	100.09	1.80
	40	104.32	1.68	103.03	1.13
	10	98.93	0.77	102.39	3.03
53	20	98.10	2.65	97.97	1.38

	40	101.58	1.21	102.57	0.94

Table 23. HPLC-MS/MS Data of the nine standard compounds

Peak No.	MW[a)]	MS (m/z)	MS/MS (m/z)	C.E[b)]	Ion mode	Identification
45	342	342	297	29	positive	magnoflorine
46	608	631	469	30	positive	isospinosin
47	608	631	469	33	positive	spinosin
48	814	837	451	33	positive	6'''-sinapoyl spinosin
49	784	807	451	31.3	positive	6'''-feruloyl spinosin
50	754	777	451	31.3	positive	6'''-coumaroyl spinosin
51	1207	1230	757	33	positive	jujuboside A
52	1207	1230	757	33	positive	jujuboside A_2
53	1045	1068	935	34	positive	jujuboside B

a) molecular weight.

b) collision energy.

Table 24. Content of nine compounds in samples of twenty-four commercial products from diverse sources (w/w, %)

sample	**45**	**46**	**47**	**48**	**49**	**50**	**51**	**52**	**53**
Z-1	0.537 ± 0.001	0.020 ± 0.000	0.132 ± 0.000	0.002 ± 0.000	0.048 ± 0.000	0.009 ± 0.000	0.078 ± 0.003	0.013 ± 0.000	0.048 ± 0.001
Z-2	0.601 ± 0.001	0.015 ± 0.000	0.136 ± 0.000	0.002 ± 0.000	0.079 ± 0.000	0.009 ± 0.000	0.085 ± 0.000	0.000 ± 0.000	0.042 ± 0.000
Z-3	0.368 ± 0.000	0.034 ± 0.000	0.160 ± 0.000	0.002 ± 0.000	0.058 ± 0.000	0.011 ± 0.000	0.092 ± 0.000	0.014 ± 0.000	0.070 ± 0.000
Z-4	0.296 ± 0.000	0.019 ± 0.000	0.160 ± 0.000	0.009 ± 0.000	0.067 ± 0.000	0.014 ± 0.000	0.045 ± 0.000	0.012 ± 0.000	0.035 ± 0.000
Z-5	0.656 ± 0.001	0.016 ± 0.000	0.138 ± 0.000	0.002 ± 0.000	0.072 ± 0.000	0.010 ± 0.000	0.072 ± 0.000	0.012 ± 0.000	0.053 ± 0.000
Z-6	0.098 ± 0.000	0.006 ± 0.000	0.140 ± 0.000	0.012 ± 0.000	0.036 ± 0.000	0.007 ± 0.000	0.000 ± 0.000	0.000 ± 0.000	0.011 ± 0.000
Z-7	0.452 ± 0.001	0.017 ± 0.000	0.127 ± 0.000	0.002 ± 0.000	0.063 ± 0.000	0.008 ± 0.000	0.053 ± 0.000	0.015 ± 0.000	0.036 ± 0.000
Z-8	0.576 ± 0.001	0.020 ± 0.000	0.146 ± 0.000	0.002 ± 0.000	0.076 ± 0.000	0.015 ± 0.000	0.086 ± 0.000	0.013 ± 0.000	0.047 ± 0.000
Z-9	0.191 ± 0.000	0.013 ± 0.000	0.219 ± 0.000	0.031 ± 0.000	0.092 ± 0.000	0.016 ± 0.000	0.000 ± 0.000	0.000 ± 0.000	0.015 ± 0.000
Z-10	0.556 ± 0.000	0.021 ± 0.000	0.128 ± 0.000	0.002 ± 0.000	0.056 ± 0.000	0.010 ± 0.000	0.090 ± 0.000	0.013 ± 0.000	0.061 ± 0.000
Z-11	0.581± 0.001	0.027 ± 0.000	0.140 ± 0.000	0.002 ± 0.000	0.065 ± 0.000	0.011 ± 0.000	0.086 ± 0.002	0.015 ± 0.000	0.049 ± 0.002
Z-12	0.623± 0.001	0.019 ± 0.000	0.131 ± 0.000	0.002 ± 0.000	0.064 ± 0.000	0.011 ± 0.000	0.072 ± 0.001	0.016 ± 0.000	0.044 ± 0.001
Z-13	0.236 ± 0.001	0.013 ± 0.000	0.222 ± 0.000	0.028 ± 0.000	0.087 ± 0.000	0.016 ± 0.000	0.000 ± 0.000	0.000 ± 0.000	0.014 ± 0.000
Z-14	0.165 ± 0.000	0.014 ± 0.000	0.260 ± 0.001	0.036 ± 0.000	0.106 ± 0.000	0.018 ± 0.000	0.000 ± 0.000	0.000 ± 0.000	0.015 ± 0.000
Z-15	0.220 ± 0.000	0.013 ± 0.000	0.178 ± 0.000	0.025 ± 0.000	0.072 ± 0.000	0.011 ± 0.000	0.000 ± 0.000	0.000 ± 0.000	0.015 ± 0.000
Z-16	0.242 ± 0.000	0.020 ± 0.000	0.222 ± 0.000	0.028 ± 0.000	0.082 ± 0.000	0.014 ± 0.000	0.000 ± 0.000	0.000 ± 0.000	0.014 ± 0.000
Z-17	0.235 ± 0.000	0.012 ± 0.000	0.222 ± 0.000	0.031 ± 0.000	0.096 ± 0.000	0.018 ± 0.000	0.000 ± 0.000	0.000 ± 0.000	0.014 ± 0.000
Z-18	0.200 ± 0.000	0.008 ± 0.000	0.199 ± 0.000	0.023 ± 0.000	0.081 ± 0.000	0.012 ± 0.000	0.000 ± 0.000	0.000 ± 0.000	0.013 ± 0.000

Z-19	0.201 ± 0.000	0.013 ± 0.000	0.175 ± 0.000	0.028 ± 0.000	0.094 ± 0.000	0.020 ± 0.000	0.000 ± 0.000	0.000 ± 0.000	0.014 ± 0.000
Z-20	0.229 ± 0.000	0.014 ± 0.000	0.178 ± 0.000	0.031 ± 0.000	0.085 ± 0.000	0.018 ± 0.000	0.000 ± 0.000	0.000 ± 0.000	0.014 ± 0.000
Z-21	0.234 ± 0.001	0.016 ± 0.000	0.234 ± 0.000	0.031 ± 0.000	0.107 ± 0.000	0.017 ± 0.000	0.000 ± 0.000	0.000 ± 0.000	0.016 ± 0.000
Z-22	0.232 ± 0.000	0.022 ± 0.000	0.211 ± 0.000	0.028 ± 0.000	0.096 ± 0.000	0.015 ± 0.000	0.000 ± 0.000	0.000 ± 0.000	0.015 ± 0.000
Z-23	0.210 ± 0.000	0.014 ± 0.000	0.218 ± 0.000	0.032 ± 0.000	0.094 ± 0.000	0.015 ± 0.000	0.000 ± 0.000	0.000 ± 0.000	0.015 ± 0.000
Z-24	0.196 ± 0.000	0.015 ± 0.000	0.206 ± 0.000	0.032 ± 0.000	0.099 ± 0.000	0.015 ± 0.000	0.012 ± 0.000	0.000 ± 0.000	0.019 ± 0.000

IV. Conclusion

The purpose of this work is the development of simultaneous analysis methods of all bioactive compounds in herbal medicines. The methods based on HPLC-DAD-ELSD-MS were established for the quantitative and qualitative analysis of two selected herbal medicines.

Various validation parameters, such as linearity, limit of detection, limit of quantification, recovery, accuracy, and precision, were successfully obtained. In addition, the efficiencies of diverse extraction methods were compared for the development of a standard analytic method. The verified methods were successfully applied to the quantitative determination of representative metabolites in commercial samples from Korea, Myanmar, and China.

These results have successfully demonstrated the potential of using developed methods for the quality control of herbal medicines.

Summary

During the four and half years of the Doctor of Philosophy studies, effort is focused on the study of isolation of secondary metabolites from marine-derived fungi and development of quantitative and qualitative analysis methods of herbal medicines.

To achieve isolation and structure determination of novel substances from marine organisms, more than two hundred fungal strains were isolated from the sea sediments and marine organisms which collected from various locations of southern coast of Korea and two of them were selected for chemical investigation on the basis of LC-ESIMS analysis and bioactivity tests. From two selected marine-derived fungi, 18 compounds have been isolated and 9 new ones among these have been structurally elucidated by combined spectroscopic and chemical analysis. The structures of these 18 compounds belonged to diverse structural classes with various biogenetic origins. Diverse bioassay tests related to anticancer, antimicrobial, and enzyme-inhibitory activities have been performed. Some of the isolated compounds showed potent bioactivities in quinone reductase and anticancer towards to HCT116, SNU638, SK-HEP1, MDA-MB231 cell lines. One of compound was studied vivo test on mice. Structure-activity relationships

were also deduced.

In addition to chemical investigation of marine fungi, the standard methods based on HPLC-DAD-ELSD-MS was established for the simultaneous analysis of two selected herbal medicines. Based upon the prior researches, all standard compounds which have significant bioactivities and large contents were analyzed. Diverse validation parameters, such as linearity, limit of detection, limit of quantification, recovery, accuracy, and precision, were successfully obtained and the efficiencies of diverse extraction methods were compared. The developed methods were successfully applied to the quantitative determination of representative metabolites in commercial samples from Korea and China.

1. Penicillipyrones A and B, Meroterpenoids from the Marine-derived Fungus *Penicillium* sp.

Two novel meroterpenoids, Penicillipyrones A (**1**) and B (**2**), together with methyl 8-hydroxy-6-methyl-9-oxo-9H-xanthene-1-carboxylate (**3**) and coniochaetone B (**4**) were isolated from the marine-derived fungus *Penicillium* sp.. Based upon the results of combined spectroscopic analyses, these compounds were structurally elucidated to be triprenyl γ-lactones from a new skeletal class derived from a unique pattern of linkage between the

prenyl and pyrone moieties.

The new compounds exhibited weak cytotoxicities against K562 and A549 cell lines. However, compounds **1** and **2** were inactive (MIC > 100 μg/mL) against various Gram-positive and Gram-negative bacteria and pathogenic fungi. Compound **2** also elicited a significant induction of quinone reductase. Contrastingly, compound **1**, which possessed the 3-hydroxy group, failed to show a noticeable induction in the given concentration, implying that the ketone moiety at C-3 of **2** plays a crucial role in its QR inducing activity. Therefore, the significant induction of penicillipyrone B (**2**) with significant induction of QR may be suggestive of a potential role in cancer prevention.

2. Alkaloidal Metabolites from a Marine-Derived *Aspergillus* sp. Fungus

Fumiquinazoline S (**5**), a new quinazoline-containing alkaloid, and the known fumiquinazolines F (**10**) and L (**11**) of the same structural class were isolated from the solid-substrate culture of an *Aspergillus* sp. fungus collected from marine-submerged wood. In addition, isochaetominines A-C (**6**-**8**) and 14-*epi*-isochaetominine C (**9**), new alkaloids possessing an unusual amino acid-based tetracyclic core framework related to the fumiquinazolines, and together with nidurufin (**12**), versiconol (**13**), sterigmatocystin (**14**), 7-deoxysterigmatocystin (**15**), and isobenzofuranone (**16**) were isolated from

the same fungal strain. The structures of these compounds were determined by combined spectroscopic methods, and the absolute configurations were assigned by NOESY, ROESY and advanced Marfey's analyses along with biogenetic considerations.

The new compounds exhibited weak inhibition against Na^+/K^+-ATPase. In our measurement of cytotoxicity, however, **5-11** were inactive (**5-9**: IC_{50} > 13-50 μM, **10** and **11**: IC_{50} > 100 μM) against the K562 and A549 cell lines. In the antimicrobial activity tests against selected strains of Gram-positive and Gram-negative bacteria and pathogenic fungi, only compound **10** displayed weak inhibition (MIC 50 μM) against *Bacillus subtilis*. These alkaloids also exhibited a weak inhibition (IC_{50} were 34, 78, 20, 38, 57, 17, and 20 μM for **5-11**, respectively) against Na^+/K^+-ATPase. None of these compounds were active against the enzymes sortase A or isocitrate lyase.

3. Asperphenins A and B, lipopeptides as anticancer agents from a Marine-Derived *Aspergillus* sp. Fungus

Asperphenins A (**17**) and B (**18**), two new lipopeptide containing aromatic compounds were isolated from the marine-derived fungus *Aapergillus* sp.. Based upon the results of combined spectroscopic analyses, these compounds were structurally elucidated to be lipopeptide containing the

phenone function group, the first example of this type.

In our bioactivity measurement, compounds **17**-**28** were studied toward the A549, HCT116, SNU638, SK-HEP1, and MDA-MB 231. Asperphenins A (**17**) and B (**18**) were significantly ative against HCT116, moderately active toward the SNU638, SK-HEP1, and MDA-MB 231, and weak activity toward the A549. However, the cycloasperphenins A (**19**) and B (**20**) were inactive toward all the cell lines, and 7-ketone reduction of asperphenins A (**21**, **22**) and B (**23**) were inactive toward the A549 and MDA-MB 231, and weak toward HCT116, SNU638 and SK-HEP1. And 7-ketone reduction of asperphenin B (**24**) and 7,15-diketone reduction of asperphenins A (**26**) and B (**27**, **28**) were inactive toward all the cell lines. The results implied that the 7-ketone and 15-ketone played the important role for activities against A549, HCT116, SNU638, SK-HEP1, and MDA-MB 231. Morever, the asperphenin B (**18**) was studied as the antitumor agent on RKO cell-implated xenografts. Asperphenin B exhibited significant inhibition of colon cancer. At a concentration of 8mg/kg, the inhibition rate was 68.7%, which was approached the inhibition rate of irinotecan with the 4 mg/kg. And the combination of asperphenin B and irinotecan improved the inhibition to 86.9%. Therefore, the significant inhibition toward the colon cancer by asperphenin B may be suggestive of a potential role in anticancer drug. The

mechanism of anti-colon cancer of asperphenin B is futher being studied.

4. Quantification and Identification of Bioactive Metabolites from Kalopanacis Cortex by HPLC with Evaporative Light Scattering Detection and ESI Quadrupole TOF MS

A method based on HPLC-ELSD-Q-TOF-MS was established for the simultaneous determination of twelve bioactive metabolites from the Kalopanacis Cortex. Validation parameters, such as linearity, limit of detection, limit of quantification, recovery, accuracy, and precision, were successfully obtained. In addition, the efficiencies of diverse extraction methods were compared for the development of a standard analytic method. The verified method was successfully applied to the quantitative determination of twelve representative metabolites in sixty-one Kalopanacis Cortex samples from Korea and China. The quantitation results demonstrated that six compounds, coniferin (**33**), kalopanaxsaponin C (**40**), septemlosides II (**38**), III (**36**), C (**39**), and D (**37**), which exhibited distinct regional patterns in KC samples, could serve as marker compounds to distinguish KC from Korea and China.

5. Simultaneous Analysis of Bioactive Metabolites from *Ziziphus jujube* by HPLC-DAD-ELSD-MS/MS

A method based on HPLC-DAD-ELSD-MS/MS was established for the simultaneous determination of nine representative metabolites from semen Ziziphus jujuba. Validation parameters, such as linearity, limit of detection, limit of quantification, recovery, accuracy, and precision, were successfully obtained. In addition, the efficiencies of diverse extraction methods were compared for the development of a standard analytic method. The verified method was successfully applied to the quantitative determination of nine representative metabolites in twenty-four commercial samples of *Z. jujuba var. spinosa* and *Z. mauritiana* from different markets in Korea, China and Myanmar were analyzed and compared to each other. The analytical results showed that the contents of the nine analytes vary significantly with two different species.

References

1. Zhao, Y.; Chen, P. *Curr. Org. Chem.* **2014**, *18*, 777-792.
2. Fenical, W. *Chem. Rev.* **1993**, *93*, 1673-1683.
3. Bugni, T. S.; Ireland, C. M. *Nat. Prod. Rep.* **2004**, *21*, 143-163.
4. Fenical, W.; Jensen, P. R. *Nat. Chem. Biol.* **2006**, *2*, 666-673.
5. Cragg, G. M.; Grothaus, P. G.; Newman, D. J. *Chem. Rev.* **2009**, *109*, 3012-3043.
6. Bhatnagar, I.; Kim, S. K. *Mar. Drugs*, **2010**, *8*, 2673-2701.
7. Blunt, J. W.; Copp, B. R.; Keyzers, R. A.; Munro, M. H. G.; Prinsep, M. R. *Nat. Prod. Rep.* **2014**, *31*, 160-258, and earlier reports in the series.
8. Hu, G. P.; Yuan, J.; Sun, L.; She, Z.-G.; Wu, J.-H.; Lan, X.-J.; Zhu, X.; Lin, Y.-C.; Chen, S.-P. *Mar. Drugs* **2011**, *9*, 514-525.
9. Jensen, P. R.; Fenical, W. *Annu. Rev. Microbiol.* **1994**, *48*, 559-584.
10. Bhakuni, D. S.; Rawat, D. S., *Bioactive Marine Natural Products*; Springer: AH Dordrecht, 2005; pp 13-17.
11. Bhadury, P.; Mohammad, B. T.; Wright, P. C., *J. Ind. Microbiol. Biotechnol.* **2006**, *33*, 325-337.
12. Rinehart, K. L., Jr.; Kobayashi, J.; Harbour, G. C.; Hughes, R. G. Jr.; Mizsak, S. A.; Scahill, T. A. *J. Am. Chem. Soc.* **1984**, *106*, 1524-1526.
13. Simons, T. L.; Andrianasolo, E.; McPhail, K., Flatt, P.; Gerwick, W. H.

Mol. Cancer Ther. **2005**, *4*, 333-342.

14. Mayer, A. M. S.; Gustafson, K. R. *Eur. J. Cancer* **2008**, *44*, 2357-2387.
15. Salomon, C. E.; Magarvey, N. A.; Sherman, D. H. *Nat. Prod. Rep.* **2004**, *21*, 105-121.
16. Gordaliza, M. *Clin. Transl. Oncol.* **2007**, *9*, 767-776.
17. Kohlmeyer, J.; Kohlmeyer, E., *Marine Mycology. The Higher Fungi*. Academic Press: New York, 1979; pp 54-69.
18. Nikapitiya, C., Bioactive Secondary Metabolites from Marine Microbes for Drug Discovery. In *Advances in Food and Nutrition Research*; Kim, S.-K., Ed; Academic Press: San Diego, 2012; Vol. 65, Chapter 24, pp 363-387.
19. Rowley, D. C.; Kelly, S.; Kauffman, C. A.; Jensen, P. R.; Fenical, W., *Bioorg. Med. Chem. Lett.* **2003**, *11*, 4263-4274.
20. Cueto, M.; Jensen, P. R.; Kauffman, C.; Fenical, W.; Lobkovsky, E.; Clardy, J., *J. Nat. Prod.* **2001**, *64*, 1444-1446.
21. Tan, L. T.; Cheng, X. C.; Jensen, P. R.; Fenical, W., *J. Org. Chem.* **2003**, *68*, 8767-8773.
22. Cueto, M.; MacMillan, J. B.; Jensen, P. R.; Fenical, W., *Phytochemistry* **2006**, *67*, 1826-1831.
23. Tan, R. X.; Jensen, P. R.; Williams, P. G.; Fenical, W., *J. Nat. Prod.*

2004, *67*, 1374-1382.

24. Garo, E.; Starks, C. M.; Jensen, P. R.; Fenical, W.; Lobkovsky, E.; Clardy, J., *J. Nat. Prod.* **2003**, *66*, 423-426.

25. Oh, D. C.; Jensen, P. R.; Fenical, W., *Tetrahedron Lett.* **2006**, *47*, 8625-8628.

26. Zheng, J.; Zhu, H.; Hong, K.; Wang, Y.; Liu, P.; Wang, X.; Peng, X.; Zhu, W., *Org. Lett.* **2009**, *11*, 5262-5265.

27. Gu, W.; Cueto, M.; Jensen, P. R.; Fenical, W.; Silverman, R. B., *Tetrahedron* **2007**, *63*, 6535-6541.

28. Mayer, A.; Glaser, K. B.; Cuevas, C.; Jacobs, R. S.; Kem, W.; Little, R. D.; McIntosh, J. M.; Newman, D. J.; Potts, B. C.; Shuster, D. E., *Trends Pharmacol. Sci.* **2010**, *31*, 255-265.

29. Lu, Z.; Zhu, H.; Fu, P.; Wang, Y.; Zhang, Z.; Lin, H.; Liu, P.; Zhuang, Y.; Hong, K.; Zhu, W., *J. Nat. Prod.* **2010**, *73*, 911-914.

30. Koizumi, Y.; Arai, M.; Tomoda, H.; Ōmura, S., *Biochim. Biophys. Acta.* **2004**, *1693*, 47-55.

31. Zheng, J.; Xu, Z.; Wang, Y.; Hong, K.; Liu, P.; Zhu, W., *J. Nat. Prod.* **2010**, *73*, 1133-1137.

32. Li, C.-S.; An, C.-Y.; Li, X.-M.; Gao, S.-S.; Cui, C.-M.; Sun, H.-F.; Wang, B.-G., *J. Nat. Prod.* **2011**, *74*, 1331-1334.

33. Lee, S. U.; Asami, Y.; Lee, D.; Jang, J. H.; Ahn, J. S.; Oh, H., *J. Nat. Prod.* **2011**, *74*, 1284-1287.

34. Oh, H.; Jensen, P. R.; Murphy, B. T.; Fiorilla, C.; Sullivan, J. F.; Ramsey, T.; Fenical, W., *J. Nat. Prod.* **2010**, *73*, 998-1001.

35. Peng, X.; Wang, Y.; Sun, K.; Liu, P.; Yin, X.; Zhu, W., *J. Nat. Prod.* **2011**, *74*, 1298-1302.

36. Julianti, E.; Oh, H.; Jang, K. H.; Lee, J. K.; Lee, S. K.; Oh, D.-C.; Oh, K.-B.; Shin, J. *J. Nat. Prod.* **2011**, *74*, 2592-2594.

37. Julianti, E.; Lee, J.-H.; Liao, L.; Park, W.; Park, S.; Oh, D.-C.; Oh, K.-B.; Shin, J. *Org. Lett.* **2013**, *15*, 1286-1289.

38. Jeon, J.-e.; Julianti, E.; Oh, H.; Park, W.; Oh, D.-C.; Oh, K.-B.; Shin, J. *Tetrahedron Lett.* **2013**, *54*, 3111-3115.

39. Mosmann, T. *J. Immunol. Methods* **1983**, *65*, 55–63.

40. Ulukaya, E.; Ozdikicioglu, F.; Oral, A. Y.; Demirci, M. *Toxicol. in Vitro* **2008**, *22*, 232–239.

41. Chung, S.-C.; Jang, K.-H.; Park, J.; Ahn, C.-H.; Shin, J.; Oh, K.-B.; Shin, J. *Bioorg. Med. Chem. Lett.* **2011**, *21*, 1958–1961.

42. Prochaska, H. J.; Santamaria A. B. *Anal Biochem.* **1988**, *169*, 328–336.

43. Hendrickx, A. P.; Budzik, J. M.; Oh, S. Y.; Schneewind, O. *Nat. Rev. Microbiol.* **2011**, *9*, 166-176.

44. Lorenz, M. C.; Fink, G. R. *Nature* **2001**, *412*, 83-86.

45. Johansson, M.; Karlsson, L.; Wennergren, M.; Jansson, T.; Powell, T. L. *J. Clin. Endocrinol. Metab.* **2003**, *88*, 2831-2837.

46. Kanokmedhakul, K.; Kanokmedhakul, S.; Suwannatrai, R.; Soytong, K.; Prabpai, S.; Kongsaeree, P. *Tetrahedron* **2011**, *67*, 5461–5468.

47. Phipps, R. K.; Petersen, B. O.; Christensen, K. B.; Duus, J. Ø .; Frisvad, J. C.; Larsen, T. O. *Org. Lett.* **2004**, *6*, 3441–3443.

48. (a) Nasu, S. S.; Yeung, B. K. S.; Hamann, M. T.; Scheuer, P. J. *J. Org. Chem.* **1995**, *60*, 7290–7292. (b) Ueda, K.; Ogi, T.; Sato, A.; Siwu, E. R. O.; Kita, M.; Uemura, D. *Heterocycles* **2007**, *72*, 655–663. (c) Fontana, A; Tramice, A.; Cutignano, A.; d'Ippolito, G.; Gavagnin, M.; Cimino, G. 2003, *69*, 2405–2409.

49. (a) Yasuo, K. *Kagaku to Seibutsu* **1983**, *21*, 321–323. (b) Jones, R. C. F. *Nat. Prod. Rep.* **1985**, *2*, 401–426.

50. Geris, R.; Simpson, T. J. *Nat. Prod. Rep.* **2009**, *26*, 1063–1094.

51. (a) Kikuchi, H.; Hoshi, T.; Kitayama, M.; Sekiya, M.; Katou, Y.; Ueda, K.; Kubohara, Y.; Sato, H.; Shimazu, M.; Kurata, S.; Oshima, Y. *Tetrahedron* **2009**, *65*, 469–477. (b) Lee, J. C.; Lobkovsky, E.; Pliam, N. B.; Strobel, G.; Clardy, J. *J. Org. Chem.* **1995**, *60*, 7076–7077. (c) Goetz, M. A.; Zink, D. L.; Dezeny, G.; Dombrowski, A.; Polishook, J.

D.; Felix, J. P.; Slaughter, R. S.; Singh, S. B. *Tetrahedron Lett.* **2001**, *42*, 1255–1257. (d) Singh, S. B.; Zink, D. L.; Dombrowski, A. W.; Dezeny, G.; Bills, G. F.; Slaughter, R. S.; Goetz, M. A. *Org. Lett.* **2001**, *3*, 247–250. (e) Kimura, Y.; Hamasaki, T.; Isogai, A., Nakajima, H. *Agric. Biol. Chem.* **1982**, *46*, 1963–1965.

52. Rubal, J. J.; Moreno-Dorado, F. J.; Guerra, F. M.; Jorge, Z. D.; Saouf, A.; Akssira, M.; Mellouki, F.; Romero-Garrido, R.; Massanet, G. M. *Phytochem.* **2007**, *68*, 2480–2486.

53. (a) Fernandez, M. A.; Ferrero, B. O.; De, P. T. J.; Rubio, G. R. *Tetrahedron* **1991**, *47*, 4375–4382. (b) Vlad, P. V.; Ungur, N. D.; Nguyen, V. H. *Khim. Prir. Soedin.* **1990**, 346–353. (c) Ungur, N. D.; Tuen, N. V.; Popa, N. P.; Vlad, P. F. *Khim. Prir. Soedin.* **1992**, 645–653.

54. Sunaka, T.; Ōmura, S. *Chem. Rev.* **2005**, *105*, 4559–4580.

55. (a) Talalay, P.; Fahey, J. W.; Holtzclaw, W. D.; Prestera, T.; Zhang, Y. *Toxicol. Lett.* **1995**, *82-83*, 173–179. (b) Park, E.-J.; Min, H.-Y.; Park, H. J.; Ahn, Y.-H.; Pyee, E.-J.; Lee, S. K. *J. Pharmacol. Sci.* **2011**, *116*, 89–96.

56. Ulukaya, E.; Ozdikicioglu, F.; Oral, A. Y.; Demirci, M. *Toxicol. in Vitro* **2008**, *22*, 232–239.

57. Chung, S.-C.; Jang, K.-H.; Park, J.; Ahn, C.-H.; Shin, J.; Oh, K.-B.;

Shin, J. *Bioorg. Med. Chem. Lett.* **2011**, *21*, 1958–1961.

58. Liao, L.; Lee, J.-H.; You, M.; Choi, T. J.; Park, W.; Lee, S. K.; Oh, D.-C.; Oh, K.-B.; Shin, J. *J. Nat. Prod.* **2014**, *77*, 406-410.

59. Afiyatullov, S. S.; Zhuravleva, O. I.; Antonov, A. S.; Kalinovsky, A. I.; Pivkin, M. V.; Menchinskaya, E. S.; Aminin, D. L. *Nat. Prod. Commun.* **2012**, *7*, 497-500.

60. Zhou, Y.; Debbab, A.; Mándi, A.; Wray, V.; Schulz, B.; Müller, W. E. G.; Kassack, M.; Lin, W. H.; Kurtán, T.; Proksch, P.; Aly, A. H. *Eur. J. Org. Chem.* **2013**, 894-906..

61. Shao, C.-L.; Xu, R.-F.; Wei, M.-Y.; She, Z.-G.; Wang, C.-Y. *J. Nat. Prod.* **2013**, *76*, 779-782.

62. Numata, A.; Takahashi, C.; Matsushita T.; Miyamoto, T.; Kawai, K.; Usami, Y.; Matsumura, E.; Inoue, M.; Ohishi, H.; Shingu, T. *Tetrahedron Lett.* **1992**, *33*, 1621-1624.

63. Takahashi, C.; Matsushita, T.; Doi, M.; Minoura, K.; Shingu, T.; Kumeda, Y.; Numata, A. *J. Chem. Soc. Perkin Trans. 1* **1995**, 2345-2353.

64. Belofsky, G.; Anguera, M.; Jensen, P.; Fenical, W.; Köck, M. *Chem. Eur. J.* **2000**, *6*, 1355-1360.

65. Heredia, M.; Cuesta, E.; Avendaño, C. *Tetrahedron* **2002**, *58*, 6163-

6170.

66. Han, X.; Xu, X.; Cui, C.; Gu, Q. *Chin. J. Med. Chem.* **2007**, *17*, 232-237.

67. Jiao, R.; Xu, S.; Liu, J.; Ge, H.; Ding, H.; Xu, C.; Zhu, H.; Tan, R. *Org. Lett.* **2006**, *8*, 5709-5712.

68. (a) Fujii, K.; Ikai, Y.; Mayumi, T.; Oka, H.; Suzuki, M.; Harada, K.-i. *Anal. Chem.* **1997**, *69*, 3346-3352. (b) Fujii, K.; Ikai, Y.; Oka, H.; Suzuki, M.; Harada, K.-i. *Anal. Chem.* **1997**, *69*, 5146-5151. (c) Woo, J.-K.; Jeon, J.-e.; Kim, C.-K.; Sim, C. J.; Oh, D.-C.; Oh, K.-B.; Shin, J. *J. Nat. Prod.* **2013**, *76*, 1380-1383.

69. Liao, L.; You, M.; Chung, B. K.; Oh, D.-C.; Oh, K.-B.; Shin, J. *J. Nat. Prod.* **2015**, *78*, 349-354.

70. Shigemon, H.; Eakuri, S.; Yazawa, K.; Nakamura, T.; Sasaki, T.; Kobayashi, J. *Tetrahedron*, **1991**, *47*, 8529-8534.

71. Xu, D.; Ondeyka, H.; Harris, G.; Zink, D.; Kahn, J. N.; Wang, H.; Bills, G.; Platas, G.; Wang, W.; Szewczak, A.; Liberator, P.; Roemer, T. *J. Nat. Prod.* **2011**, 74, 1721-1730.

72. (a) Lee, Y. M.; Dang, H. T.; Li, J.; Zhang, P.; Hong, J.; Lee, C.-O.; Jung, J. H. *Bull. Korean Chem. Soc.* **2011**, *32*, 3817-3820. (b) Wu, C.-J.; Li, C.-W.; Cui, C.-B. *Mar. Drugs* **2014**, *12*, 1815-1838.

73. Ui, H.; Shiomi, K.; Suzuki, H.; Hatano, H.; Morimoto, H.; Yamaguchi, Y.; Masuma, R.; Sakamoto, K.; Kita, K.; Miyoshi, H.; Tomoda, H.; Tanaka, H.; Omura, S. *J. Antibiot.* **2006**, *59*, 591-596.

74. (a) Ahn, J. H.; Shin, M. S.; Jung, S. H.; Kang, S. K.; Kim, K. R.; Rhee, S. D.; Jung, W. H.; Yang, S. D.; Kim, S. J.; Woo, J. R.; Lee, J. H.; Cheon, H. G.; Kim, S. S. *J. Med. Chem.* **2006**, *49*, 4781-4784. (b) Chanda,T.; Chowdhury, S.; Ramulu, B. J.; Koley, S.; Jones, R. C. F.; Singh, M. S. *Tetrahedron*, **2014**, *70*, 2190-2194.

75. Matsumori, N.; Kaneno, D.; Murata, M.; Nakamura, H.; Tachibana, K. *J. Org. Chem.* **1999**, *64*, 866-876.

76. Chan, K. *J. Ethnopharmacol.* **2005**, *96*, 1-18.

77. Tindle, H. A.; Davis, R. B.; Phillips, R. S.; Eisenberg, D. M. *Altern. Ther. Health Med.* **2005**, *11*, 42-49.

78. Kim, D.; Kim, B.; Yun, E.; Kim, J.; Chae, Y.; Park, S. *J. Nat. Med.* **2013**, *67*, 27-35.

79. Zhu, Y.-P., *Chinese Materia Medica: Chemistry, Pharmacology and Applications*. London: Taylor & Francis: 1998.

80. Normile, M. *Science* **2003**, *299*, 188-190.

81. Sano, K., Sanada, S., Ida, Y., Shoji, J. *Chem. Pharm. Bull.* **1991**, *39*, 865-870.

82. Kim, T. J. *In Korean Resources Plants*, Seoul National University Press, Seoul **1996**, pp. 169-200.

83. Shao, C. J., Kasai, R., Xu, J. D., Tanaka, O. *Chem. Pharm. Bull.* **1989**. *37*, 311-314.

84. Lee, M. W., Hahn, D. R. *Arch. Pharm. Res.* **1991**, *14*, 124-129.

85. Tindle, H. A.; Davis, R. B.; Phillips, R. S.; Eisenberg, D. M. *Altern. Ther. Health Med.* **2005**, *11*, 42-49.

86. Lee, E., Choi, M. Y., Park, H. J., Cha, B. C., Cho, S. H. *Kor. J. Pharmacogn.* **1995**, *26*, 122-129.

87. Choi, J., Huh, K., Kim, S. H., Lee, K. T., Park, H. J., Han, Y. N. *J. Ethnopharmacol.* **2002**, *79*, 199-204.

88. Jung, H. J., Park, H. J., Kim, R. G., Shin, K. M., Ha, J., Choi, J. W., Kim, H. J., Lee, Y. S., Lee, K. T. *Planta. Med.* **2003**, *69*, 610-616.

89. Park, H. J., Kim, D. H., Choi, J. W., Park, J. H., Han, Y. N. *Arch. Pharm. Res.* **1998**, *21*, 24-29.

90. Bang, S. Y., Park, G. Y., Park, S. Y., Kim, J. H., Lee, Y. K., Lee, S. J., Kim, Y. *Immune. Netw.* **2010**, *10*, 212-218.

91. Kim, I. T., Park, Y. M., Shin, K. M., Ha, J., Choi, J., Jung, H. J., Park, H. J., Lee, K. T. *J. Ethnopharmacol.* 2004, *94*, 165-173.

92. Lee, E. B., Li, D. W., Hyun, J. E., Kim, I. H., Whang, W. K. *J.*

Ethnopharmacol. **2001**, *77*, 197-201.

93. Lee, K. T., Sohn, C., Park, H. J., Kim, D. W., Jung, G. O., Park, K. Y. *Planta. Med.* **2000**, *66*, 329-332.

94. Quang, T. H., Nguyen, T. T. N., Minh, C. V., Kiem, P. V., Boo, H. J., Hyun, J. W., Kang, H. K., Kim, Y. H. *Phytochem. Lett.* **2012**, *5*, 177-182.

95. Kim, D. H., Bae, E. A., Han, M. J., Park, H. J., Choi, J. W. *Biol. Pharm. Bull.* **2002**, *25*, 68-71.

96. Hong, S. S., Hwang, J. S., Huh, J. D., Ro, J. S., Lee, K. S. *Kor. J. Pharmacogn.* **2002**, *33*, 277-284.

97. Kim, M. Y., Yoo, Y. M., Nam, J. H., Choi, J., Park, H. J. *Kor. J. Pharmacogn.* **2007**, *38*, 270-276.

98. Men, C. V., Jang, Y. S., Lee, K. J., Lee, J. H., Quang, T. H., Nguyen, V. L., Hoang, V. L., Kim, Y. H., Kang, J. S. *Arch. Pharmacal. Res.* **2011**, *34*, 2065-2071.

99. Liang, Y., Xie, P., Chan, K. *Planta. Med.* **2010**, *76*, 1997-2003.

100. Liu, L., Lu, Y., Shao, Q., Cheng, Y,-Y., Qu, H.-B. *J. Sep. Sci.* **2007**, *30*, 2628-2637.

101. Kong, W., Jin, C., Xiao, X., Zhao, Y., Liu, W., Li, Z., Zhang, P. *J. Sep. Sci.* **2010**, *33*, 1518-1527.

102. Yin, J. Y., Meng, Q., Wang, E. S. *Chin. Chem. Lett.* **2005**, *16*, 53-56.

103. Yin, J. Y. *Structural elucidation of triterpenoid saponins from Kalopanax septemlobus and investigation of relationship between their structures and activities* (doctoral dissertation). 2005. Available from www.dissertationtopic.net database. Dissertation ID:1588727.

104. Tanaka, T., Nakashima, T., Ueda, T., Tomii, K., Kouno, I. *Chem. Pharm. Bull.* **2007**, *55*, 899-901.

105. Lee, M. K., Choi, O.-K., Park, J.-H., Cho, H.-J., Ahn, M.-J., Kim, S. H., Kim, Y. C. Sung, S. H. *J. Sep. Sci.* **2007**, *30*,2345-2350.

106. Zhang, W.-D., Wang, Y., Wang, Q., Yang, W.-J., Gu, Y., Wang, R., Song, X.-M., Wang, X.-J. *J. Sep. Sci.* **2012**, *35*,2054-2062.

107. Watanabe, I., Saito, H., Takagi, K. *Japan. J. Pharmocol.* **1973**, *23*, 563-571.

108. Shi, Q. R., Zhou, Y., Zhou, P., Zhang, W. D. *J. Pharm. Practice* **2004**, *22*, 94-102.

109. Liu, J. J., Chen, B., Yao, S. Z. *Talanta* **2007**, *71*, 668-675.

110. Wang, Y., Liu, T. H., Wang, W., Wang, B. X. *Acta. Pharm. Sinica.* **2000**, *35*, 284-288.

111. Moln´ar-Perl, I., Füzfai, Z. *J. Chromatogr. A* **2005**, *1073*, 201-227.

112. Zheng, Y., Qian, S.Y., You, Z. L. *J. Physiol. Sci.* **2006**, *28*, 35-37.

113. Tripathi, M., Pandey, M. B., Jha, R. N., Pandey V. B., Tripathi, P. N., Singh, J. P. *Fitoterapia* **2001**, *72*, 507-510.

114. Ghaly, I. S., Said, A., Abdel-Wahhab, M. A. *Environ.Toxicol. Pharmacol.* **2008**, *25*, 10-19.

115. Han, B. H., Park, M. H., Park, J. H. *Pure & Appl. Chem.* **1989**, *61*, 443-448.

116. Zhao, J., Li, S. P., Wang, Y. T., Yang, F. Q., Li, P. *J. Chromatogr. A* **2006**, *1108*, 188-194.

117. Pawlowska, A. M., Camangi, F., Braca, A. *Food Chem.* **2009**, *112*, 858-862.

118. Bao, K. D., Li, P., Qi, L. W., Li, H. J., Yi, L., Wang, W., Wang, Y. Q. *Chem. Pharm. Bull.***2009**, *57*, 144-148.

119. Bao, K. D., Li, P., Li, H. J., Qi, L. W. *J. Chin. Nat. Med.* **2009**, *7*, 47-53.

120. Cheng, G., Bai, Y. J., Zhao, Y. Y., Tao, J., Liu, Y., Tu, G. Z., Ma, L. B., Liao, N., Xu, X. J. *Tetrahedron* **2000**, *56*, 8915-8920.

121. Li, Y. J., Liang, X. M., Xiao, H. B., Bi, K. S. *J. Chromatogr. B* **2003**, *787*, 421-425.

122. Ma, Y. R., Chai, G. L., Zhang, L. X. *J. Chin. Inf. Tradit. Chin. Med.* **2004**, *11*, 368-371.

123. Niu, C. Y., Wu, C. S., Sheng, Y. X., Zhang, J. L. *J. Asian Nat. Prod. Res.*

2010, *12*, 300-312.

APPENDIX A:
^{1}H and ^{13}C NMR Spectroscopic Data of Isolated Compounds

List of Figures

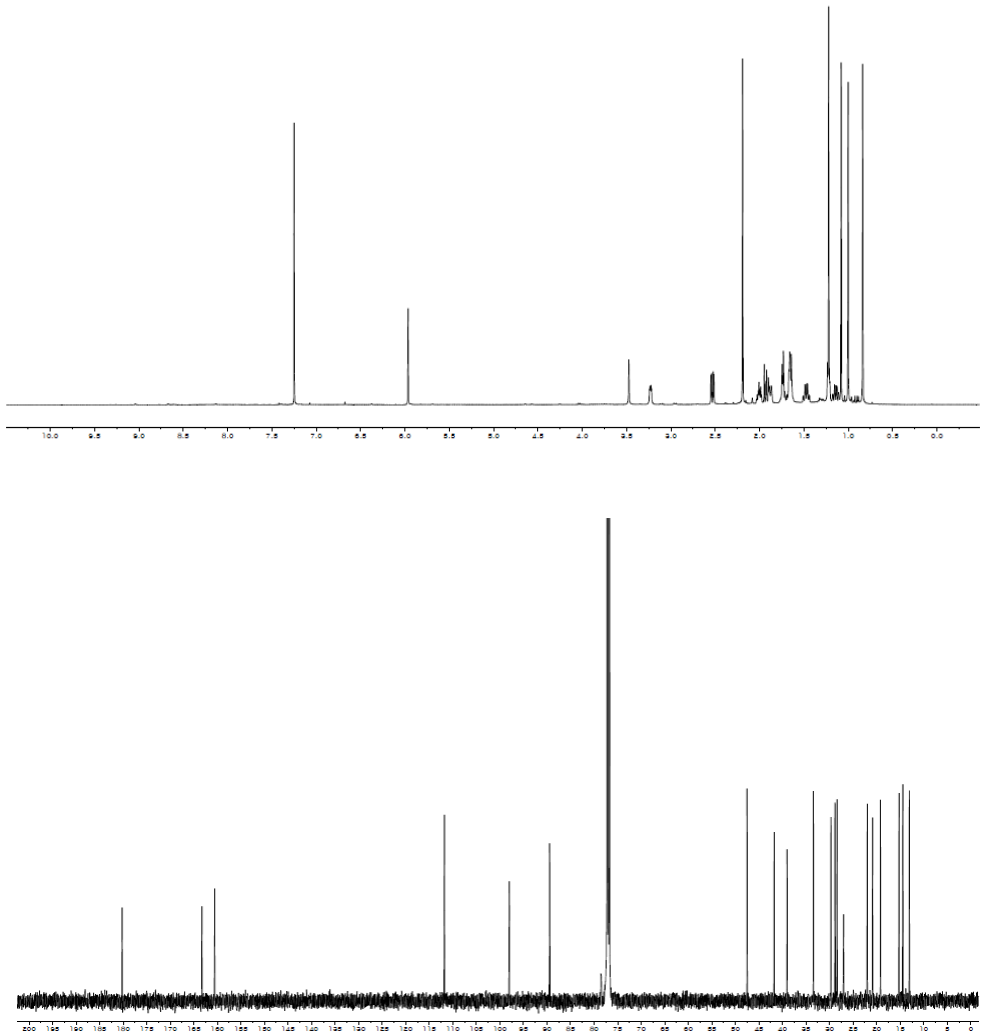

Figure A1. ^{1}H (500 MHz) and ^{13}C (125 MHz) NMR spectra of compound **1** ($CDCl_3$)

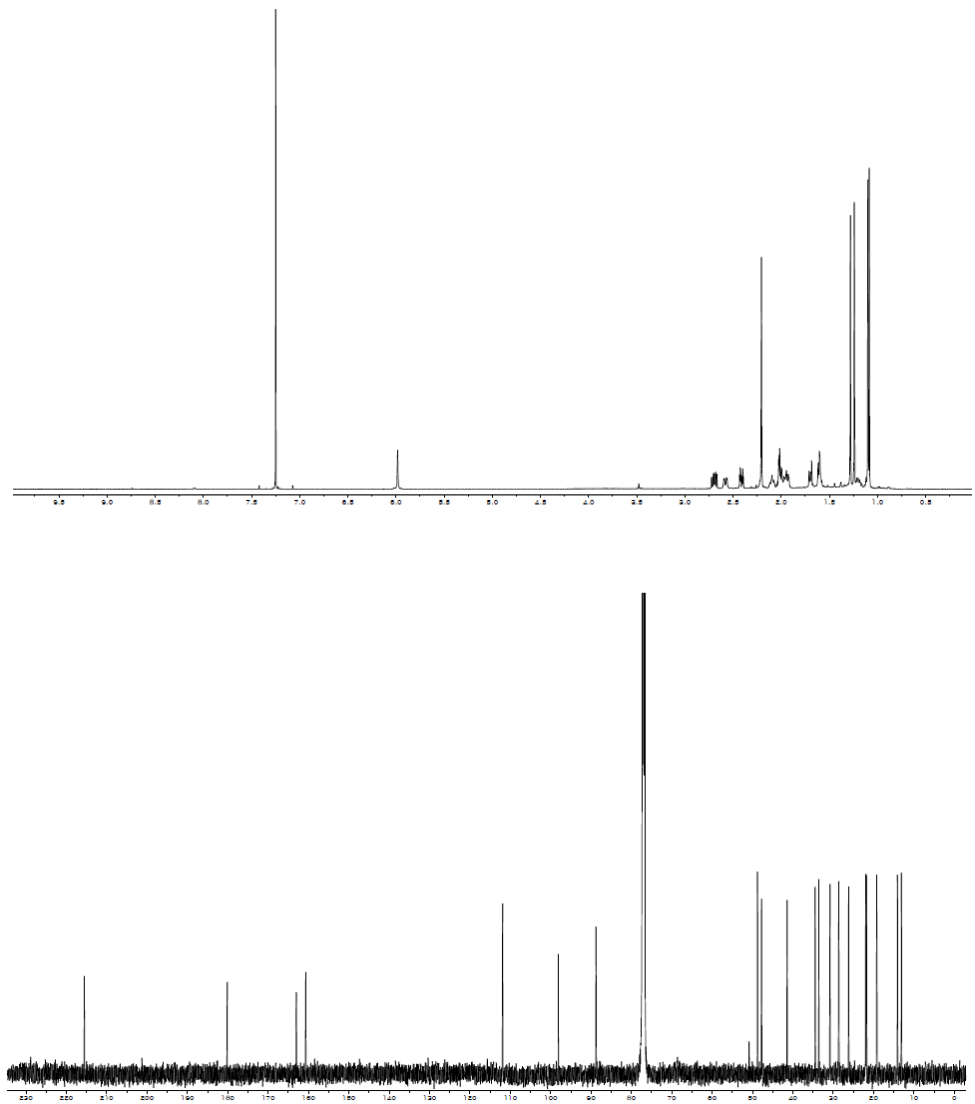

Figure A2. ^{1}H (500 MHz) and ^{13}C (125 MHz) NMR spectra of compound **2** ($CDCl_3$)

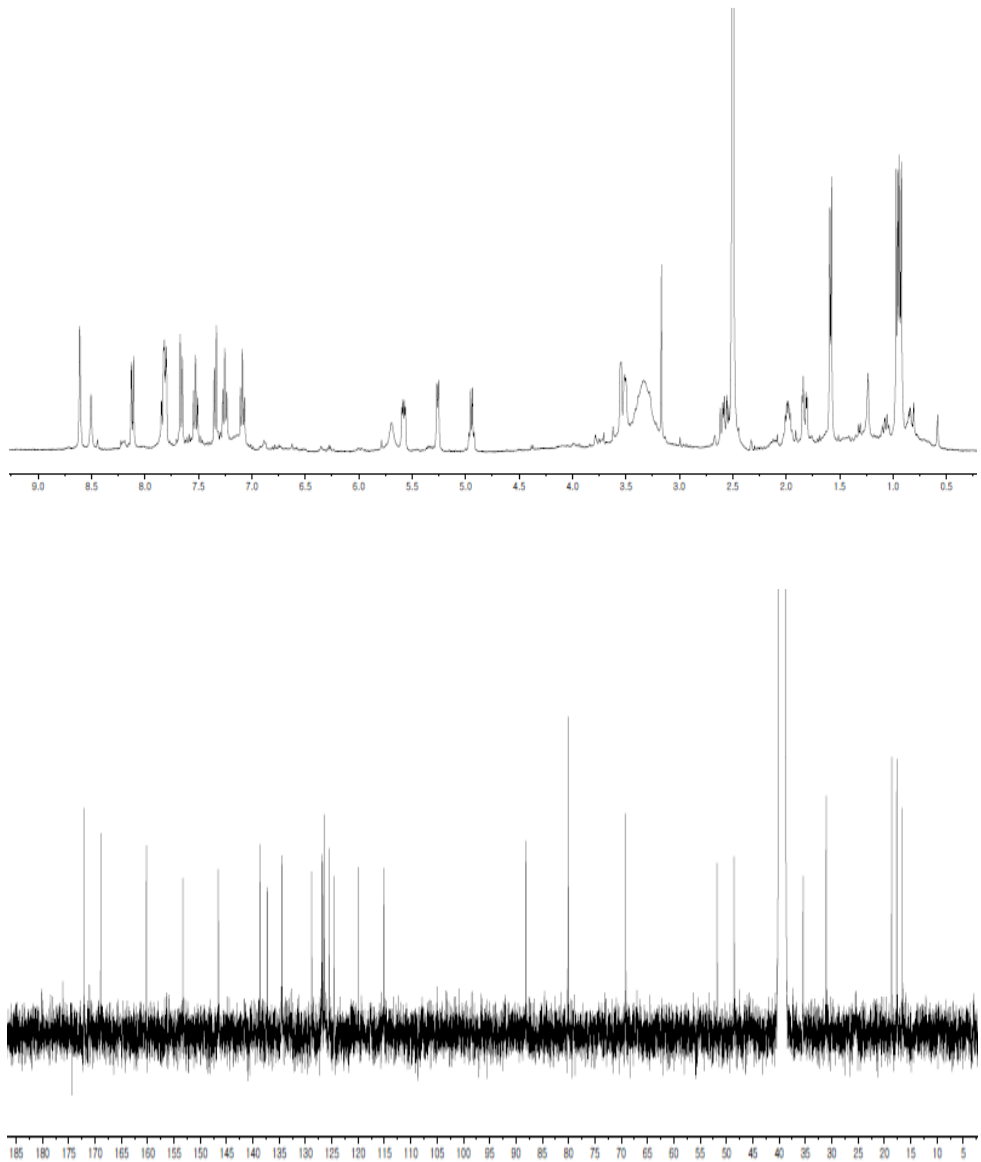

Figure A3. ^{1}H (400 MHz) and ^{13}C (100 MHz) NMR spectra of compound **5** (DMSO-d_6)

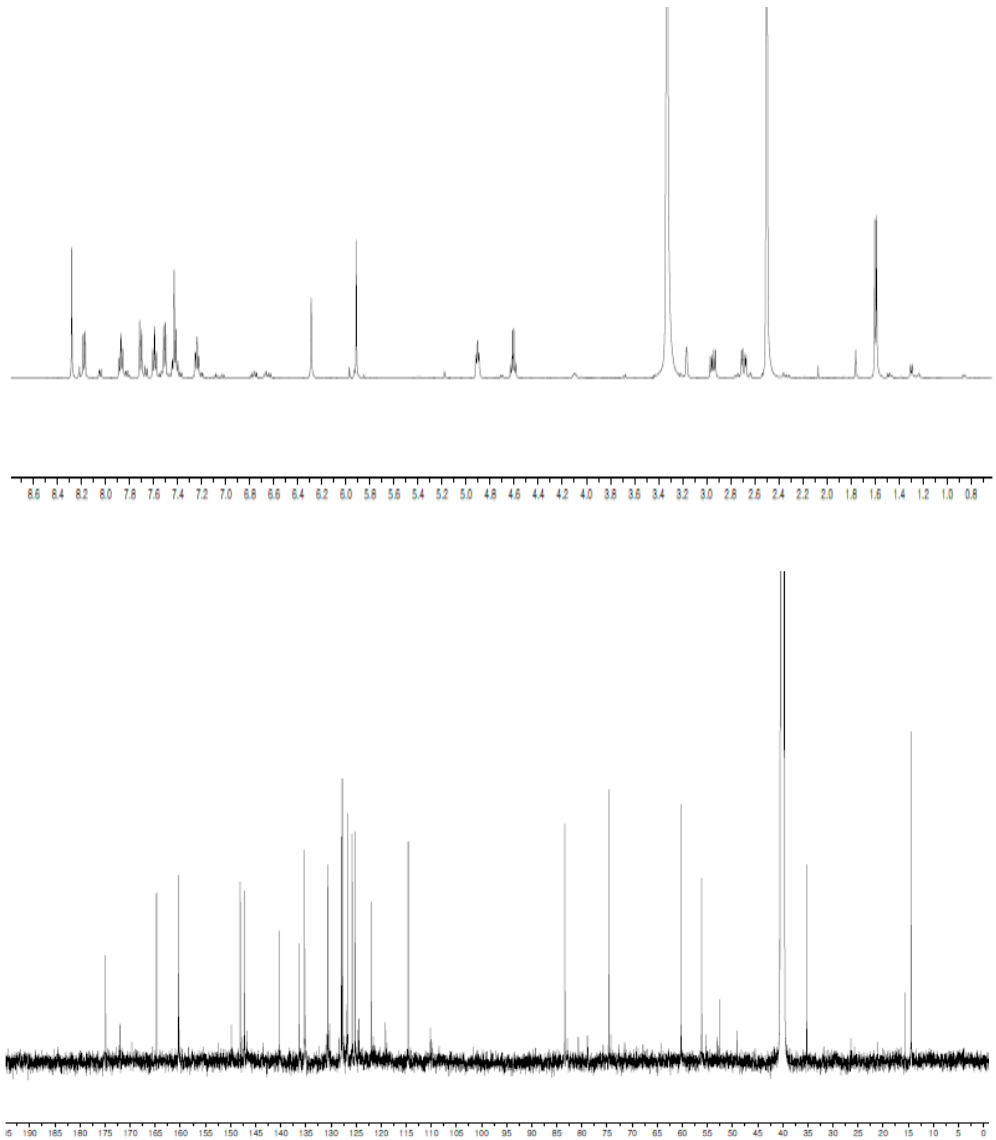

Figure A4. ^{1}H (600 MHz) and ^{13}C (150 MHz) NMR spectra of compound **6** (DMSO-d_6)

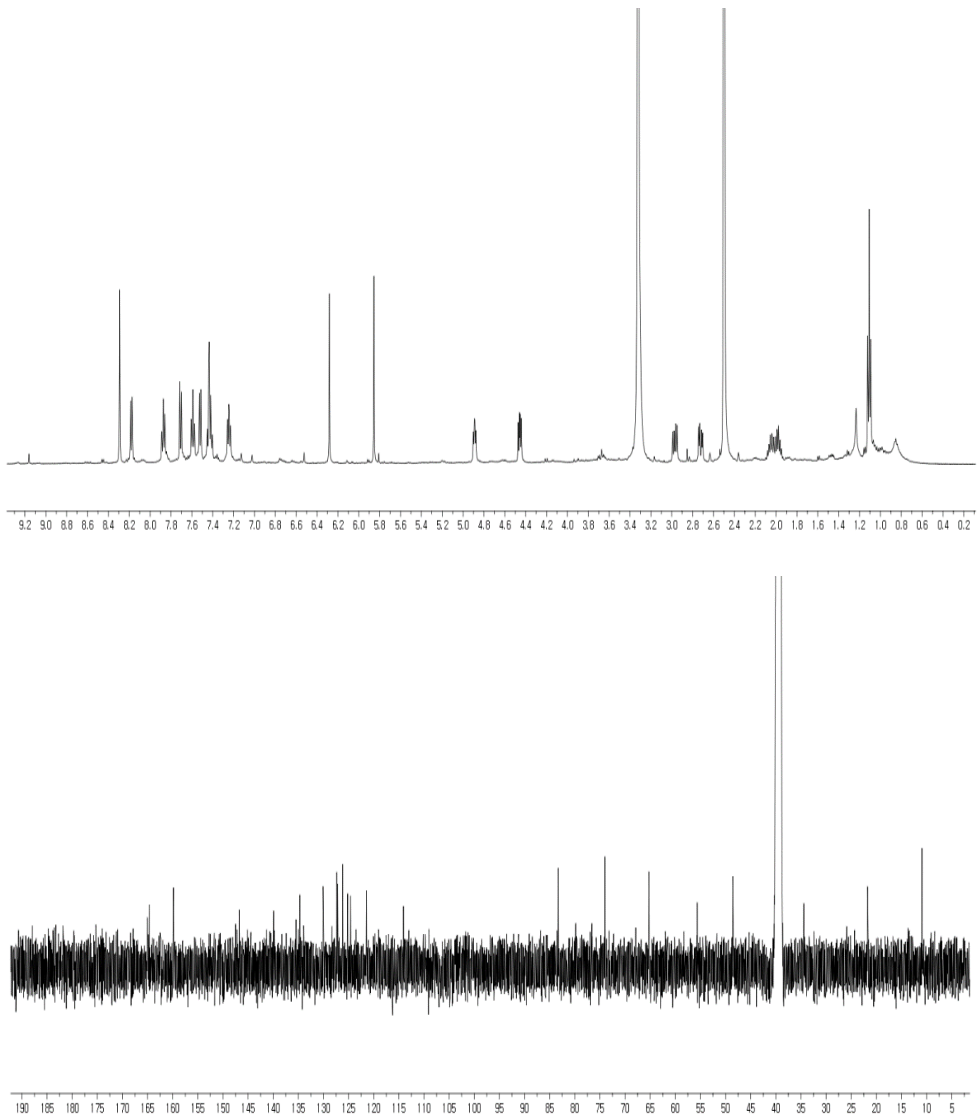

Figure A5. ^{1}H (500 MHz) and ^{13}C (125 MHz) NMR spectra of compound **7** (DMSO-d_6)

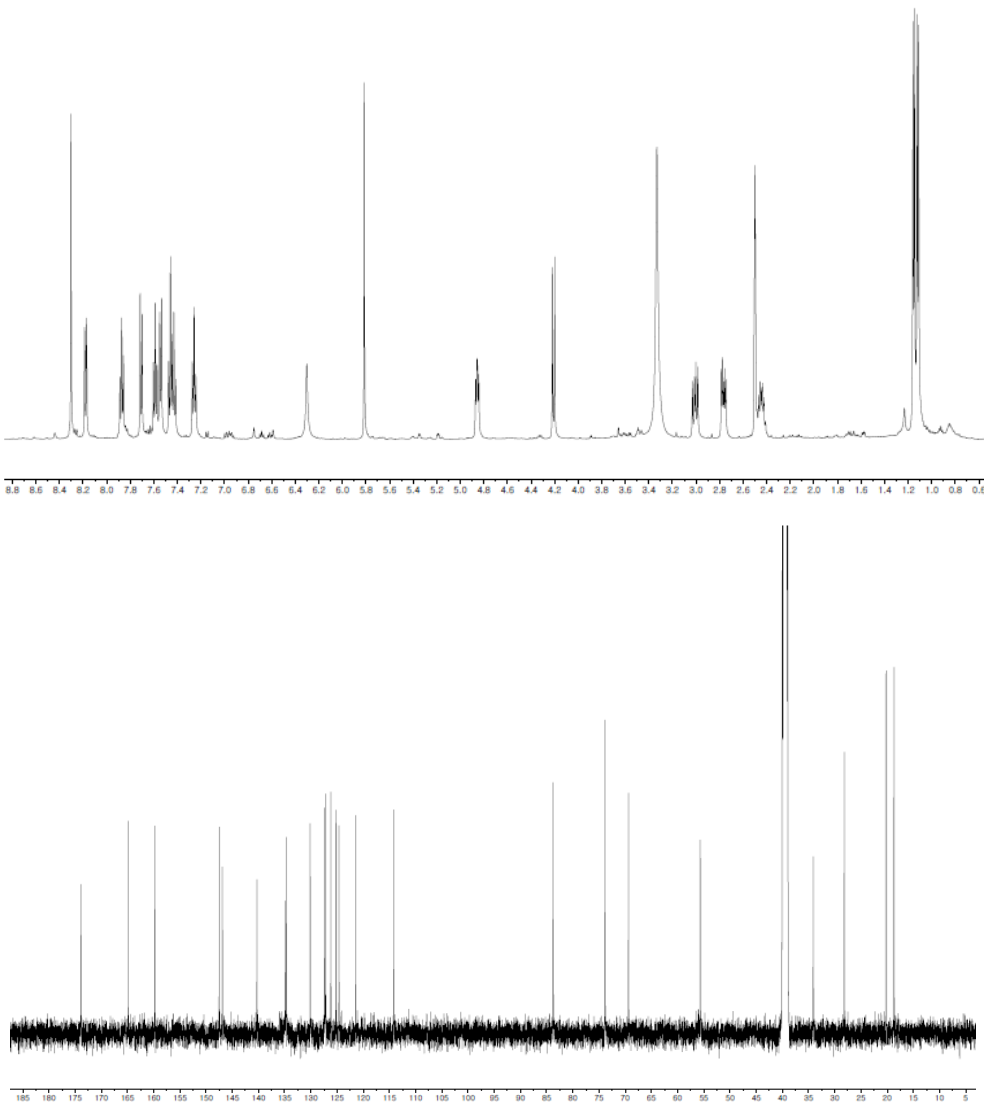

Figure A6. ^{1}H (500 MHz) and ^{13}C (125 MHz) NMR spectra of compound **8** (DMSO-d_6)

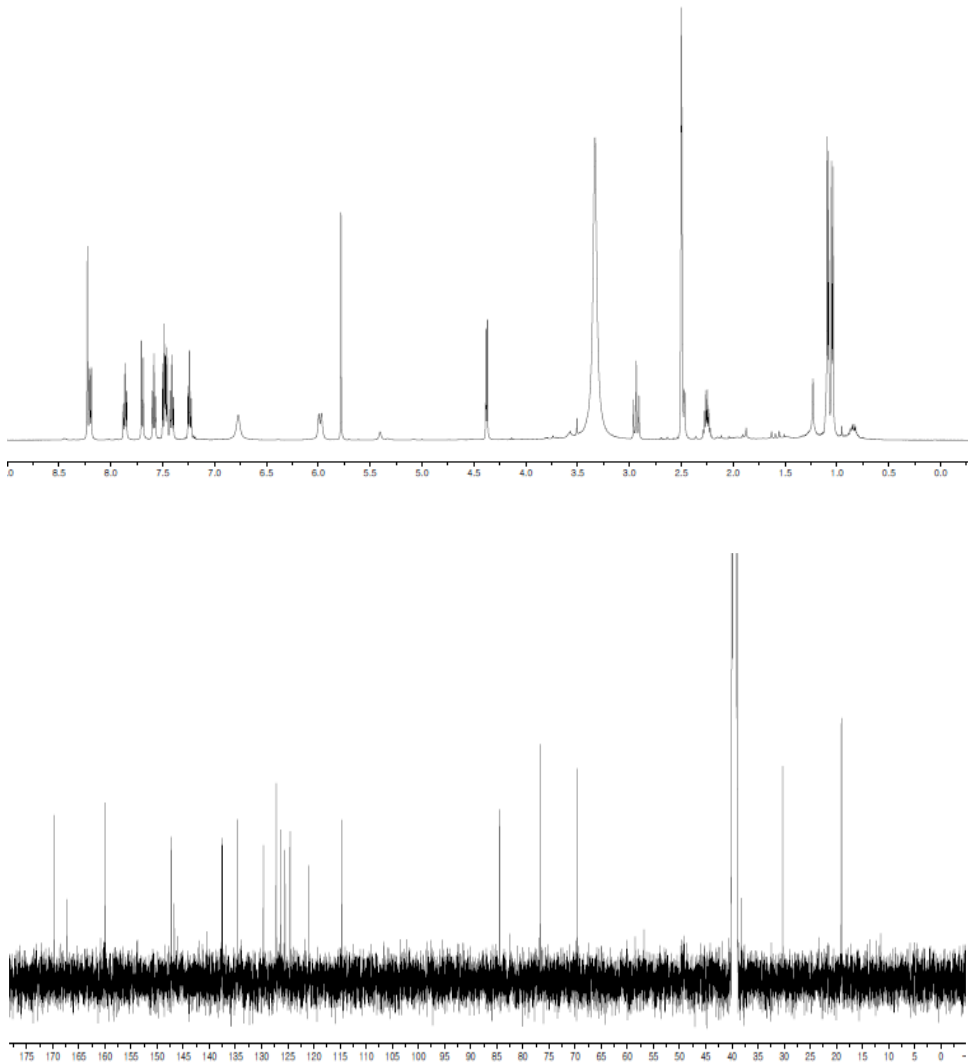

Figure A7. ^{1}H (500 MHz) and ^{13}C (125 MHz) NMR spectra of compound **9** (DMSO-d_6)

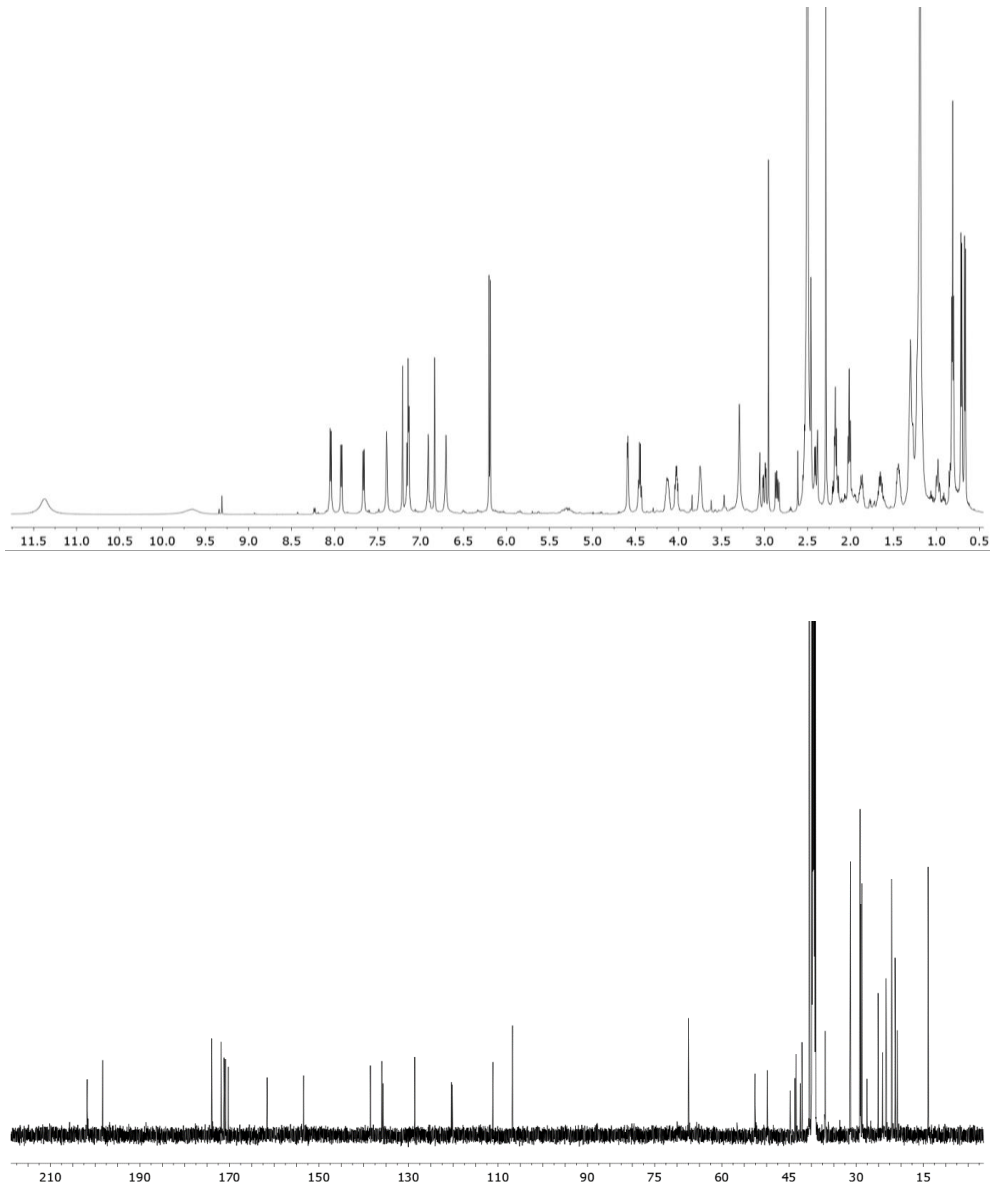

Figure A8. ^{1}H (600 MHz) and ^{13}C (150 MHz) NMR spectra of compound **17** ($CDCl_3$)

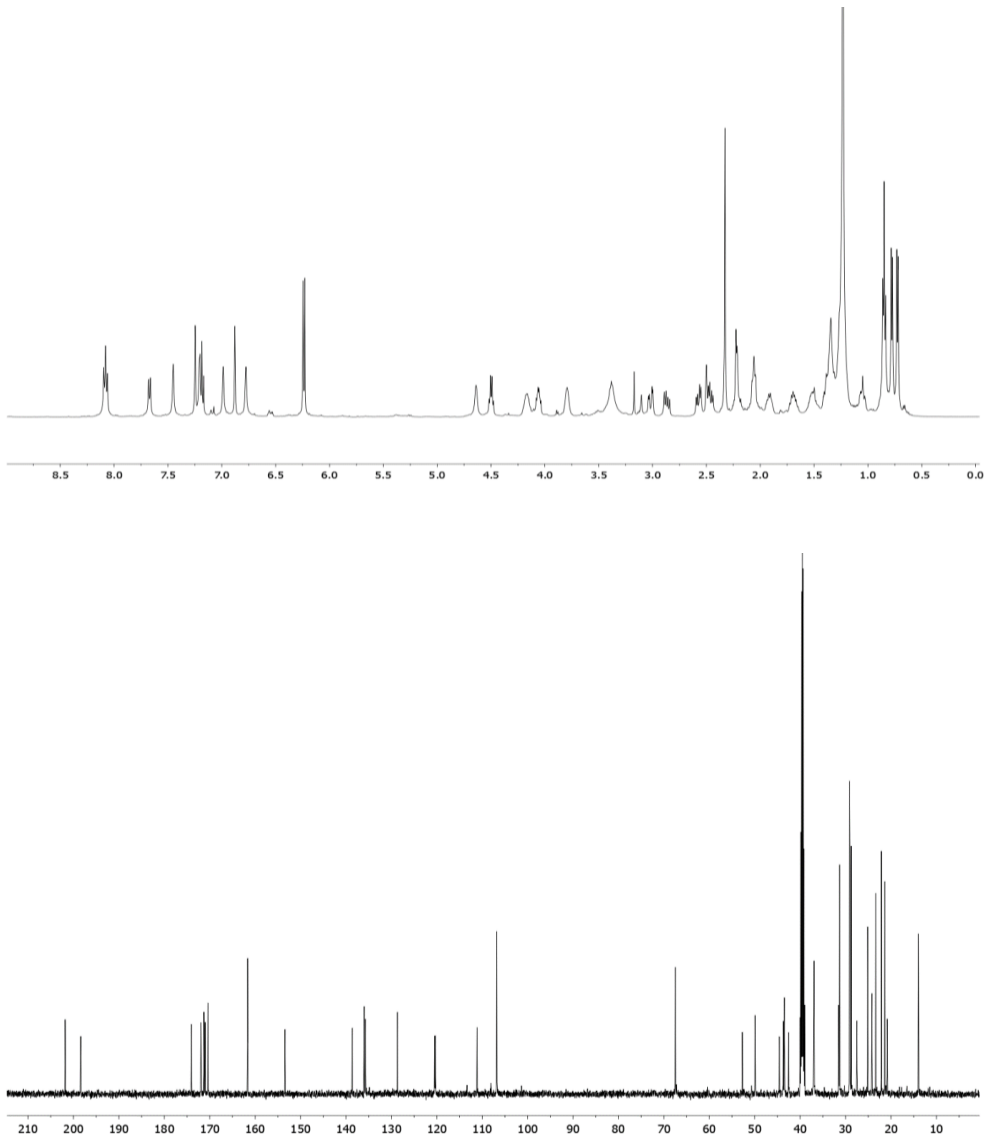

Figure A9. ^{1}H (500 MHz) and ^{13}C (125 MHz) NMR spectra of compound **18** ($CDCl_3$)

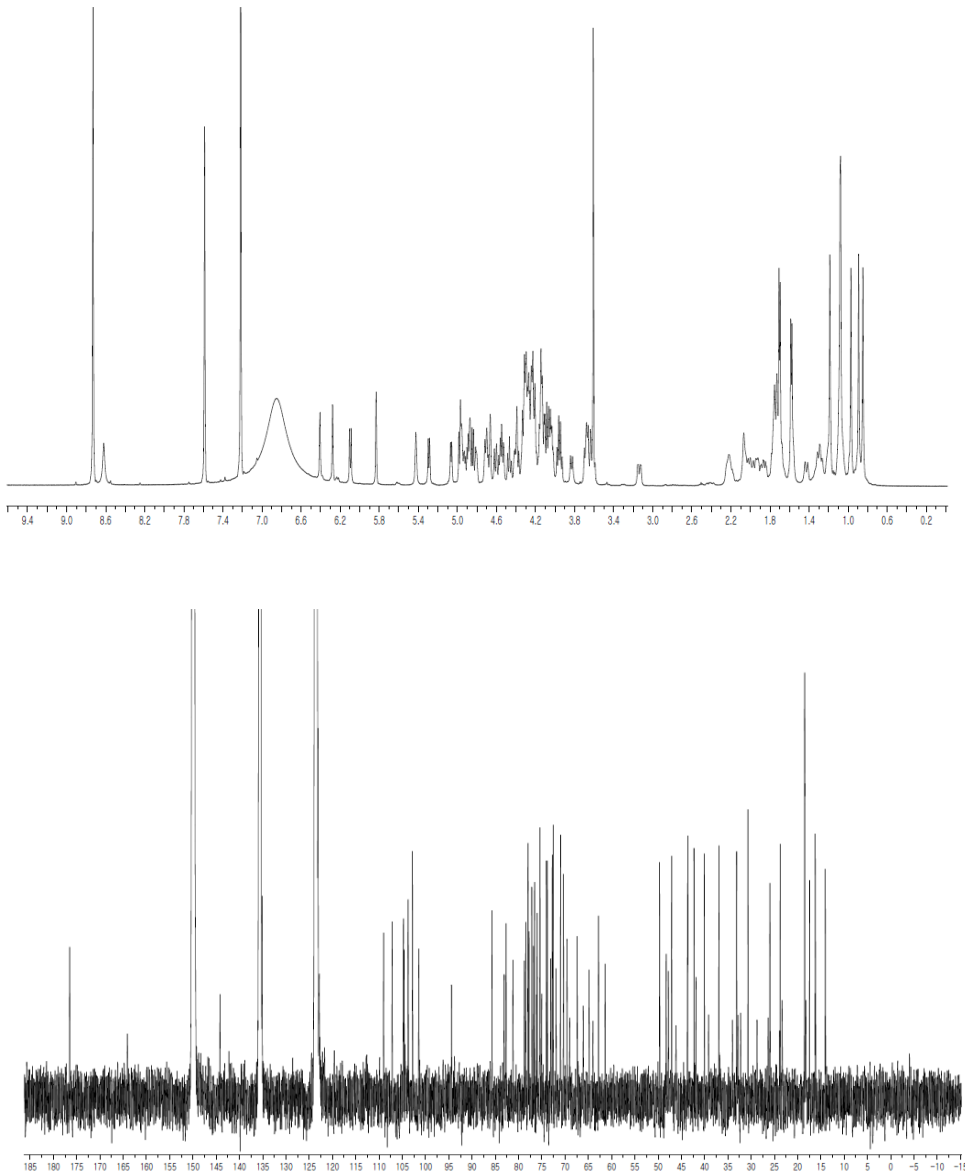

Figure A10. ^{1}H (600 MHz) and ^{13}C (150 MHz) NMR spectra of compound **37** (Pyridine-d_5)

APPENDIX B:

Supporting Information

List of Contents

B1. Biological Assays Methods

Cytotoxicity assays, antimicrobial assays, and isocitrate lyase, sortase A, and Na^+/K^+-ATPase inhibition assays were performed as described previously.[21, 42, 45, 47, 49] For the cytotoxicity test, an MTT viability assay was performed as previously described with slight modifications.[47] MTT was first prepared as a stock solution of 5 mg/mL in phosphate buffered saline (PBS, pH 7.2) and was filtered. At the end of the treatment period (24 h, 48 h, and 72 h), with three different test drug concentrations in triplicate, MTT solution (20 μL) was added to each well and then incubated for 4 h at 37 °C; then solubilizing buffer (10% sodium dodecyl sulfate dissolved in 0.01 N HCl, 100 μL) was added to each well. After overnight incubation, the 96-well plate was read by an enzyme-linked immunosorbent assay (ELISA) reader at 570 nm for absorbance to determine the cell (A549 cell line and/or K562) viability. The viable cells produced a dark blue formazan product, whereas no such staining was formed by dead cells. The LC_{50} value was defined as the concentration that resulted in a 50% decrease in cell viability compared to that of control reactions in the absence of an inhibitor. The values (mean ± SD) were calculated from the dose–response curves of three concentrations of each test sample in three independent experiments (n = 3).

Quinone reductase (QR) activity. Hepa 1c1c7 cells were purchased from American Type Culture Collection (ATCC CRL-2026) and were grown in alpha minimum essential medium without nucleosides, supplemented with 2 mM glutamine, 100 U/mL penicillin G, 100 μg/mL streptomycin and 10% fetal bovine serum. Cultures were maintained at 37 ºC in a 5% CO_2/95%

air atmosphere. QR activities were determined spectrophotometrically according to the reported microtitre method with some modification. Hepa 1c1c7 cells were plated at a density of 1.0×10^4 cells/mL and were grown for 24 h in a humidified incubator in a 5% CO_2 at 37 ^oC. The cells were exposed to test compounds, and then incubated for an additional 24 h. After the plates had been exposed to the test sample for 24 h, the media were decanted, and the cells were lysed by incubation at 37 ^oC for 10 min with 250 μL in each well of a solution containing 10 mM Tris-HCl, pH 8.0, 140 mM NaCl, 15 mM $MgCl_2$, and 0.5% NP-40 (IGEPAL CA-630) (Sigma, St Louis, MO). The plates were then agitated on an orbital shaker for an additional 10 min at 25 ^oC, after which 1 mL of the complete reaction mixture was added to each well. The final assay mixture contained 10 mM Tris-HCl, pH 7.4, 0.5 mg/mL bovine serum albumin (BSA), 0.008% Tween-20, 40 μM flavin adenine dinucleotide (FAD), 0.8 mM glucose-6-phosphate, 2 U/mL glucose-6-phosphate dehydrogenase, 25 μM NADP, 40 μg/mL 3-(4,5-dimethylthiazo-2-yl)-2,5-(diphenyltetrazolium bromide) (MTT), and 1 mM menadione. A blue colour developed and the reaction was stopped after 5 min by addition of 250 μL of a solution containing 0.3 mM dicoumarol in 0.5% pyridine and 5 mM potassium phosphate, pH 7.4. The rate of the NADPH-dependent, menadiol-mediated reduction of MTT was measured at

610 nm. Protein was determined by crystal violet staining of an identical set of test plates. The specific activity (SA) of quinone reductase (nmol/min/mg of protein) was calculated from the equation:

$$SA = [MTT_{abs}/CV_{abs}] \times 3{,}345$$

where MTT_{abs} is the absorbance change of MTT per min; CV_{abs} is the absorbance of crystal violet; and 3,345 is the ratio of the proportionality constant determined for crystal violet and the extinction coefficient of MTT, and has the units of nmol/(min·mg protein).

B2. Computational Calculation of Compounds 5, 6, and 9.

Computational analysis. The groud-state geometries were optimized with density functional theory (DFT) calculations, using Turbomole 6.5 at the basis set def-SV(P) for all atoms and functional B3LYP/DFT level, the ground states were further confirmed by the harmonic frequency calculation. Lowest energy conformations were calculated for the structures of compounds **5** with 3*S*, 14*R*, 17*R*, 18*R*, and 20*S* configurations, **6** with 2*R*, 3*R*, 11*S*, and 14*R* configurations, and **9** with 2*R*, 3*R*, 11*S*, and 14*S* configurations. The DFT settings (functional B3-LYP/Gridsize M3) and geometry optimization options (energy 10^{-6} hartree, gradient norm $\left| dE / dxyz \right| = 10^{-3}$ hartree/bohr) were used.

The result of DFT calculation of compound **5**.

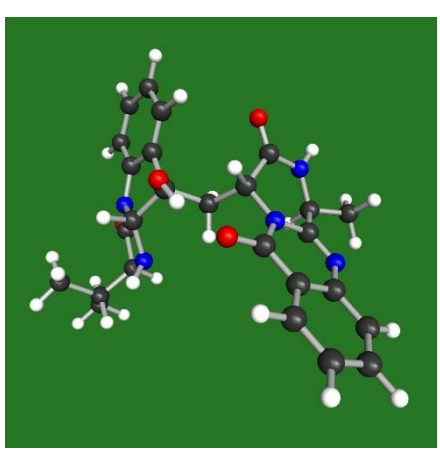

Compound **5** (3*S*, 14*R*, 17*R*, 18*R*, and 20*S* configurations)
total energy = -1579.61023575168
---
kinetic energy = 1564.99522787312
potential energy = -3144.60546362481

The result of DFT calculation of compound **6** (left) and **9** (right).

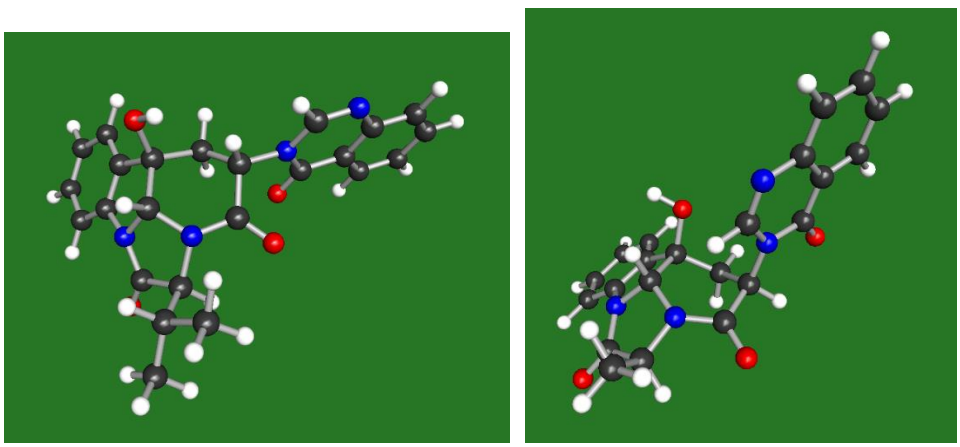

Left; compound **6** (2*R*, 3*R*, 11*S*, and 14*R* configurations)

total energy = -1367.31823420808
---
kinetic energy = 1354.91548967183
potential energy = -2722.23372387990

Right; compound **9** (2*R*, 3*R*, 11*S*, and 14*S* configurations)
total energy = -1445.85318732708
---

kinetic energy = 1432.44233243421

potential energy = -2878.29551976129

B3. The LC/MS spectra of Advanced Marfey's analysis of compounds 5-9.

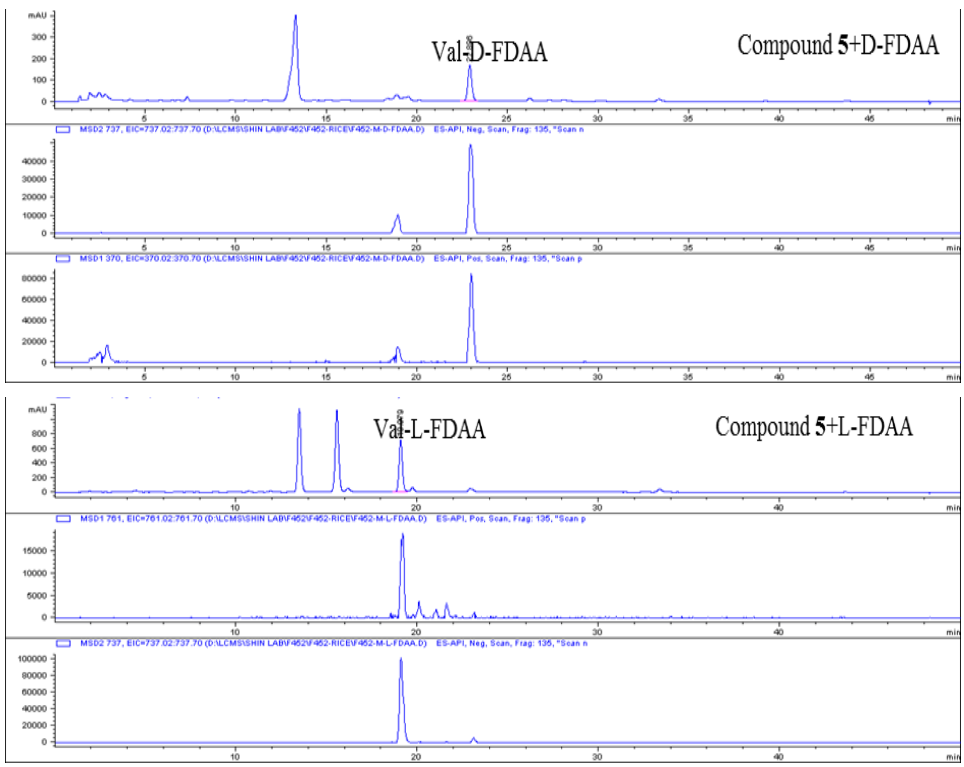

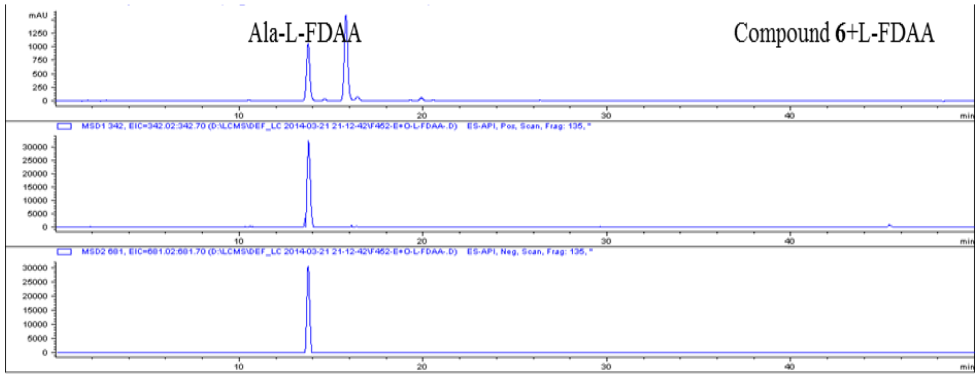
Ala-L-FDAA
Compound 6+L-FDAA

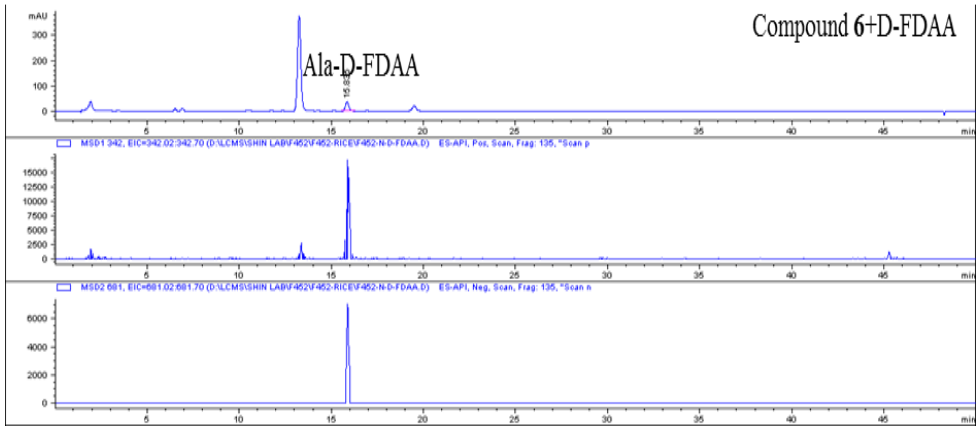
Ala-D-FDAA
Compound 6+D-FDAA

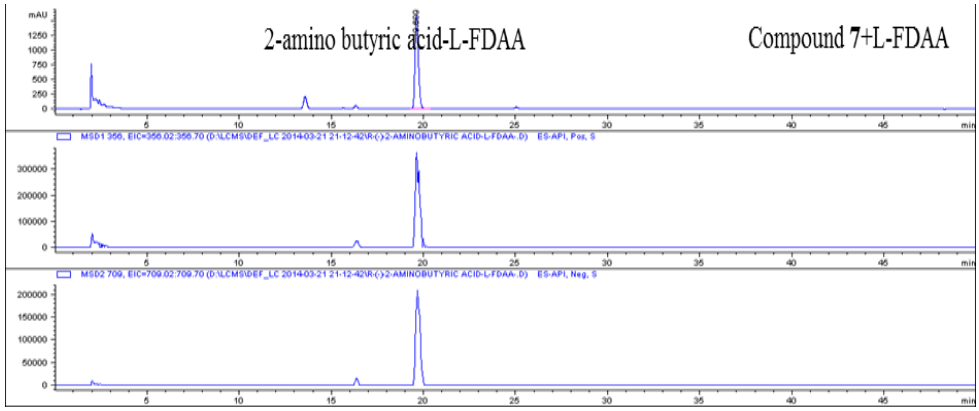
2-amino butyric acid-L-FDAA
Compound 7+L-FDAA

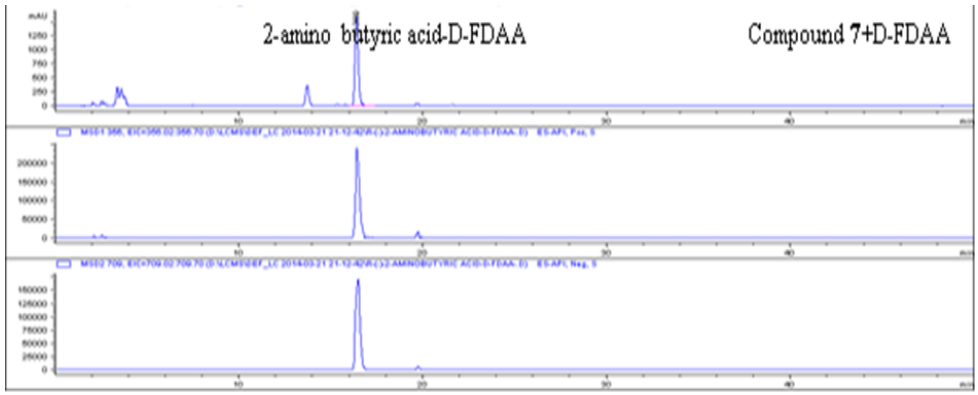
2-amino butyric acid-D-FDAA
Compound 7+D-FDAA

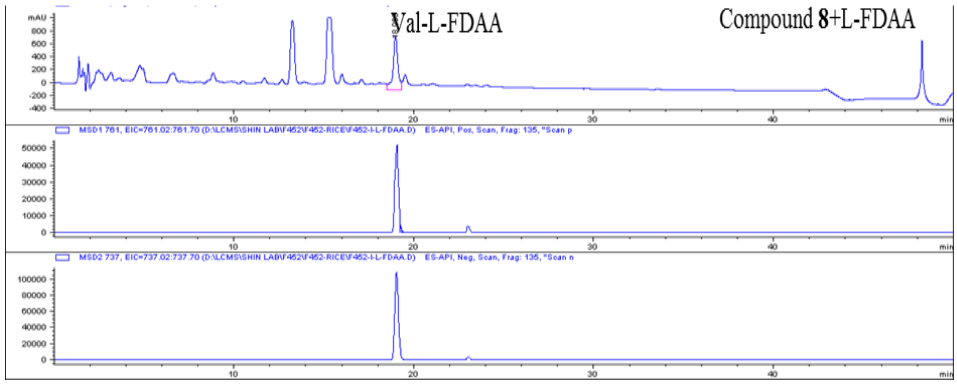
Val-L-FDAA
Compound 8+L-FDAA

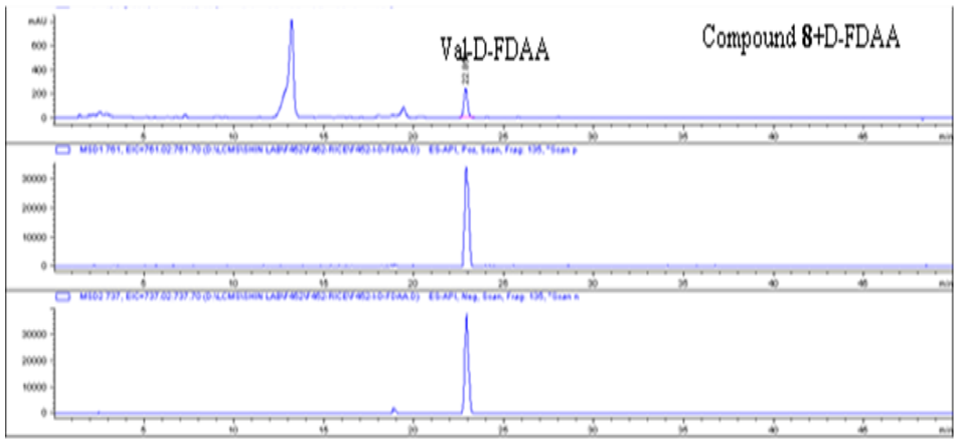
Val-D-FDAA
Compound 8+D-FDAA

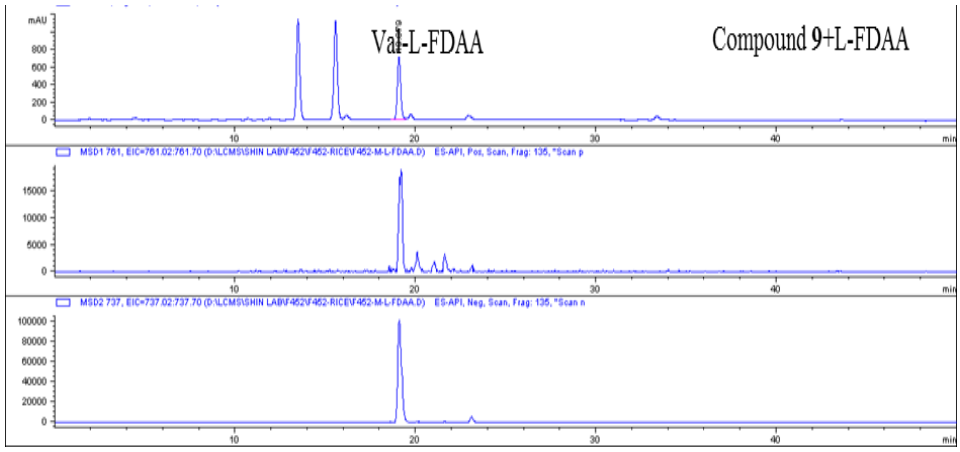
Val-L-FDAA
Compound 9+L-FDAA
mAU
min
MSD1 761, EIC=761.02:761.70 (D:\LCMS\SHIN LAB\F462\F462-RICE\F462-M-L-FDAA.D) ES-API, Pos, Scan, Frag: 135, *Scan p
MSD2 737, EIC=737.02:737.70 (D:\LCMS\SHIN LAB\F462\F462-RICE\F462-M-L-FDAA.D) ES-API, Neg, Scan, Frag: 135, *Scan n

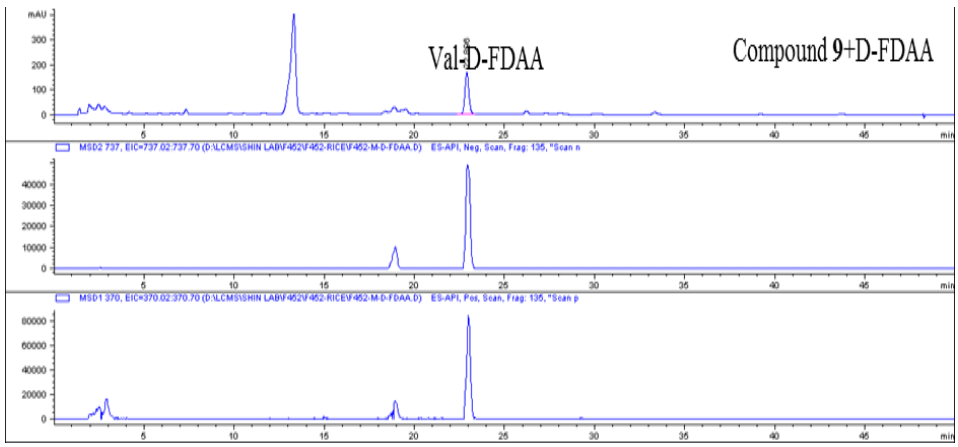
Val-D-FDAA
Compound 9+D-FDAA
mAU
min
MSD2 737, EIC=737.02:737.70 (D:\LCMS\SHIN LAB\F462\F462-RICE\F462-M-D-FDAA.D) ES-API, Neg, Scan, Frag: 135, *Scan n
MSD1 370, EIC=370.02:370.70 (D:\LCMS\SHIN LAB\F462\F462-RICE\F462-M-D-FDAA.D) ES-API, Pos, Scan, Frag: 135, *Scan p

Table S1. The reference number of voucher specimens of Kalopanacis Cortex.

Samples	Voucher specimens	Samples	Voucher specimens	Samples	Voucher specimens
K-01	10H1001	C-04	10H3025	C-25	10H2029
K-02	10H1007	C-05	10H2024	C-26	10H2030
K-03	10H1026	C-06	10H2002	C-27	10H2034
K-04	10H1027	C-07	10H2003	C-28	10H2035
K-05	10H1031	C-08	10H2008	C-29	10H2036
K-06	10H1032	C-09	10H2010	C-30	10H2037
K-07	10H1039	C-10	10H2011	C-31	10H2038
K-08	10H2005	C-11	10H2012	C-32	10H2043
K-09	10H2006	C-12	10H2013	C-33	10H2044
K-10	10H2007	C-13	10H2014	C-34	10H2045
K-11	10H2009	C-14	10H2015	C-35	10H2046
K-12	10H2032	C-15	10H2017	C-36	10H2049
K-13	10H2033	C-16	10H2018	C-37	10H2054
K-14	10H2053	C-17	10H2019	C-38	10H2039
K-15	10H2052	C-18	10H2020	C-39	10H2004
K-16	10H2001	C-19	10H2021	C-40	10H2016
K-17	10H2040	C-20	10H2022	C-41	10H2041
K-18	10H2042	C-21	10H2023	C-42	10H2050
C-01	10H2016	C-22	10H2025	C-43	10H2051
C-02	10H3023	C-23	10H2027		
C-03	10H3024	C-24	10H2028		

Table S2. Comparison of effectiveness of KC metabolites by extraction method (mg/g, n = 3).

Compounds	Sonication	Vortex	Reflux
33	0.92 ± 0.02	0.73 ± 0.01	0.89 ± 0.02
34	5.40 ± 0.08	5.41 ± 0.07	5.15 ± 0.07
35	6.13 ± 0.11	5.93 ± 0.11	6.23 ± 0.10
36	4.98 ± 0.14	4.32 ± 0.12	5.03 ± 0.10
37	6.47 ± 0.08	6.15 ± 0.09	6.27 ± 0.10
38	2.10 ± 0.00	2.00 ± 0.01	1.90 ± 0.01
39	0.53 ± 0.01	0.54 ± 0.01	0.51 ± 0.00
40	29.79 ± 0.51	29.34 ± 0.49	29.42 ± 0.55
41	8.25 ± 0.00	8.14 ± 0.09	8.20 ± 0.10
42	34.20 ± 1.22	34.01 ± 1.25	34.00 ± 1.01
43	0.41 ± 0.00	0.42 ± 0.00	0.41 ± 0.00
44	0.52 ± 0.00	0.51 ± 0.00	0.52 ± 0.01

Table S3. Comparison of effectiveness of KC metabolites by extraction solvent (mg/g, n = 3).

Compounds	70% MeOH	50% MeOH	70% EtOH	50% EtOH
33	0.88 ± 0.02	0.92 ± 0.02	0.79 ± 0.03	0.82 ± 0.05
34	5.38 ± 0.10	5.40 ± 0.08	5.14 ± 0.12	5.30 ± 0.18
35	6.02 ± 0.09	6.13 ± 0.11	5.93 ± 0.08	6.10 ± 0.16
36	4.57 ± 0.15	4.98 ± 0.14	4.59 ± 0.11	4.97 ± 0.09
37	6.45 ± 0.13	6.47 ± 0.08	6.21 ± 0.18	6.10 ± 0.21
38	2.02 ± 0.01	2.10 ± 0.00	2.10 ± 0.02	2.15 ± 0.02
39	0.53 ± 0.01	0.53 ± 0.01	0.51 ± 0.01	0.48 ± 0.01
40	29.22 ± 0.49	29.79 ± 0.51	29.24 ± 0.62	29.39 ± 0.58
41	8.37 ± 0.08	8.25 ± 0.00	8.20 ± 0.10	8.32 ± 0.10
42	33.94 ± 1.34	34.20 ± 1.22	34.34 ± 1.32	34.25 ± 1.03
43	0.39 ± 0.01	0.41 ± 0.00	0.40 ± 0.00	0.38 ± 0.02
44	0.51 ± 0.01	0.52 ± 0.00	0.51 ± 0.01	0.48 ± 0.01

Table S4. Comparison of effectiveness of KC metabolites by extraction time (mg/g, n = 3).

Compounds	10 min	20 min	30 min	60 min	90 min
33	0.72 ± 0.02	0.81 ± 0.02	0.92 ± 0.02	0.92 ± 0.02	0.87 ± 0.04
34	4.87 ± 0.07	5.33 ± 0.08	5.40 ± 0.08	5.39 ± 0.05	5.23 ± 0.10
35	5.67 ± 0.09	5.94 ± 0.11	6.13 ± 0.11	6.07 ± 0.07	6.07 ± 0.13
36	4.17 ± 0.08	4.75 ± 0.14	4.98 ± 0.14	4.89 ± 0.09	4.68 ± 0.09
37	6.02 ± 1.00	6.23 ± 0.08	6.47 ± 0.08	6.38 ± 0.11	6.24 ± 0.11
38	1.90 ± 0.01	2.00 ± 0.01	2.10 ± 0.00	2.11 ± 0.01	2.02 ± 0.00
39	0.50 ± 0.01	0.53 ± 0.01	0.53 ± 0.01	0.50 ± 0.01	0.43 ± 0.01
40	29.00 ± 0.57	29.46 ± 0.65	29.79 ± 0.51	29.67 ± 0.76	29.54 ± 0.71
41	7.39 ± 0.08	7.95 ± 0.10	8.25 ± 0.00	8.20 ± 0.02	8.25 ± 0.10
42	34.01 ± 1.01	34.18 ± 1.20	34.20 ± 1.22	34.25 ± 1.34	33.87 ± 1.45
43	0.32 ± 0.01	0.41 ± 0.01	0.41 ± 0.00	0.40 ± 0.01	0.31 ± 0.00
44	0.41 ± 0.01	0.49 ± 0.00	0.52 ± 0.01	0.53 ± 0.01	0.43 ± 0.01

Publication List

1. "Comparative Analyses of Bioactive Constituents from *Forsythia suspensa* and *Forsythia viridissima* by HPLC-DAD" Won, T. H.; Liao, L.; Lee, S. H.; Son, J. K.; Shin, J. *Nat. Prod. Sci.* **2011**, *17*, 328-336.

2. "Simultaneous Analysis of Bioactive Metabolites from *Ziziphus jujuba* by HPLC-DAD-ELSD-MS/MS" Liao, L.; Won, T. H.; Kang, S. S.; Shin, J. *J. Pharm. Investig.* **2012**, *42*, 21-31.

3. "New Polyaromatic Metabolites from a Marine-Derived Fungus Penicillium sp." Julianti, E.; Lee, J.-H.; Liao, L.; Park, W.; Park, S.; Oh, D.-C.; Oh, K.-B.; Shin, J. *Org. Lett.* **2013**, *15*, 1286-1289.

4. "Simultaneous Analysis of Furfural Metabolites from *Rehmanniae Radix* Preparata by HPLC-DAD-ESI-MS" Won, T. H.; Liao, L.; Kang, S. S.; Shin, J. *Food Chem.* **2014**, *142*, 107-113.

5. "Cytotoxic Diterpenoid Pseudodimers from the Korean Sponge Phorbas gukulensis" Jeon, J.-e.; Liao, L.; Kim, H.; Sim, C. J.; Oh, D.-C.; Oh, K.-B.; Shin, J. *J. Nat. Prod.* **2013**, *76*, 1679-1685.

6. “Penicillipyrones A and B, Meroterpenoids from a Marine-Derived Penicillium sp. Fungus” Liao, L.; Lee, J.-H.; You, M.; Choi, T. J.; Park, W.; Lee, S. K.; Oh, D.-C.; Oh, K.-B.; Shin, J. *J. Nat. Prod.* **2014**, *77*, 406-410.

7. “Quantification and Identification of Bioactive Metabolites from *Kalopanacis Cortex* by HPLC with Evaporative Light Scattering Detection and ESI Quadrupole TOF MS” Liao, L.; Won, T. H.; Kim, Y. H.; Shin, J. *J. Sep. Sci.* **2014**, *37*, 505-514.

8. “Alkaloidal Metabolites from a Marine-Derived Aspergillus sp. Fungus” Liao, L.; You, M.; Chung, B. K.; Oh, D.-C.; Oh, K.-B.; Shin, J. *J. Nat. Prod.* **2015**, *78*, 349-354.

9. “Lumazine Peptides from the Marine-Derived Fungus Aspergillus terreus” You, M.; Liao, L.; Hong, S. H.; Park, W.; Kwon, D. I.; Lee, J.; Noh, M.; Oh, D.-C.; Oh, K.-B.; Shin, J. *Mar. Drugs* **2015**, *13*, 1290-1303.

Acknowledgements

I would like to thank all who in one way or another helped me during my four and a half years Ph.D study in Seoul National University and contributed in the completion of this thesis.

First and foremost the deepest gratitude must go to my advisor Professor Jongheon Shin for his guidance, caring, patience, encouragement, immense knowledge, and financial supportment during my research to finish the thesis. I could not have imagined having a better advisor and mentor for my Ph.D study.

I would also like to express the gratitude to the Professor Ki-Bong Oh, who provided the biological assays and the identification of fungi strains for my thesis.

And I would like to thank Professor Dong-Chan Oh, whose valuable guidance on the fungi strains' selection based on his professional knowledge and the LC-EISMS data interptation and encouragement when I was in difficulties.

Thanks will also go to Professor Sang-Jip Nam and Professor Sung Won Kwon for their best suggestions as committee on my defense.

I wish I can express my sincere gratitude to Professor Sang Kook Lee for his biological assays and Professor Yeong Shik Kim for his excellent and deep lectures.

I want to express my warm and deep gratitude to all the lab members for their friendships and assistances: Song Jueun, Oh Ikhoon, Elin Julianti, Jeon Ju-eun, Won Tae Hyung, Lee Jung-Ho, Oh Hana, Lee Sooryun, Lee Yoonyeong, Song Jinhaeng, Riswanto, Kim Chang-Kwon, Song Inn-Hye, Woo Jung-Kyun, You Minjung, Kim Hyung Joong, Cho Hyun Joo, Ryu Yeon Hwa, Kwon O Seok, Woo Yeon Soo, Yun Jung-Ho, and Hwang Ji Yeon.

I wish to extend my warmest thanks to all the NMR and IR/MS operators in the College of Pharmacy and National Center for Inter-University Research Facilities for their providing data for all the tested samples.

I especially appreciate my husband (for his encouragement and financial supportment), my lovely baby (she is my motivation and the source of enthusium), my parents (for their encouragement and well undserstanding), my mother-in-law (for her kindness and help me care the baby), my elder sister and young brother (for their encouragement).